Purity Control of Pharmaceutical and Chemical Substances for Application in Process Environments using Spectroscopy in the Middle and Near Infrared

Instrumentelle Analytische Chemie

Fakultät für Chemie

der Universität Duisburg-Essen

Zur Erlangung des akademischen Grades eines
Doktors der Naturwissenschaften

Dr. rer. nat

genehmigte Dissertation

vorgelegt von

Fayaz Kondagula

aus

Hyderabad, Indien

Referent: **Prof. Dr. Karl Molt**

Korreferent: **Prof. Dr. H. W. Siesler**

Vorsitzender: : **Prof. Dr. Thomas Schrader**

Tag der mündlichen Prüfung: 19 April 2011

Declaration

I herewith declare that I have produced this thesis without the prohibited assistance of third parties and without making use of aids other than those specified; notions taken over directly or indirectly from other sources have been identified as such. This thesis has not previously been presented in identical or similar form to any other German or foreign examination board.

The thesis work was conducted from 01.12.2007 to 30.12.2010 under the supervision of Prof. Dr. Karl Molt at the department of Instrumental Analytical Chemistry in University-Duisburg Essen.

(Fayaz Kondagula)

Essen.

Dedicated

To my parents K. Khadeer Saheb, K. Tamijunnisa Begum and my guru Prof. Dr. Karl Molt

Acknowledgements

Foremost, I express my sincere gratitude to my advisor Prof. Dr. Karl Molt for the continuous support of my PhD study and research, for his patience, motivation, enthusiasm, and immense knowledge. His guidance helped me in all the time of research and writing of this thesis. I could not have imagined having a better advisor and mentor for my PhD study.

Besides my advisor, I would like to thank Prof. Dr. H. W. Siesler for being my co-referee.

I thank Mr. Wolfgang Ritter, CEO of QuantaRed Technogies GmbH (Vienna), for the opportunity to take measurements with the ERACHECK instrument.

My special thanks to my lab mate and colleague Dr. Jessica Trockel. Her discipline was a great inspiration for completion of my thesis. My sincere thanks to my colleagues of the Department Instrumental Analytical Chemistry especially Robert Knerim and Lydia Vassen.

Special thanks to my friends and wonderful human beings Srinivas Satyanarayana, Chitumalla Ramesh, Meike Stute, Syed Ansar Basha, Sreedhar Nagandla and Abdul Kareem Ragaz who made life more bright and sunny. I would like to express my sincere gratitude to my beloved parents Khadeer Saheb and Tamijunnisa Begum and my three sisters Nazneen, Nasreen and Nadiya who were the real source of inspiration and emotional support which have enabled to complete this work with success.

I would like to acknowledge the thousands of individuals who have coded for the **R**-Project and LaTeX project for free. Last but not least I would like to ask for an excuse to the other individuals who supported me whom I could not mention due shortage of space.

Finally I would like end this acknowledgment by a proverb around which the life of a Analytical Chemist revolves:

“Vertrauen ist gut, Kontrolle ist besser”

Abstract

All organic and most inorganic compounds show characteristic Infrared spectra. Therefore IR Spectroscopy can be used as an effective tool for quality control. Middle and Near Infrared with modern instrumentation and accessories like Diamond ATR and Diffuse Reflectance accessories, provide spectra which are highly reproducible making it possible to detect even minor spectral deviations caused by impurities. In this thesis the focus is on quality control in chemical process environments where the purity of materials has to be determined more or less automatically.

The correlation between the spectrum of a potentially contaminated sample and the reference spectrum of the corresponding pure compound can be used as measure for purity in terms of the correlation coefficient r. r is obtained by regressing the sample spectrum on the reference spectrum. A simulation study showed that it is advantageous to transform r to Fisher's z coefficient because z is much better suited than r for detecting small spectral deviations caused by impurities. On this basis two spectral purity parameters SPR_1 and SPR_2 were obtained by multiplying the correlation coefficient resp. the normalized z coefficient with 100.

As a second way for discovering impurities a method of dynamic difference spectroscopy was developed, by which the difference between the spectrum of the sample and the reference and the corresponding difference factor are calculated automatically. As spectral purity parameters the obtained difference factor itself, SPR_3, and alternatively the integral of the difference spectrum, SPR_4, are used.

The methods based on linear regression proved to be more effectual and detection limits of impurities down to 0.002 g/100 g for liquids and 0.03 g/100 g for solids could be achieved. Further it could be shown that by using a Quantum Cascade Laser spectrometer instead of a FT-IR instrument still lower limits of detection can be attained.

Contents

List of Figures

List of Tables

1

Introduction and Objectives

Spectroscopy in the Middle and Near Infrared region is a widely used routine analytical method for both the qualitative and quantitative control of incoming (raw materials) and outgoing (finished) products in the Pharmaceutical, Polymer and Chemical industries [1, 2] on par with other analytical methods like Nuclear Magnetic Resonance, Mass Spectroscopy, Ultraviolet Spectroscopy and High Performance Liquid Chromatography. This is due to the fact that all organic and many inorganic compounds have characteristic Infrared spectra, which allows the discrimination of one substance from another. In addition the availability of modern accessories like Diamond ATR Units (MIR) and Diffuse Reflectance Units (NIR) ensures fast and easy sample preparation, and in most of the instances, analyses can be performed on as received samples without previous dilutions or other preparative steps [3]. The resultant spectra show a high signal-to-noise ratio and in many cases have excellent reproducibility.

Raw materials control is the basic and first step in quality assurance and is in compliance with GMP (Good Manufacturing Practice) [4], it is obligatory since numerous factors may contribute to contamination of the products such as organic impurities, e.g. starting materials or intermediates, by-products, degradation products, etc. and inorganic impurities, e.g. reagents, ligands, catalysts, heavy metals, etc. Another source of false raw materials can be human errors during acceptance of delivery, confusion of containers or wrong labelling. Raw materials control not only involves identification of the basis materials, but also monitoring

and control if the incoming products comply to the specifications with respect to the degree of allowed impurities [5].

The most common analytical methods employed for this purpose are HPLC, GC, UV-Spectroscopy, Infrared Spectroscopy, etc. Chromatographic methods score over IR/NIR spectroscopy in achieving high specificity and very low limits of detection. However for most of the practical purposes such low limits are seldom needed and limits of about 0.1% would be enough in many industrial applications [6]. Moreover chromatographic techniques have their own limitations like economic factors (cost per analyte), the demand of highly skilled labour and the fact that they are time consuming, prone to errors during sample preparation and destroying the sample irreversibly providing no information of the matrix. Infrared spectroscopy with its diverse sampling accessories (both in Middle and Near Infrared) in many cases can be a good alternative to these chromatographic techniques [7].

1.1 Infrared Spectroscopy

1.1.1 Direct Evidence on Constitution

Infrared Spectrometry is particularly important in analytical sciences because of the information content of a spectrum and its variety of possibilities for sample measurement and substance preparation. Moreover it gives direct evidence on constitution due to inherent structural information in a spectrum of an unknown sample that can be derived alone, without the aid of comparative substances, through theoretical or empirical correlations. In IR spectroscopy, such correlations exist between the position of absorption bands within certain abscissa ranges of the spectrum and particular structural groups. For instance, the presence or absence of carbonyl functions, hydroxy groups, amino groups, nitriles but also double bonds, aromatics and many other structural elements can most likely be recognized upon first glance [8, 9]. By considering other areas of the spectrum and, if need be, by enlisting empirical correlation tables from the literature and libraries, a closer examination of the position and intensity of these bands allows, in most cases, a precise classification of the recognized structural group:

ketone, acid or ester, primary, secondary or tertiary alcohol, substitution type of aromatics etc.

1.1.2 Identification by Spectral Comparison

The position and intensity of absorption bands of a substance are highly specific to that substance. Like a fingerprint of a person, the IR spectrum is characteristic for a substance and can be used for identifying it unequivocally. The best suited bands for identification are those found in the fingerprint region between 1800 and 650 cm^{-1}. Two factors are decisive for successful substance identification through the IR spectrum:

- The generally high number of absorption maxima occurring. Aside from molecules with high symmetry and a low number of atoms, in most cases 10-30 and more bands appear in IR spectrum.

- The large number of available IR spectral libraries. The number of spectra categorized in different collections and published in the literature currently is about 225,000 and this number is constantly raising [10, 11].

Among the comparison methods for spectral identification, the most simple one is the visual comparison method, were the sample spectrum is compared with the reference spectrum. This is regarded as a valid method of identity control in many instances, e.g. for the identity control of pharmaceuticals [12]. Nevertheless, this method demands reasonable expertise and is only possible in the Middle Infrared, because NIR spectra have very broad and usually overlapping bands calling for chemometric recognition procedures.

In computer based spectral searches a parameter has to be defined, which describes the similarity or dissimilarity between the sample and the reference spectrum. If this parameter is above respectively below a certain threshold then the sample spectrum is considered to be identical with the reference spectrum.

Such a comparison can either be performed by comparing peak tables [13] or with complete spectra. With the advent of more powerful computers and the availability of high capacity hard disks comparison of complete spectra nowadays is prevailing.

One of the most widely used qualification methods is calculating Euclidean distances between the sample and the reference spectrum [14]. These can be calculated either in the space of individual wavelengths [15] or - after a proceeding Principal Component Analysis (PCA) - in factor space [16–18].

Another way to check for identity is the use of correlation coefficients which are obtained by regressing the sample spectrum on the reference spectra in the library [7, 19]. In case of perfect agreement between the sample and the reference, the correlation coefficient should be equal to 1, however random noise associated with any type of spectral measurement precludes obtaining the correlation coefficient of exactly becoming 1. This parameter - in contrast to distances in factor space - has the advantage of being independent from the set of reference spectra.

This method was first applied by K. Tanabe and S. Saeki for the automatic spectral search from libraries [20] and still is widely applied, e.g. in the "Compare Function" implemented in the PerkinElmer software "Spectrum for Windows™" [21]. Van der Vlies and co-workers used the correlation coefficient which they called the spectral match value (SMV) for identifying different types of cellulose and ampicillin trihydrate [22]. Blanco *et al.* demonstrated the discriminating ability of the correlation coefficient that they called the match index (MI) in identification of a pharmaceutical preparation by use of a library consisting of 163 substances including excipients, active compounds, amino acids and vitamins [7]. Griffith *et al.* used weighted correlation coefficients as a measure of spectral similarity [23].

1.2 Motivation and Objective

Raw material control is defined as the check of incoming materials through sampling (or selecting products), followed by subsequent judgment. Judgment of the safety level or check of compliance to the specifications is sometimes performed by visual inspection but in most cases by wet chemical or instrumental analysis of incoming materials, and then comparing the results to certain criteria or limit values resulting in the acceptance or rejection of a batch or product. Impurities present in the raw materials can be classified into three main categories [6]:

- Organic impurities (apart from residual solvents)
- Inorganic impurities
- Residual solvents

Organic impurities can arise during manufacturing process or during storage of the chemical and drug substances. They can be identified or unidentified, volatile or non-volatile species, and include:

- Starting materials
- By-products
- Intermediates
- Degradation products
- Reagents, ligands and catalysts

Inorganic impurities often result from the manufacturing process and then normally known and identified and include:

- Reagents, ligands and catalysts
- Heavy metals or other residual metals
- Inorganic salts
- Other materials (e.g. filter aids, charcoal)

Solvents are mostly organic liquids used as vehicles for the preparation of solutions or suspensions in the synthesis of a chemical or drug substance.

Due to the presence of such impurities laboratory studies are mandatory to be conducted to detect impurities. Analytical procedures should be developed for those potential impurities that are exceptionally potent, toxic or which may cause problems in further processing. Such analytical procedures should have documented evidence that they are suitable and are validated for detection and quantification of impurities (see the recommendations of ICH Q2A and Q2b guidelines [6] and cGMP of US-FDA [24]). Also technical factors (e.g. manufacturing

capability and control methodology) and economic pragmatism can be reasons for selecting certain methods for checking for impurities of commercial products. Thus, even the use of lower precision techniques (e.g. Thin Layer Chromatography) can be acceptable when justified and appropriately validated.

Organic impurity levels can be measured by a variety of techniques, including those that compare an analytical response for an impurity to that of an appropriate reference standard, e.g. Certified Reference Materials (CRMs) [25–27]. Reference standards used in analytical procedures for control of impurities should be evaluated and characterized according to the intended purposes. In the simplest case a sample of the drug or chemical compound with a defined degree of purity can be used as a standard to estimate levels of impurities.

Common occurrence of various types of impurities (organic and inorganic) in raw materials along with guidelines stated in the document Q3A(R2) of ICH form the motivating factors to develop efficient but also fast methods which are capable of detecting various kinds of commonly occurring impurities. Therefore Infrared spectroscopic methods form an interesting alternative to traditional chromatographic techniques. The fact that all organic and most inorganic compounds are Infrared active implies that Infrared spectroscopy has good chances to detect a broad range of impurities.

One of the longtime applied computational methods for identification control in Infrared spectroscopy is that of regression between the sample and the reference spectrum (see section 1.1.2). Probably the first one to use it in purity control were H. Weitkamp and D. Wortig (Pharma-Analytisches Laboratorium der Bayer AG, Werk Wuppertal). They used the standard error of regression as a measure of dissimilarity between the sample and reference spectrum [28]. The standard error of regression has the drawback that it is sensitive to intensity changes between the spectra. Therefore in this thesis, as parameter for the purity of a sample the correlation coefficient r is used. This doesn't get influenced by baseline shifts and intensity changes. This property is of especial significance when measuring solid samples.

Another useful technique is that of difference spectroscopy. In principle, this is the compensation of the reference spectrum in the sample spectrum by subtraction after multiplication with a difference factor.

Based on these two main principles, i.e. regression and difference spectroscopy, in this thesis altogether four spectral purity parameters were developed and tested with simulated examples and experimental data. One of the aims was to develop these methods in such a way that they are robust and can be performed automatically, i.e. with minimal human interaction which makes them suitable for process environments.

2

Theory and basic principles of MIR/NIR-spectroscopy

Infrared spectroscopy is one of the most prevalent spectroscopic techniques employed by organic and inorganic analytical chemists. Simply speaking it is the absorption measurement at different IR frequencies of a sample positioned in the path of an IR beam. The main goal of IR spectroscopic analysis is to determine the chemical functional groups in the sample. Different functional groups absorb characteristic frequencies of IR radiation [29].

2.1 The electromagnetic spectrum

Infrared (IR) refers to the part of the electromagnetic spectrum between the visible and microwave regions (Fig. 2.1 on page 9).

The frequency ν is the number of wave cycles that pass through a point in one second. It is measured in Hz, where 1 Hz = 1 cycle/sec. The wavelength λ is the length of one complete wave cycle. Wavelength and frequency are inversely related:

$$\nu = \frac{c}{\lambda} \tag{2.1}$$

The wavenumber $\bar{\nu}$ is the inverse of the wavelength in cm^{-1}:

$$\bar{\nu} = \frac{1}{\lambda} \tag{2.2}$$

Energy is related to wavelength and frequency by following formula:

$$E = h\nu = \frac{hc}{\lambda} = h \cdot c \cdot \bar{\nu} \tag{2.3}$$

The IR region which is spanning from 13000 to 10 cm^{-1}, or wavelengths from 0.77 to 1000 μm, is divided into three regions: the Near, Mid and Far IR [30]. The Mid and Near IR regions are of great practical use for analytical chemists. Mid IR range is from 4000 to 400 cm^{-1} and Near IR spans from 13000 to 4000 cm^{-1} an increase in wavenumber corresponds to an increase in energy.

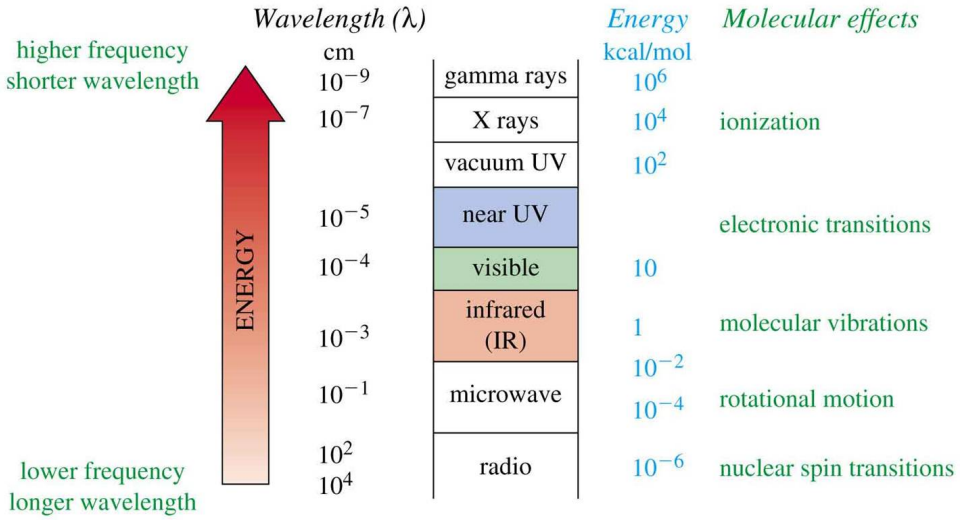

Figure 2.1: The electromagnetic spectrum [31].

2.1.1 Molecular vibrations

At the temperatures above absolute zero, all the atoms in molecules are in continuous vibration with respect to each other. When the "eigen-frequency" of a specific vibration of a molecule is equal to the frequency of the IR radiation directed on it, the molecule absorbs the radiation.

Each atom has three degrees of freedom, corresponding to motions along any of the three Cartesian coordinate axes (x, y and z). A polyatomic molecule consisting of n atoms has a total of $3n$ degrees of freedom. In a nonlinear molecule, 3 of these are rotational and 3 translational and the remaining correspond to

fundamental vibrations; in a linear molecule, 2 degrees are rotational and 3 are translational. Thus the number of fundamental internal vibrations are $3n$-6 for nonlinear and $3n$-5 for linear molecules. The major types of molecular vibrations are stretching and bending. Various types of these vibrations are shown in Fig. 2.2 with an example of a methylene group.

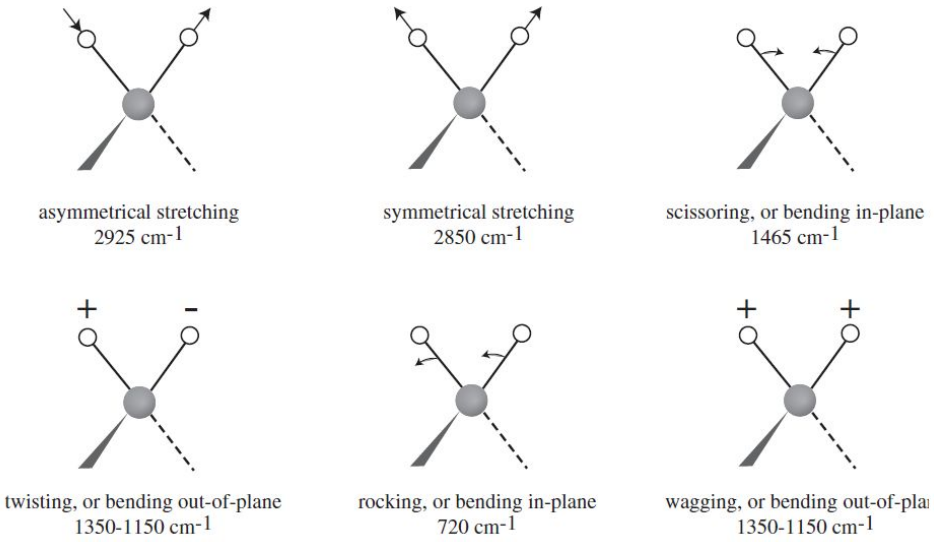

Figure 2.2: Stretching and bending vibrational modes of a CH_2- group [31].

2.1.2 Harmonic and anharmonic oscillator

The stretching frequency of a bond can be approximated by Hooke's Law. In this approximation, two atoms and the connecting bond are treated as a simple mechanical oscillator composed of 2 masses (atoms) joined by a spring as shown in Fig. 2.3.

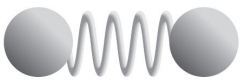

Figure 2.3: Two masses joined by a spring [31].

The energy curve for a simple harmonic oscillator is illustrated in Fig. 2.4 on page 12. According to Hooke's Law, the frequency of the vibration ν is related

to the mass and the force constant of the spring by the following equation:

$$\bar{\nu} = \frac{1}{2\pi c}\sqrt{\frac{k}{\mu}} \tag{2.4}$$

where k, is the force constant and μ is the reduced mass:

$$\mu = \frac{m_1 \cdot m_2}{m_1 + m_2} \tag{2.5}$$

In the classical harmonic oscillator, $E = 1/2kx^2$, where x is the displacement of the spring [32]. Thus, the energy is dependent on how far one stretches or compresses the spring, which can be any value. If this simple model is assumed to be true, a molecule could absorb energy of any wavelength. However, vibrational motion is quantized and must follow the rules of quantum mechanics, and the only energy levels which are allowed fit the following equation:

$$E = (n + 1/2)h\nu \tag{2.6}$$

where ν is the frequency of the vibration, $h = 6.626.10^{-34} Js$ (Planck's constant) and n the vibrational quantum number (0, 1, 2, 3,....). The lowest energy level is $E_0 = 1/2\mathrm{h}\nu$, the next highest is $E_1 = 3/2\mathrm{h}\nu$ etc. According to the selection rule, only transitions to the next energy level are allowed; therefore a harmonic oscillator can only absorb an amount of energy equal to $\mathrm{h}\nu$. However in real molecules transitions of $2\mathrm{h}\nu$, $3\mathrm{h}\nu$, or higher are observed. These correspond to bands called overtones which show up especially in the Near Infrared. They are of lower intensity than fundamental vibration bands.

This is due to the fact that molecules actually are not harmonic but anharmonic oscillators. On one side a bond can dissociate and on other side it cannot be compressed beyond a certain point [33] (Fig. 2.5 on page 12). Note how the energy levels become more closely spaced with increasing interatomic distance in the anharmonic oscillator. Therefore overtones are lower in wavenumbers than predicted by the harmonic oscillator theory.

Equation 2.4 describes the relationship between the bond strength and the atomic masses with the wavenumber at which a molecule will absorb IR radiation. As the force constant increases, the vibrational frequency (wavenumber)

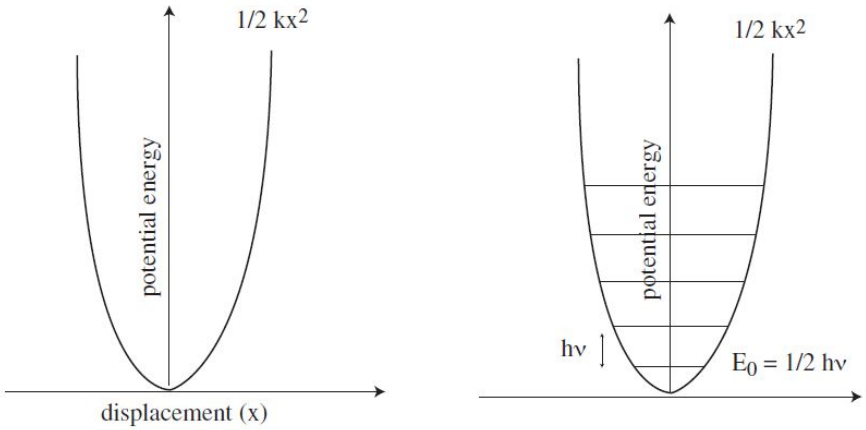

Figure 2.4: Energy curve for a vibrating spring (left) and energy constrained to quantum mechanical model (right) [31].

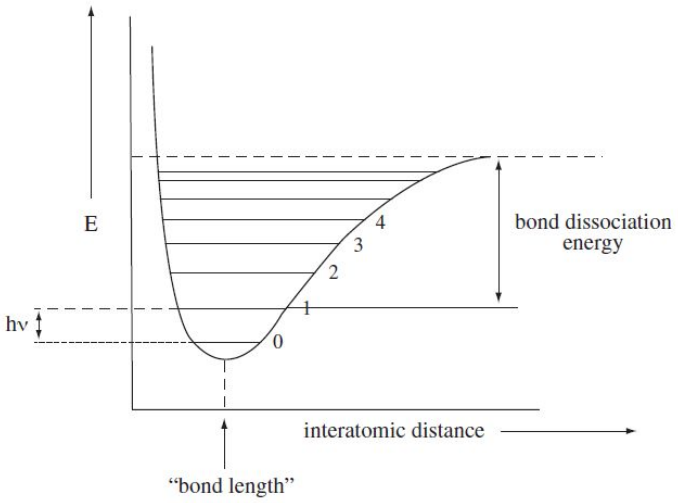

Figure 2.5: Energy curve for an anharmonic oscillator (showing the vibrational levels for a vibrating bond) [31].

also increases. Opposite to this as the masses of atoms increase, the vibrational frequency decreases. Although a useful approximation, the motion of two atoms in a large molecule cannot be isolated from the motion of the atoms in the rest of the molecule. In a molecule, two oscillating bonds can share a common atom.

When this happens, the vibrations of the two bonds are coupled. As one bond contracts, the other bond can either contract or expand, as in asymmetrical and symmetrical stretching, which in general show different frequencies.

2.2 Spectrometers

2.2.1 Spectrometers as tools for quantitative analysis and purity control

If I_0 is the intensity or radiation power of a monochromatic radiation entering a sample and I is the intensity transmitted by the sample, then the ratio I/I_0 is called the transmittance of the sample (T). This is the primary property of samples measured by spectrometers and often expressed as percentage, i.e. $\%T$. If the sample cell has the thickness b, and the absorbing component has a concentration c, then the fundamental equation governing the absorption of the radiation is:

$$T = I/I_0 = 10^{-abc} \tag{2.7}$$

The constant a is called the absorptivity and is characteristic for a specific sample at a specific wavelength. This relation can be expressed in a logarithmic form:

$$log_{10} I_0/I = abc \tag{2.8}$$

The term $log_{10} I_0/I = -log_{10} T$ is given the symbol A and called the absorbance. Then from equation 2.8 we get $A = abc$. This is called Bouguer-Lambert-Beer Law or commonly Beer's Law. The product of the concentration c and the thickness b is a measure of the relative number of absorbing molecules in the Infrared beam.

Beer's Law is considered to be additive. In a mixture, the absorbance at a given wavelength is equal to the sum of the abc values for each component:

$$A = \sum_{i}^{n} a_i b c_i \tag{2.9}$$

where the summation is over all the n components present. This implies that the radiation absorption by one component will not be affected by the presence of other components. Two conditions are implied in the derivation of Beer's Law:

1. The resolution element being measured is monochromatic, i.e. the intensity of the region of the spectrum that is actually measured must have a small spread of wavelengths.

2. The absorptivity a should not change with concentration, e.g. by aggregation effects.

If cell thickness and wavelength are held constant, a plot of concentration versus absorbance for a single component will be a straight line, if Beer's Law holds, if it doesn't, the plot will be slightly non-linear but in most cases still can be used for quantitative analysis.

Based on these principles, each component of a mixture can be quantitatively determined from both the Middle and Near IR spectrum, if a sufficiently intensive absorption band can be found that is not disturbed or is disturbed to a known extent by the other components of the mixture or by a solvent.

However today with computer-aided methods even in the case of strongly overlapping bands quantitative analysis can be performed by applying multivariate evaluation methods which utilize the principle of superposition (eq. 2.9). The standard procedure for this purpose is Partial Least Squares Regression (PLS) which has been widely described in literature [34, 35] and which is also used in this thesis.

In the case of the control of a substance for unknown impurities a quantitative calibration of course cannot be performed. But due to the above described laws also for the case of purity control some general principles can be derived:

1. Only Infrared active substances can be detected.

2. The sensitivity of purity control increases with increasing absorptivities of the impurities.

3. The sensitivity of the purity control can be increased by increasing the optical path lengths. Of course this is possible only to a certain extent and demands spectrometers with high optical throughput like FT-IR or Laser spectrometers.

4. To be universally applicable and sensitive, multivariate methods utilizing a broad spectral range have to be used in quality control. This is inherent in FT-IR spectrometers. In the case of laser spectrometers however it has to be required that the IR lasers used should be broadly tunable.

2.2.2 FT-IR spectrometers

Depending on the spectral apparatus used, one can differentiate spectrometers into non-dispersive, dispersive and Fourier Transform (FT) spectrometers. For our studies we have used FT spectrometers for both Middle and Near IR. They overcome the problem of slow scanning process in dispersive spectrometers and all frequencies can be measured simultaneously rather than individually [33, 36–39]. This is achieved by a simple optical device called Michelson interferometer (Fig. 2.6). Some of the major advantages of FT instruments over dispersive

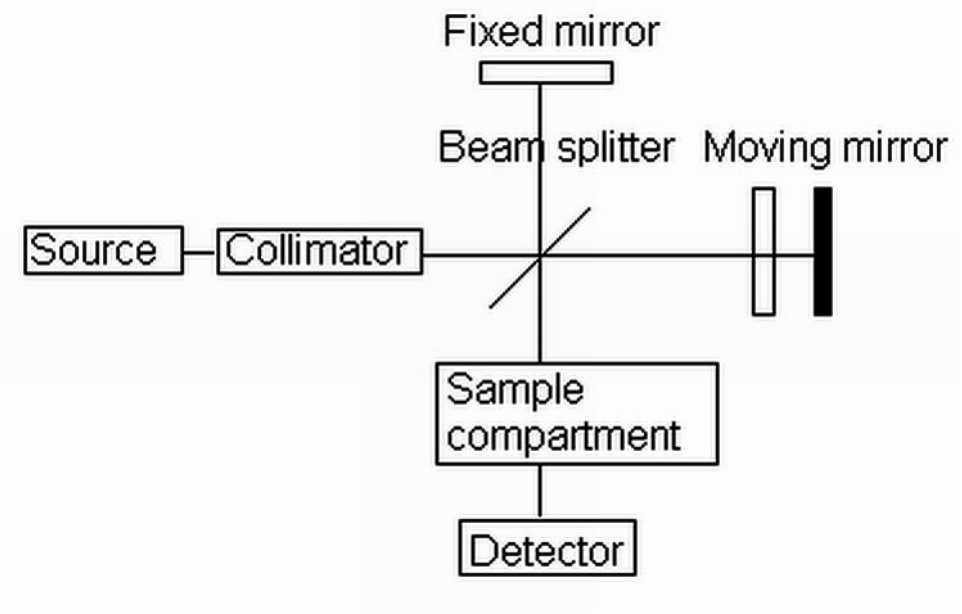

Figure 2.6: Schematic diagram of a FT-IR spectrometer [40].

spectrometers have often been described in literature [36–39] and are as follows:

1. **Multiplex advantage/Felgett advantage:** All wavelengths are measured simultaneously in the interferometer, while these are measured in the

monochromator successively. This reduces significantly the time for acquiring a spectrum. With dominating detector noise typically observed in the Mid and Far IR region, FT spectrometers are superior to dispersive instruments for two reasons: at the same measurement time and the same numbers of spectral elements $N = (\bar{\nu}_{max} - \bar{\nu}_{min})/\Delta\bar{\nu}$, a measurement time per element that is a factor N longer can be realized, whereby the noise is reduced by a factor $\sqrt{N}$. On the other hand for a given signal-to-noise ratio measurement time is reduced by a factor of 1/N.

2. **Throughput advantage/Jacquinot advantage:** At the same spectral resolution, the light conductance of a FT-IR spectrometer, with its circular aperture, is generally higher than that of a dispersive instrument, which is equipped with two slits within the monochromator. This in addition to the multiplex advantage leads to a further improvement of the signal-to-noise ratio.

3. **Connes advantage:** The wavenumber stability of spectra obtained via an interferometer is clearly higher than with dispersive spectrometers. The reason for this is that the frequency scale of the FT instrument is linked to the He-Ne laser, which provides an internal reference for every interferogram. Therefore these instruments can be regarded as self-calibrating and never need to be calibrated by the user.

2.2.3 Radiation sources

As continuous radiation sources in Infrared spectroscopy thermic radiation sources are used which obey Planck's radiation Law. Due to Wien's displacement Law this means that the frequency of highest intensity shifts to higher values with increasing temperature of the radiation source.

The most frequently used radiation source in Mid-IR spectral region is the Globar, consisting of silicon carbide in the form of rods or helixes. As the result of its electrical conductivity in cold state, a Globar can be directly ignited. The burning temperature is about 1500 K. A source used often in the past for Mid-IR region was the Nernst rod, which has a higher working temperature and consists

of rods made of zirconium oxide with additives of yttrium oxide and oxides of other rare earths. The normal operation temperature lies at about 1900 K. Other sources are metallic helices, mainly of chromium-nickel alloys or tungsten with operating temperatures lying at about 1300 K. For the Near-IR region, tungsten halogen lamps are used exclusively, which have a much higher operating temperature and thus emit radiation of higher frequency [41].

In the past lasers were used in Infrared spectroscopy for special purposes only, especially high resolution spectroscopy. For this mainly lead salt lasers were used. However these are expensive, have to be operated at very low temperatures and can be tuned only over very small spectral ranges.

But now tunable Quantum Cascade Lasers (QCLs) which have relatively large scan ranges are fastly coming up and in the future may even replace the traditional radiation sources [42–44]. QC lasers are tiny pieces of semiconductors generally micrometers to millimeters in size that feature nanometer-deep trough like structures known as quantum wells. The devices were invented and demonstrated at Bell Laboratories in 1994 [45].

QC lasers operate like an electronic waterfall. Each quantum well is associated with a characteristic electron energy level determined by the well's depth. Electrons can tunnel between adjacent wells of successively lower energies in a cascading process reminiscent of water flowing down a flight of stairs (see Fig. 2.7 on page 18). At each level, the electron emits a photon with a defined wavelength. By tailoring the depth of the wells, which are often made by growing layers of aluminum indium arsenide and gallium indium arsenide on indium phosphide the laser's wavelength can be determined.

With their ability to emit laser light across the fingerprint region for many types of molecules, QC lasers are natural tools for chemical analysis. The inherent high spectral radiance (or brightness) of QC laser systems is one of their key advantages relative to conventional radiation sources used in FT-IR instruments. This feature enables high energy throughput and by this very high optical thicknesses can be measured with good signal-to-noise ratio.

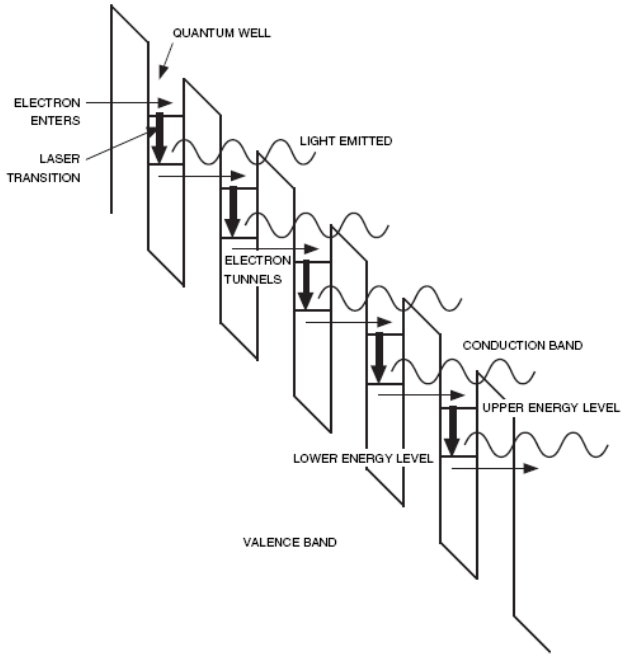

Figure 2.7: Electrons emit a cascade of photons as they undergo sub-band transitions while passing through a stack of quantum wells. The slant represents the electric field applied across the QCL [44].

2.2.4 IR Detectors

Detectors have to convert optical into electrical signals. They can be broadly classified into thermal detectors and photoelectric detectors [29, 46].

Thermal detectors use physical effects based on changes of the detector material resulting from temperature influences. A thermally produced photosignal depends only on the incident flow of radiation independent from its wavelength.

Its principle is based on the temperature dependent change in the thermotension that forms on the contact site between two different metal or semiconductor alloys. The bolometer used much earlier, has greatly lost importance compared to the thermoelement. Its principle is based on the change in resistance with temperature change resulting from radiation absorption.

Other types of detectors in this category are Golay detectors and photoacoustic detectors. For modern FT-IR spectrometers the most frequently used thermic detectors are pyroelectric detectors made of Triglycine Sulfate (TGS). They can

be used for both Mid and Near IR regions.

Another type are photoelectric detectors (quantum detectors) where the incident photons cause a certain quantum transition in a semiconductive material. Consequently, their sensitivities depend on the wavelength. The basic principle behind this kind of detectors is the internal photoelectric effect, whereby the phenomena of photoconductivity as well as photovoltage can be exploited for the detection of radiation.

In the Middle Infrared MCT (Mercury Cadmium Telluride) detectors are often used because they are much more sensitive than thermic detectors. However they have to be cooled with liquid nitrogen and may become saturated if too much radiation is impinging on them.

The standard photoelectric detector used in the NIR is the PbS (Lead Sulfide) detector. In this case Peltier cooling is sufficient.

2.3 Sampling

Sample preparation for solids in the Middle Infrared involves grinding the material to a fine powder and dispersing it in a matrix. The two most common matrix materials are mineral oil (Nujol) and Potassium bromide (KBr). Typically not more than 20 mg of solid is ground with one or two drops of nujol. This paste is applied on middle IR transparent windows, e.g. NaCl, KBr, etc. Potassium bromide is probably the most widely used matrix. Between 1 and 3 mg of sample is mixed with about 350 mg of ground KBr and this mixture is pressed into to the die at a pressure of about 12000 psi. This results into a disk which is can be analyzed by transmission (Fig. 2.8 on page 20). Liquids are traditionally analyzed as thin films in cells. A Mid IR cell consists of two IR transparent windows separated by a Teflon or lead (Pb) spacer with desired path length. In Near IR, these measurements are more convenient due to higher pathlengths (due to lower absorption coefficients) and mostly quartz cuvettes are used. Overall, sample preparation is easier for liquid transmission studies when compared to solids. Preparation of solid samples is facilitated by ATR accessories in the Middle Infrared and by Diffuse Reflectance in the Near Infrared.

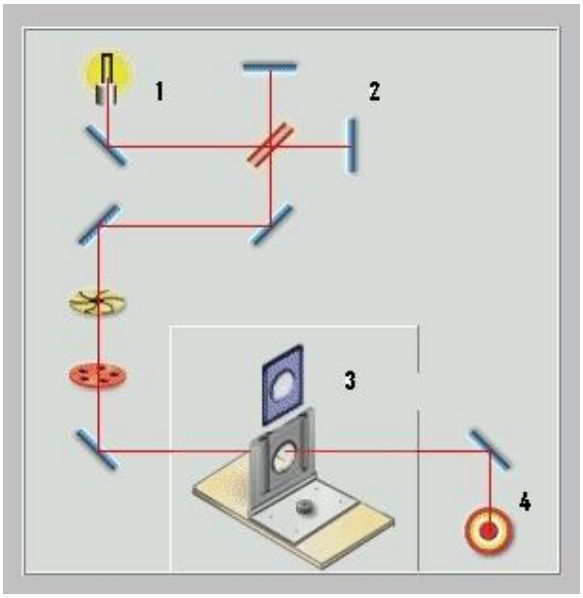

Figure 2.8: Schematic diagram of optical path for transmission measurements (both middle and near IR). 1) Source 2) Interferometer 3) Sample holder 4) Detector.

2.3.1 Attenuated Total Reflectance (ATR)

Attenuated total reflectance (ATR) is a convenient, versatile, non destructive technique for obtaining an Infrared spectrum which can be generally applied and is especially useful where materials are too thick or too strongly absorbing to be analyzed by transmission spectroscopy [47, 48]. In this technique, the sample is placed in contact to an external internal reflection element (ATR crystal). The light is totally reflected, one or several times, and the sample interacts with the evanescent wave resulting in the absorption of radiation by the sample at each point of reflection. The internal reflection element is made from a material with a high refractive index, e.g. KRS-5 (TlBrI), Zinc Selenide (ZnSe), Silicon (Si), Germanium (Ge) and Diamond (nowadays most widely used). To obtain total internal reflection the angle of incident radiation must exceed the critical angle θ_c which is defined as:

$$\theta_c = sin^{-1}\frac{n_2}{n_1} \tag{2.10}$$

Here n_1 is the refractive index of the internal reflection element and n_2 is the

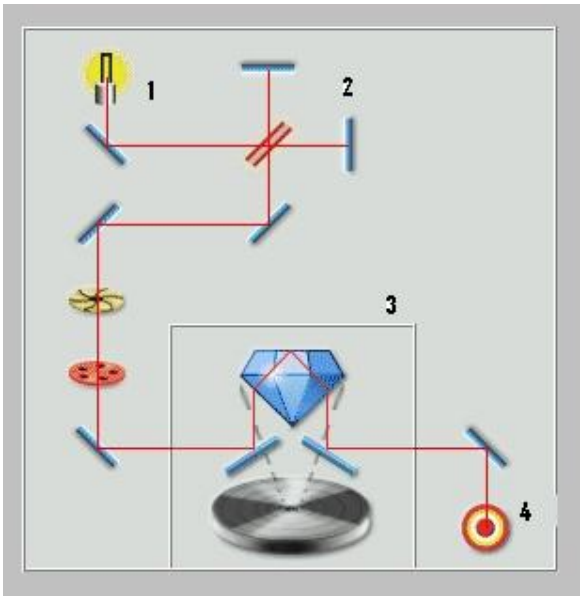

Figure 2.9: Schematic diagram of optical path for ATR measurements. 1) Source 2) Interferometer 3) ATR crystal and sample holder 4) Detector.

refractive index of the sample. The intensity of the resulting spectra is dependent on the penetration depth of the evanescent wave which decays exponentially into the sample with the distance from the surface of the ATR crystal. As the effective penetration depths into the sample is usually a fraction of the wavelength, total internal reflectance is independent from the physical sample thickness and so permits thick or strongly absorbing samples to be analyzed. The penetration depth d_p, is defined as the distance required for the electrical field amplitude to fall to e^{-1} of its value at the interface and is given by:

$$d_p = \frac{\lambda_1}{2\pi(sin^2\theta - n_{21}^2)^{1/2}} \tag{2.11}$$

where $\lambda_1 = \lambda/n_1$ is the wavelength in the denser medium, and $n_{21} = n_2/n_1$ is the ratio of the refractive index of the sample divided by that of ATR crystal. Although ATR and transmission spectra of the sample closely resemble each other there are differences due to the dependency of the penetration depth on the wavelength. The depth of penetration also depends on the angle of incidence. Further the degree of physical contact between sample and the ATR crystal determines the intensity of the ATR spectrum. Therefore liquids are ideally suited

for this type of analysis. Nevertheless, solids can be also analyzed by assuring good contact with help of applying external pressure. Due to the ease and speed of analysis we used extensively this method of sampling for our studies.

2.3.2 Diffuse reflection

When light is directed onto the surface of a solid sample, two types of reflections can occur: Specular reflection and diffuse reflection. The specular component is the radiation that reflects directly off the sample surface according to the normal reflection law where the angle of reflection is equal to angle of incidence. Diffuse reflection is the radiation that penetrates into the sample and then emerges at all angles after suffering multiple reflections and refractions by the sample particles. A Diffuse reflection accessory is designed so the diffusely reflected energy is optimized and the specular component is minimized (see Fig. 2.10 on page 23). Suitable optical devices are the gold integration sphere in the NIR and the praying mantis accessory in the Middle Infrared [47]. The theory of diffuse reflectance at scattering surfaces was derived by Kubelka and Munk in 1931 [49]. The Kubelka and Munk model relates the sample concentration to the intensity of the measured spectrum. The Kubelka and Munk function is given by:

$$f(R) = (1 - R^2)/2R = k \cdot c/s \tag{2.12}$$

Here R is the absolute reflectance of the sample, k is the molar absorption coefficient and s the scattering coefficient. The Kubelka-Munk theory predicts a linear relationship between spectral intensity and sample concentration under conditions of a constant scattering coefficient and infinite sample dilution in a non absorbing matrix. In the Mid Infrared Diffuse reflection can only be applied to samples diluted in a non absorbing matrix such as KBr or weakly absorbing matrix such as PVC. Due to the weaker molar absorption coefficients in the Near Infrared organic substances can be measured in the NIR without need for dilution or further sample preparation. This is one of big advantages of NIR over MIR. The measurements results however are not only influenced by the absorption coefficient but additionally by the scattering coefficient which is a function of particle size. The samples must therefore have a reproducible particle

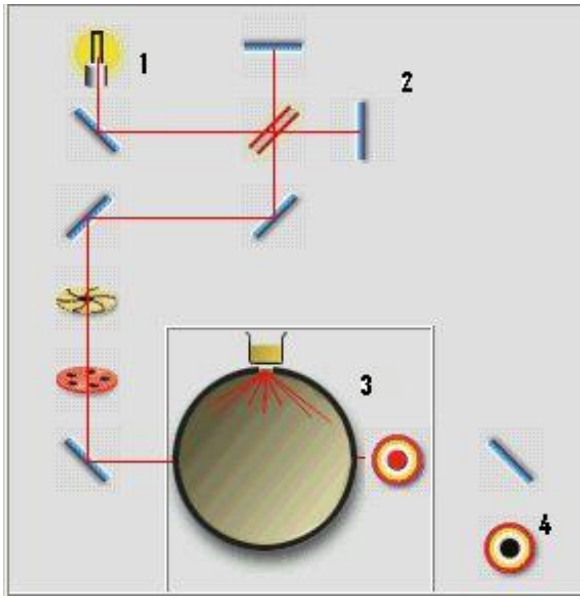

Figure 2.10: Schematic diagram of optical path for diffuse reflection measurements. 1) Source 2) Interferometer 3) Diffuse reflectance accessory 4) Detector.

size distribution, if quantitatively valid measurements are desired. Finally the Kukelka-Munk equation only applies to an infinitely thick sample layer, which in Infrared spectroscopy occurs at a sample thickness of approximately 3 mm. Typically, quantitative Diffuse reflection measurements are presented in log (1/R) units (as a useful approximation to Kubelka-Munk equation). Summarizing, the factors affecting Diffuse reflection data are:

- Refractive index of the sample and matrix
- Particle size and homogeneity
- Density of packing and concentration

The application of Diffuse reflectance is widely spread in the NIR while it is rarely used in the Middle Infrared.

2.4 Limit of detection, capture and quantification

If the aim of an analytical method like Infrared spectroscopy consists in determining small concentrations of an analyte in a matrix there arises always the question about the smallest detectable concentration. It is evident that the answer to this question is especially important in purity control. Therefore some definitions related to this problem are given in the following. These considerations cannot only be applied to the quantitative determinations of concentrations but in an analogous ways also to the spectral purity parameters developed in this thesis. All following definitions are in accordance with DIN 32645 [50, 51]. The parameters can be determined by two different methods, viz. the blank value method and the calibration line method.

2.4.1 Blank value method

The Limit of detection (LOD) is the smallest concentration or quantity x that can be detected with a specificity, i.e. false positive rate, of $1-\alpha$ where normally $\alpha = 0.05$ is chosen. When using the blank value method, the limit of detection is given by the upper limit of a one-sided prediction interval as follows:

$$x_{LOD} = \bar{x}_{bl} + k \cdot s_{bl} \tag{2.13}$$

$\bar{x}_{bl}$ and s_{bl} are the mean and standard deviation of the blank measurements respectively. A blank is a sample which does not contain the analyte but otherwise has the same matrix as usual samples. k is a numerical factor given as:

$$k = \Phi_t^{-1}(\alpha, df = n-1) \tag{2.14}$$

Φ_t^{-1} is the one-sided quantile of a t-distribution for probability $1-\alpha$ ("confidence level") and $n-1$ degrees of freedom, where n is the number of blanks measured.

The Limit of capture (LOC) is the smallest concentration or quantity x that can be detected with a specificity $(1-\alpha)$ and a sensitivity (true positive rate) of $(1-\beta)$, where $\alpha = \beta$. Due to this definition one can show that the limit of capture is the double of the limit of detection.

$$x_{LOC} = 2 \cdot x_{LOD} \tag{2.15}$$

2.4.2 Calibration line method

Here it is assumed that there is a linear relationship between the measured signals y and the concentration values x given by:

$$y = bx + a \tag{2.16}$$

which can be determined in a calibration step by linear regression. Further it is assumed that the usual prerequisites for such a least-squares regression hold, like normal distribution of the residuals and homoscedasticity of the y-values.

With the calibration line method the critical value y_{crit} for the measured signal values can be calculated with the ordinate segment a of the calibration curve and the width Δa of the one-sided prognosis interval at $x = 0$ [50, 51]:

$$y_{crit} = a + \Delta a \tag{2.17}$$

With m repetitive or parallel measurements with the analysis sample and n calibration samples one gets:

$$\Delta a = s_y.t_{f,\alpha}.\sqrt{\frac{1}{m} + \frac{1}{n} + \frac{\overline{x}^2}{Q_{xx}}} \tag{2.18}$$

with $t = \Phi_t^{-1}(\alpha, df = n-2)$ where Φ_t^{-1} is the one-sided quantile of the t-distribution for the probability $1-\alpha$ and $n-2$ degrees of freedom.

Q_{xx} is term coming from the linear regression and given by:

$$Q_{xx} = \sum_{i=1}^{n} x_i^2 - \frac{(\sum_{i=1}^{n} x_i)^2}{n} \tag{2.19}$$

With equations 2.17 and 2.18 we get:

$$y_{crit} = a + s_y.t_{f,\alpha}.\sqrt{\frac{1}{m} + \frac{1}{n} + \frac{\overline{x}^2}{Q_{xx}}} \tag{2.20}$$

Inserting this into the equation of the regression line $y = bx + a$ gives the limit of detection as follows:

$$x_{LOD} = \frac{s_y}{b}.t_{f,\alpha}.\sqrt{\frac{1}{m} + \frac{1}{n} + \frac{\overline{x}^2}{Q_{xx}}} \tag{2.21}$$

As in the blank value method the limit of capture is taken as the twofold value of the limit of detection:

$$x_{LOC} = 2 \cdot x_{LOD} \tag{2.22}$$

Further for quantitative analysis the limit of quantification (LOQ) is defined as the lowest concentration which can be determined with a relative error of 33%. This is approximately given by:

$$x_{LOQ} \approx 3 \cdot x_{LOD} \tag{2.23}$$

A more elaborate determination of the LOQ is described in DIN 32645 and explained in detail in an article published in the GIT Journal [51]. Corresponding **R**-code was developed in our department and used in this thesis.

3

Materials and software

In this chapter a brief description of the spectrometers, equipments, chemicals and software used in this study is given.

3.1 Materials

3.1.1 FT-IR Spectrometer

The spectrometer employed for obtaining spectra in Middle Infrared is the 'PerkinElmer-System 2000 FT-IR' from PerkinElmer Ltd, Buckinghamshire, England (see Fig. 9.1 in Appendix on 107). It is a versatile instrument having a scan range of 7500 - 350 cm^{-1}. Various accessories can be utilized for obtaining the spectra, e.g. ATR unit, Praying Mantis unit, etc. Other technical data are:

- Radiation source: Globar
- Detector: MIRTGS
- Interferometer type: Michelson interferometer
- Spectral range: 7500 to 350 cm^{-1}
- Optical resolution: 0.2 - 64 cm^{-1}

3.1.2 Diamond ATR Unit

An external Diamond ATR Unit from SensIR Technologies (now part of Smiths Detection Inc, USA) was employed. This unit has an option to select between multiple (see Fig. 5.3 on 49) and single reflection crystals (both of Diamond) (see Fig. 9.2 in Appendix on page 108). The multiple reflection unit (approx. with 6-9 internal reflections) is well suited for liquid samples and the single reflection unit for solid samples as it is equipped with a screw to apply force on the sample to have good contact between the crystal and the solid sample. Both have an angle of incidence of around 45°.

3.1.3 NIR Spectrometer

'PerkinElmer- Spectrum One NTS' from PerkinElmer Ltd, Buckhinghamshire, UK, is the instrument used for recording spectra in Near Infrared (see Fig. 9.3 in Appendix on page 108). It is equipped with a diverse range of accessories for measurements of solid (Diffuse reflection accessory) and liquid samples. The technical specifications of this instruments are as follows:

- Radiation source: Tungsten halogen lamp
- Detector: InGaAs
- Interferometer type: Michelson interferometer
- Spectral range: 15000 to 3500 cm^{-1}
- Optical resolution: 0.5 - 64 cm^{-1}

The Diffuse reflection accessory is ideally suited for measuring the spectra of solid samples. The sample is irradiated from below and the reflected radiation is collected by a spherical mirror and transmitted to the detector (see Fig. 2.10 on page 23).

3.1.4 Eracheck Spectrometer with QCL-IR technology

Eracheck from Quantared Technologies, Austria, is a bench top spectrometer with a quantum cascade laser as radiation source (Fig. 9.4 on page 109 in Appendix). It is specially manufactured for the measurement of very low concentrations of total petroleum hydrocarbons in water and in soil in the lab as well as in the field. The technical details of this device are:

- Radiation source: QC Laser, fixed wavenumber (between 1370-1380 cm^{-1})
- Precision: repeatability < 1 ppm
- Measuring time: 2 min
- Sample volume: 4 ml
- Sampling unit: Internal CaF_2-cuvette (Thickness ca. 2-3 mm)
- B x H x T: 220 x 320 x 280 mm

3.1.5 Auxiliary accessories

For weighing purpose the electronic balance AE 240 manufactured by Mettler-Toledo GmbH, Giessen, Germany (sensitivity 0.00001 g to 40 g) was used (Fig. 9.5 on page 109 in Appendix). The samples were stored in glass vials produced by SCHOTT DURAN, Mainz, Germany (Fig. 9.6 on page 110 in Appendix).

The measurements of solutions in Middle Infrared and Near Infrared were carried out in a CaF_2 cell (PerkinElmer, varying thickness by using spacers) and quartz cell (Hellma, 1 mm thickness) respectively (Fig. 9.7 on page 111 in Appendix). Transfer of samples from the vials to the diamond crystal and quartz cell was accomplished by Eppendorf pipettes. Cleaning of the diamond crystals and the cuvettes was done by Tetrahydrofuran (THF), Merck, Darmstadt, Germany. The rest of the chemicals used will be discussed in Chapters 5 and 6 along with their spectra.

For uniform mixing of solids to simulate contamination, a Vibratory Micro-Mill "Pulverisette 0", Fritsch GmbH, Idar-Oberstein, Germany was employed. (Fig. 9.8 on page 111 in Appendix)

3.2 Software

3.2.1 Software for acquiring spectra

The system 2000 FT-IR spectrometer is operated by software called 'Spectrum version 5.3', a proprietary software of PerkinElmer Inc. Spectrum One NTS is operated by 'Spectrum One version 3.02.01' also from PerkinElmer. All the spectra are obtained .sp format (a special format of PerkinElmer). This format is only readable with the 'Spectrum' software. To be generally readable the obtained spectra are converted and saved in ASCII format (American Standard Code for Information Interchange) with help of 'QUIRA' software [52].

3.2.2 Software for analysis of spectra

The aim of this thesis was to develop new methods and algorithms for the purpose of purity control. Because no commercial or public software suitable for this purpose was available it was decided to write our own programmes using the programming language **R**.

R is a language and environment for statistical computing and graphics [53]. It is a GNU project which is similar to the S language developed at Bell Laboratories (formerly AT&T, now Lucent Technologies) by John Chambers and colleagues. Similar as in Matlab [54] inherent in **R** there are a lot of operators for direct calculations on arrays and matrices which is important for handling of spectral data.

R software is freely available for download and runs in various environments, e.g. Windows, Unix, Linux and Macintosh.

All **R**-programmes (codes) were written using a special editor named **Tinn-R**. **Tinn-R** is a feature-rich replacement of the basic script editor provided within the **R**-gui [55]. It provides syntax-highlighting, submission of code in whole, or line-by-line, and many other useful tools to ease developing the **R**-code. The written algorithms can be directly sent to the **R**-console for evaluation and display of results.

Before further processing of the spectral data transmittance values (%T) are transformed to absorbance values. Two features of **R** were especially useful for

our purposes. One was the "*lm*-function" by which linear regression can be performed easily and which we utilized for calculating the correlation coefficients. Another was the PLS-package. This is a programme library by Ron Wehrens and Mevik [56] which we used for performing quantitative Partial-Least-Squares-Analysis of the spectral impurities in our experimental model systems. Some of the developed **R**-programmes are listed in the Appendix.

4

Development of spectral purity parameters and a simulated example

The main objective of this thesis was to find generally applicable methods for comparing the spectrum of a substance containing impurities with the reference spectrum of the pure substance and thereby confirming the presence of impurities. The other objective in this context is to find suitable parameters for describing the degree of impurities which can be applied in process environments in a simple, fast and efficient way. In order to achieve this goal, suitable robust parameters should be derived and formulated. The most promising parameters are based on "Linear regression" and "Difference spectroscopy".

4.1 Spectral purity parameters based on linear regression

Linear regression is probably one of the most widely used and useful computational technique in analytical chemistry. Regression analysis utilizes the relation between two quantitative variables so that one variable can be applied to predict the another. The variable which is to be predicted is called the response or dependent variable and the variable predicting it, is termed as explanatory or

independent variable. Relationship between variables can be either functional or statistical. A functional relationship is exactly defined, while a statistical relationship has random errors associated with it. Regression analysis servers three purposes:

- Description
- Control
- Prediction

The simple linear regression function is expressed as:

$$Y_i = \beta_0 + \beta_1 X_i + \epsilon_i \tag{4.1}$$

In this model β_0, β_1 are parameters, ϵ_i is the random error and Y, X are measured values. This is called a "first order model" because it is linear in both the parameters and the independent variable. In order to to derive the first spectral purity parameter (SPR_1), the sample spectrum X is regressed onto reference spectrum Y and the correlation coefficient (r) is calculated. If two spectra originate from the same substance they may differ only by their intensities ($\beta_1 \neq 1$) and their baseline ($\beta_0 \neq 0$) and apart from that and some noise are identical and the correlation coefficient is close to 1. Both baseline shifts and intensity changes of the spectra do not influence the correlation coefficient.

4.1.1 Correlation coefficient

The correlation coefficient is a measure of the strength of relationship between the variables X and Y. The population correlation between these variables is defined as:

$$\rho_{X,Y} = \mathrm{corr}(X,Y) = \frac{\mathrm{cov}(X,Y)}{\sigma_X \sigma_Y} = \frac{E[(X-\mu_X)(Y-\mu_Y)]}{\sigma_X \sigma_Y} \tag{4.2}$$

ρ is called the product moment correlation coefficient or Pearson's correlation coefficient. The sample value is called as correlation coefficient r and computed according to the equation:

$$r = \frac{\sum_{i=1}^{N}[(x_i - \bar{x}).(y_i - \bar{y})]}{\sqrt{\sum_{i=1}^{N}(x_i - \bar{x})^2 . \sum_{i=1}^{N}(y_i - \bar{y})^2}} \tag{4.3}$$

It can take values between -1 and +1. The sign (- or +) indicates the direction of the relationship. A positive sign indicates that as one variable gets larger the other also tends to get larger, while a negative sign indicates that as one variable gets larger the other tends to get smaller. The magnitude of the correlation describes the strength of the relation. The further that a correlation is from zero, the stronger the relation is between the two variables. A zero correlation would indicate that the two variables aren't related to each other at all.

Cohen established a set of guidelines for interpreting the strength of correlations [57]. He claimed that a correlation of 0.1 is a "small" effect, a correlation of ≥ 0.3 is a "medium" effect, and that of a correlation of 0.5 is a "large" effect. Cohen stated the "medium" effect size to be one that was large enough so that people would naturally recognize it in everyday life, the small effect size to be one that was noticeably smaller but not trivial, and the large effect size to be the same distance above the medium effect size as the small effect size.

Based on the correlation coefficient r, the first parameter for spectral purity is computed by the following equation:

$$\mathbf{SPR_1 = r \times 100} \tag{4.4}$$

The main advantage of this approach is that the correlation coefficient r is unaffected by baseline shifts and intensity changes. However, r does not supply a scale of equal units of detectability of deviations. Consequently, an equal difference in r of 0.001 is easier to detect between $r_1 = 0.998$ and $r_2 = 0.999$ than between $r_3 = 0.980$ and $r_4 = 0.981$. This discrepancy is due to the result of a non normal distribution of r values approaching 1.

In order to demonstrate this, a simulated example was performed as in Fig. 4.1 on page 35. Here A is assumed to be the spectrum of one (hypothetical) concentration unit of pure substance A, and B is the spectrum of one concentration unit of a substance B. Substance B is used for inducing impurities into the substance A. The B′ curves show the spectra of substance B in concentrations between 0.001 and 0.1 with increments of 0.001 units. The B′ spectra were added to spectrum A to simulate increasing contamination. The resultant spectra are designated with C and are assumed to be spectra of substance A containing different amounts of impurity B. The spectra C were in addition overlaid with white

noise of amplitude 0.001. r values were calculated by regressing the spectra C against the reference spectrum A. The result is shown in Fig. 4.2 on page 36. From this figure it can be seen that at the onset of the contamination the r values move away very slowly from 1 (the curve shows convex behavior).

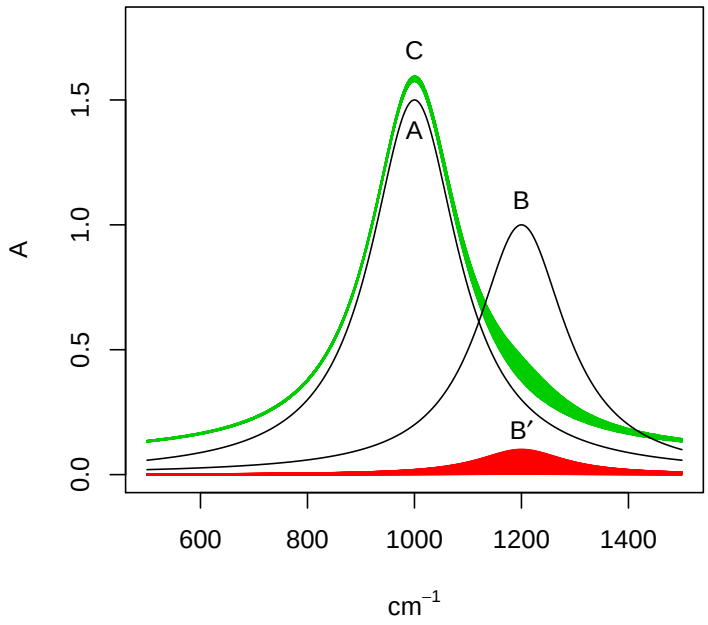

Figure 4.1: Simulated example for calculating r and z values. A and B are the spectra of one (hypothetical) concentration unit of the components A and B. B is added to the component A in steps of 0.01-0.1 concentration units (spectra B′). C shows the corresponding mixtures, onto which slight noise (amplitude 0.001) was imposed.

4.1.2 Distribution of r

When performing experiments for determining the correlation coefficient, the population correlation (ρ) is usually not known. Therefore, the sample statistic r is used to estimate ρ and to carry out tests of hypotheses or calculate confidence intervals which rest on statements of probability. For example, we might say that

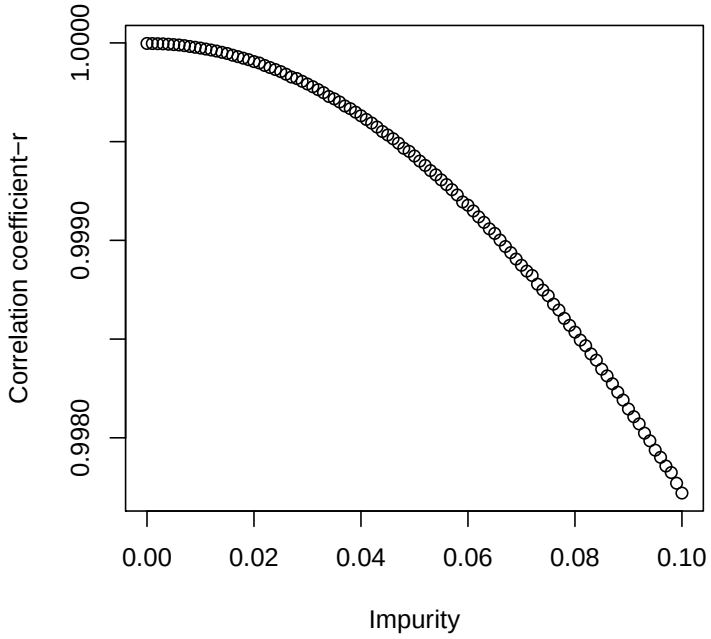

Figure 4.2: Dependency of the correlation coefficient r from the degree of contamination.

an observed value of r of 0.3 is very unlikely if $\rho = 0$. In our case if we compare the spectral correlation of a pure substance and a slightly impure sample of this substance with the corresponding reference spectrum we have to test if correlation coefficients which are quite similar and close to 1 still are significantly different. For being able to perform such a test r should be normally distributed.

But now let's look at the sampling distribution of r. Recall that r is bounded by +1 and -1, i.e. it can take no larger or smaller values. When $\rho = 0$, r is distributed around 0 symmetrically, and the mean of the sampling distribution does equal ρ. As ρ increases from zero (becomes more positive), the sampling distribution becomes negatively skewed. This is also the reason of the unsymmetric histogram (Fig. 4.3 on page 37) of the correlation coefficients obtained by the experiment in Fig. 4.1 on page 35. As ρ approaches +1 or -1, the sampling variance decreases, so that when ρ is either at +1 or -1, all sample values equal

ρ and the sampling variance is zero. This means that as $\mid \rho \mid$ approaches 1, the sampling variance approaches zero. The consequence of all this is that the direct use of r is not the optimal way for testing significant differences between very similar spectra.

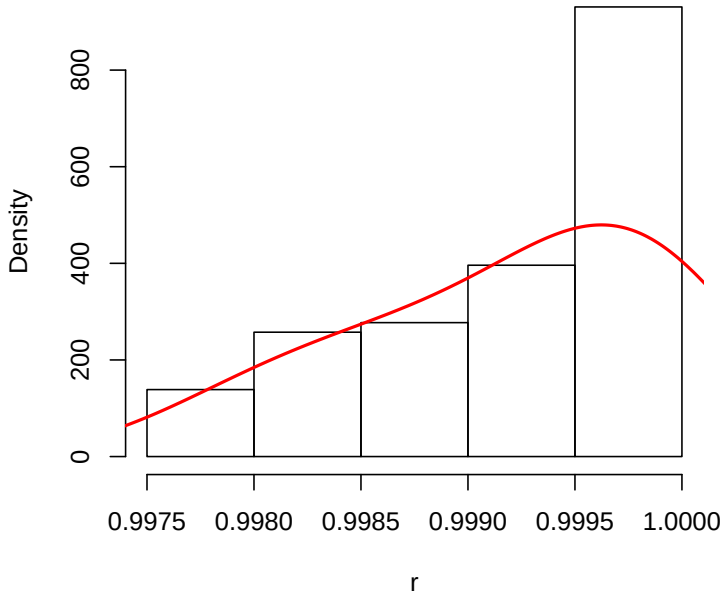

Figure 4.3: Histogram of r values calculated by regressing the spectra of mixtures C in Fig. 4.1 on the reference spectrum A.

4.1.3 Fisher's z transformation

Fisher developed a transformation of r to a parameter called z that tends to become distributed normally quickly as the sample size increases. This is also the reason why the histogram of the z-values in Fig. 4.5 becomes more symmetrical compared to Fig. 4.3. This transformation is called the r to z transformation, and z is termed as Fisher's z coefficient [58].

$$z = \frac{1}{2} \times \ln \frac{1+r}{1-r} \tag{4.5}$$

When this transformation is applied to the r values obtained from the simulation experiment (Fig. 4.2 on page 36) we get a concave behavior as shown in Fig. 4.4 on page 38, which implies that the first contamination steps cause the largest effects. This property of z is very favorable if the aim is to detect small impurities. A further advantage of z is that its variance is maintained as r approaches 1 [59, 60]. This can be seen in Fig. 4.6(b) on page 43. The z values as such can be

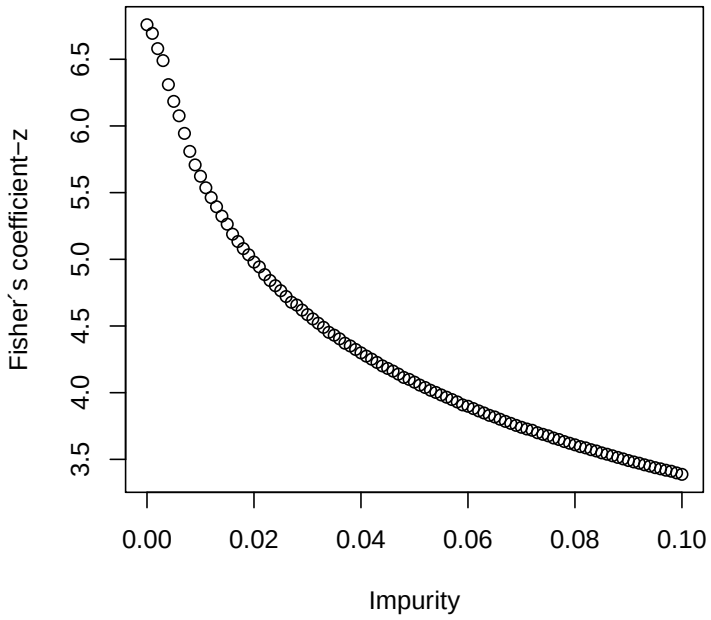

Figure 4.4: Dependency of the Fisher's coefficient z from the degree of contamination.

used as a parameter for purity by determining the threshold value[1], below which the z values are considered to originate from an impure sample. For obtaining a generalized parameter useful for quantification of purity the following 2-step normalization is performed. At first, repetitive measurements of the spectra of the pure substance are performed and from these a mean spectrum is calculated.

[1] A simulated example for the calculation of the threshold value z_{crit} is given in section 4.3.1 on page 41.

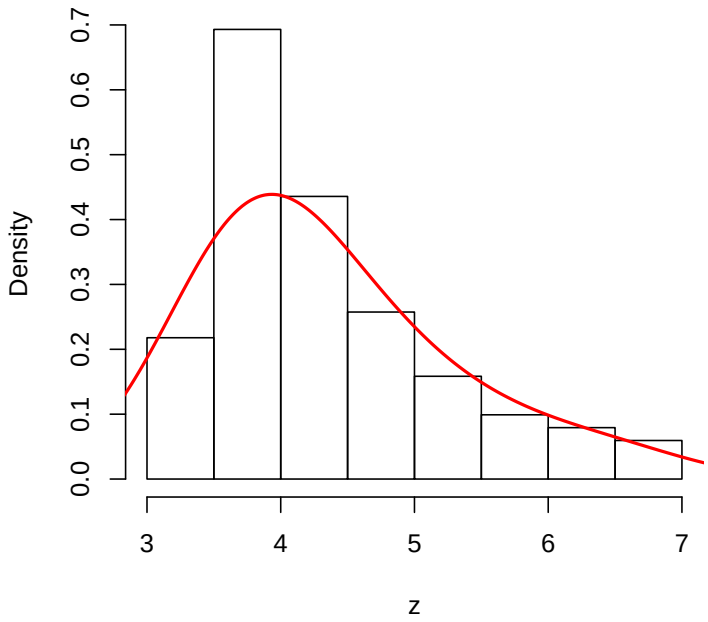

Figure 4.5: Histogram of z-values calculated by transforming the r-values of the Fig. 4.3.

Then each single spectrum is compared with this mean spectrum. From the resulting z-values a one-sided confidence interval for z is determined. Its lower limit is the critical z-value and calculated as:

$$z_{crit} = \bar{z_{bl}} - ts_{z,bl} \tag{4.6}$$

with $t = \Phi_t^{-1}(\alpha, df = n - 1)$ and $\alpha = 0.05$, where Φ_t^{-1} are the one-sided quantile of the t-distribution. The index bl stands for the fact that the critical z-value is determined from spectra of the pure substance A ("blanks"). In the second step the z values are normalized by dividing with z_{crit}:

$$z' = \frac{z}{z_{crit}} \tag{4.7}$$

The corresponding spectral purity parameter is then calculated by the following equation:

$$\mathbf{SPR_2} = \mathbf{z'} \times \mathbf{100} \tag{4.8}$$

4.2 Spectral purity parameters based on difference spectroscopy

The principle of difference spectroscopy is simple and the results sensitive to small changes in the shapes and positions of the bands caused by impurities. It means simply a subtraction of the reference spectrum Y from the sample spectrum X. Prior to subtraction the reference spectrum is multiplied with a factor f.

$$D = X - f \times Y$$

D is the difference spectrum. By visual or computer-aided inspection of this spectrum, there is a chance of detecting the chemical nature of the impurity present in the sample. The factor f is chosen in such a way that an optimal compensation of the reference is obtained. This optimal factor is termed as f_{opt} and is used for deriving the spectral purity parameter SPR_3:

$$\mathbf{SPR_3 = f_{opt} \times 100} \tag{4.9}$$

Another way is utilizing the obtained difference spectrum (D) as spectral purity parameter is by integrating the difference spectrum and dividing it with the integrated spectrum of Y.

$$\mathbf{SPR_4 = (1 - \frac{\int D}{\int Y}) \times 100} \tag{4.10}$$

4.3 Testing the spectral purity parameters SPR_1 and SPR_2 with a simulated example

Before applying the above discussed purity parameters to the measured spectra, one of the best way to find out their practical applicability and limitations is that of a simulation. A simulated example was developed analogous to the example stated in Fig. 4.1 on page 35.

The only difference is that the reference spectrum of the pure substance A is now calculated as the mean of 9 single spectra of A on which random noise with an amplitude of 0.001 was superimposed. These nine spectra are regarded to

originate from blanks of A and by regressing them on their mean (reference spectrum) the critical z-value due to equations 4.6 and 4.7 on page 39 is calculated. As already mentioned, two spectral purity parameters are determined from the regression (see Fig. 4.1 on page 44):

$$\mathrm{SPR}_1 = \mathrm{r} \times 100$$

$$\mathrm{SPR}_2 = \mathrm{z}' \times 100$$

Diagrams for SPR_1 and SPR_2 vs concentration of impurity were plotted in Fig. 4.6(a) and Fig. 4.6(b) on page 43. The threshold for SPR_1 was derived from the conversion of z_{crit} to r_{crit} and multiplying this with 100.

$$r_{crit} = \frac{e^{2z_{crit}} - 1}{e^{2z_{crit}} + 1} \tag{4.11}$$

4.3.1 Limit of detection (LOD) and limit of capture (LOC) for the impurity

If we take z as a measure for the purity of the sample we can determine the limit of detection by measuring blank values in an analogous way to section 2.4.1 on page 24 and calculating:

$$z_{crit} = \bar{z}_{bl} - k \cdot s_{z,bl} \tag{4.12}$$

The minus sign in the equation is due to the fact that z is decreasing with increasing concentration of the impurity. $\bar{z}_{bl}$ is the mean of the nine z-values obtained by comparing the blanks with the reference spectrum and $s_{z,bl}$ is the corresponding standard deviation. k is the one-sided quantile of the t-distribution for probability $(1 - \alpha)$ and $n - 1$ degrees of freedom:

$$k = \Phi_t^{-1}(\alpha, df = n - 1)$$

Then the concentration of the impurity corresponding to z_{crit} is the limit of detection.

The purity parameter SPR_2 is calculated as $SPR_2 = z' \times 100$ where $z' = z/z_{crit}$. To find the detection limit of the method one has to locate the concentration corresponding to $SPR_2 = 100$. This is shown in the Fig. 4.6(b) on page 43.

How is this performed mathematically? We use a numeric solution. The r values obtained by linear regression of each spectrum of the blanks and the samples B on the reference spectrum are subjected to quadratic regression with weighting coefficients (1/(1-r)) using the *'lm'* function of **R**. With this regression model the fitted curve (red color) of Fig. 4.6(a) on page 43 is obtained. The data values of this curve are then transformed to z respectively SPR_2 values as described above. The detection limit then can be found easily as the concentration value closest to $SPR_2 = 100$.

In addition to $\alpha = 0.05$ for the limit of capture (LOC) an additional constraint of $\beta = 0.05$ has to be considered. z can be regarded as being approximately homoscedastic (see Fig. 4.6(b) on page 43) and in this case the z value corresponding to the limit of capture is:

$$z_{crit,LOC} = \bar{z}_{bl} - 2k \cdot s_{z,bl} \tag{4.13}$$

After transforming this to the corresponding SPR_2 value the LOC can be determined numerically in the same way as before for the LOD. The result is shown in the Fig. 4.6(b) on page 43.

For this simulated example, a limit of detection of 0.0018 conc. units and limit of capture of 0.0025 conc.units were obtained by the spectral purity parameter SPR_2 described above.

4.3.2 Influence of noise on limits of detection and capture

This simulation also presents an opportunity to analyze the influence of random noise on the LOD and LOC. For this purpose white noise imposed on the simulated spectra (both standards and blanks) was linearly increased between amplitudes of 0.0002 to 0.04. The obtained values for the limit of detection (LOD) and limit of capture (LOC) were plotted against the noise amplitude in Fig. 4.7 on page 43. From this graph it can seen that noise has a direct strong linear influence on these parameters. As the noise increases the LOD and LOC will increase. So, in order to attain low LOD and LOC values care has to be exercised to provide for high signal-to-noise ratio(S/N) and also avoid artifacts which cause spurious noise.

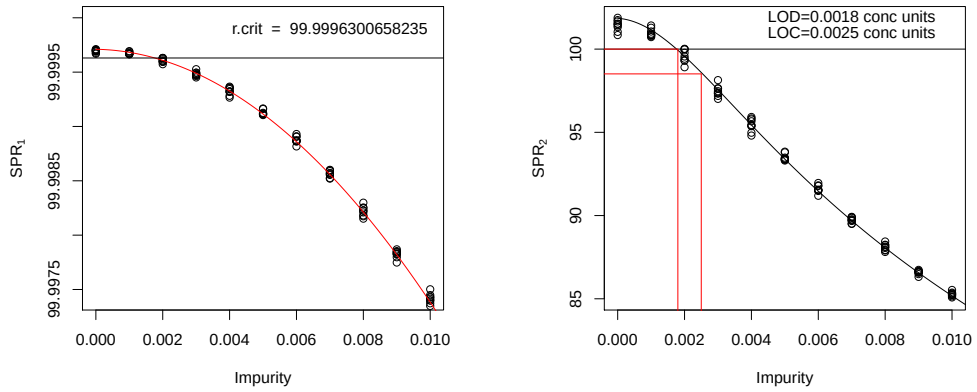

(a) Dependency of the Spectral purity parameter SPR_1 from the degree of contamination.

(b) Dependency of the Spectral purity parameter SPR_2 from the degree of contamination.

Figure 4.6: Results obtained by regressing the spectra of the mixtures C on the reference spectrum A. The impurity concentrations belonging to z_{crit} and $z_{crit,LOC}$ corresponds to LOD and LOC respectively.

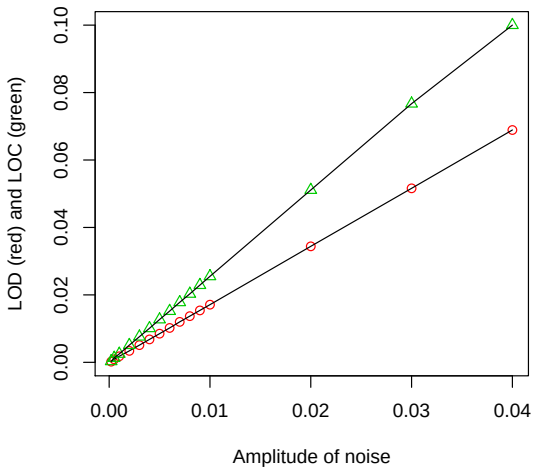

Figure 4.7: Limit of detection (LOD) and limit of capture (LOC) as function of noise.

Table 4.1: Results of the simulated example: Spectral purities SPR_1 and SPR_2 of spectra (A) as a function of the concentration of an impurity (B)

$CONC$	SPR_1	SPR_2	$CONC$	SPR_1	SPR_2
0	99.9997061	101.743749	0.005	99.9991111	93.3587656
0	99.9996969	101.50857	0.005	99.9991253	93.4807658
0	99.9996933	101.419046	0.005	99.9991163	93.4035942
0	99.9996893	101.322214	0.005	99.9991183	93.4205615
0	99.9996774	101.036033	0.005	99.9991164	93.4042938
0	99.9997114	101.881662	0.006	99.9988723	91.5559738
0	99.9996977	101.530424	0.006	99.9988675	91.52423
0	99.999703	101.663546	0.006	99.9988689	91.5332567
0	99.9996691	100.845082	0.006	99.9989305	91.9577422
0.001	99.999669	100.843028	0.006	99.9989101	91.8146598
0.001	99.9996637	100.721899	0.006	99.9988607	91.4787877
0.001	99.9996933	101.419162	0.006	99.9989051	91.7796163
0.001	99.9996725	100.924	0.006	99.9988678	91.5259681
0.001	99.9996877	101.283116	0.006	99.9988165	91.1904755
0.001	99.9996663	100.780515	0.007	99.9985247	89.5210603
0.001	99.9996693	100.848617	0.007	99.9985897	89.8622872
0.001	99.9996698	100.859666	0.007	99.9985545	89.675293
0.001	99.9996783	101.057359	0.007	99.9985204	89.4988239
0.002	99.9996299	99.9965513	0.007	99.998601	89.9228952
0.002	99.9996291	99.9805194	0.007	99.9985678	89.7452645
0.002	99.9995729	98.9116272	0.007	99.9985729	89.7723097
0.002	99.9995949	99.3122009	0.007	99.9985606	89.707564
0.002	99.999631	100.018541	0.007	99.9985976	89.904936
0.002	99.9996191	99.7777553	0.008	99.9981815	87.9365872
0.002	99.9996079	99.5592099	0.008	99.9982989	88.4418934
0.002	99.9996008	99.4240317	0.008	99.9981738	87.9045975
0.002	99.9995951	99.3164764	0.008	99.9982252	88.1206223
0.003	99.9994745	97.341085	0.008	99.9982274	88.1301887
0.003	99.9994737	97.3296138	0.008	99.9982093	88.05321
0.003	99.9994776	97.3851559	0.008	99.9981519	87.8140707
0.003	99.9994936	97.6209077	0.008	99.9982546	88.2471298
0.003	99.9994512	97.0115632	0.008	99.99825	88.2272076
0.003	99.9994835	97.4710745	0.009	99.9978533	86.6795608
0.003	99.999527	98.1374789	0.009	99.9977482	86.317427
0.003	99.9994638	97.1886227	0.009	99.9978226	86.5720111
0.003	99.9994958	97.6537587	0.009	99.9978695	86.7368488
0.004	99.9993208	95.3970225	0.009	99.9978321	86.6049299
0.004	99.9993444	95.6646827	0.009	99.9978272	86.587851
0.004	99.9993663	95.9226427	0.009	99.9978419	86.6394213
0.004	99.9992822	94.9781619	0.009	99.9978457	86.652817
0.004	99.9992657	94.8065338	0.009	99.9977969	86.4829572
0.004	99.9993184	95.3703711	0.01	99.9973985	85.223757
0.004	99.999359	95.8354341	0.01	99.9973492	85.0814768
0.004	99.9993538	95.7747066	0.01	99.9974485	85.3709815
0.004	99.9993246	95.4400161	0.01	99.997373	85.149935
0.005	99.9991609	93.7953104	0.01	99.9974267	85.3062766
0.005	99.999105	93.3074014	0.01	99.997502	85.5312218
0.005	99.9991657	93.8388427	0.01	99.9974326	85.3236526
0.005	99.9991108	93.3565958	0.01	99.9973994	85.2264847
			0.01	99.9974144	85.2703838

5

Application of the developed spectral purity parameters to experimental models

After having developed parameters relevant for purity control and tested them with a simulated example (see Chapter 4), the next step is to apply these methods to the spectra of real samples and check their applicability and suitability in process environments, which means minimal human interaction. For this purpose sampling methods must be fast, convenient and should demand minimal sample preparation. Versatile IR accessories like Diamond ATR units (Middle IR) and Diffuse reflection units (Near IR) fulfill these requirements and were subsequently used in this study. These accessories are also appropriate for online purity control [61, 62].

For performing a purity control the spectrum of a sample from a potentially contaminated material has to be compared with a reference spectrum, i.e. a spectrum of the pure material to check if there are significant spectral deviations. The potential impurity usually is not known in advance but if it is Infrared active there are good chances that it will be discovered already at relatively low concentrations, which will be demonstrated by the experiments described in this and the following sections. In these experiments to imitate a contamination, to a pure compound there are added small amounts of another compound which serves as 'impurity'. Because in these model experiments the substances causing the

contamination are known, critical concentrations (i.e. LOD/LOC) with respect to the detectability of these impurities can be determined. Also the amount of the impurity causing the contamination can be quantitatively analyzed.

5.1 Purity control of Palatinol-N

Palatinol-N is a phthalate plasticizer with the chemical name Diisononyl Phthalate. Palatinol is a registered trade name of BASF AG, Germany. The structural formula and other physical and chemical properties are shown in Fig. 5.1(a) and Table 5.1 on page 47 respectively. In this model experiment, Palatinol-N forms the pure substance and the samples whose purities are to be determined, are prepared by addition of other plasticizers and a phosphate flame retardant. These are impurities chosen in a particular way so that one differs mainly in the finger print region (1800-400 cm^{-1}), another mainly in the C-H stretch region (3200-2800 cm^{-1}) and a third in both of these regions. These choices of contaminants allows to test the purity parameters and thereby to prove their versatility of use and general applicability.

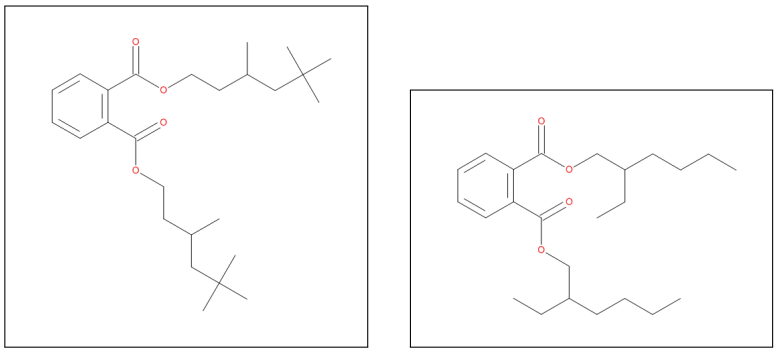

(a) Molecular structure of Palatinol-N.

(b) Molecular structure of Palatinol-AH.

Figure 5.1: Molecular structures of Plasticizers used for the model experiments.

In the first experiment, the impurity chosen to simulate a contamination in the samples is Palatinol-AH (Dioctyl Phthalate) (Fig. 5.1(b)). This compound has very similar physical and chemical characteristics to that of Palatinol-N. Since it has nearly the same density it forms homogeneous binary solutions when an

Table 5.1: Chemical and physical properties of Palatinol-N and Palatinol-AH

Specifications	Palatinol-N	Palatinol-AH
Formula	$C_{26}H_{42}O_4$	$C_{24}H_{38}O_4$
Mol. Wt	418	391
Refractive index n_D^{20}	1.484	1.482
Density at 20°C (g/ml)	0.970-0.977	0.980-0.984

addition is made to Palatinol-N. Such a kind of impurity could be detected, e.g. with HPLC, but spectroscopic methods are much faster and easier to handle than the chromatographic methods, making them favorable and suitable in process environments.

5.1.1 Spectral purity control employing Middle IR Palatinol-AH as impurity in Palatinol-N

When a visual spectral comparison of Palatinol-AH is performed against the spectrum of Palatinol-N, one notices only minor spectral deviations in the fingerprint region of 1400-750 cm^{-1}. So, e.g. a sample contaminated with 10 g/100 g of impurity Palatinol-AH shows very small spectral deviations from Palatinol-N. This is shown in Fig. 5.2 on page 48. These deviations are so minute that a lot of expertise would be needed to differentiate and interpret them visually.

5.1.1.1 Preparation of samples

In order to imitate the contamination, ten samples were prepared by addition of Palatinol-AH. Approximately 1 g of Palatinol-AH was added to a clean empty vial, then Palatinol-N is used to make up to the weight of 10 g approx., so that a concentration of 1 g/100 g obtained. This procedure is followed analogously to prepare the rest of the samples in order to have a desired range of concentration between 1 g/100 g - 10 g/100 g of Palatinol-AH in Palatinol-N.

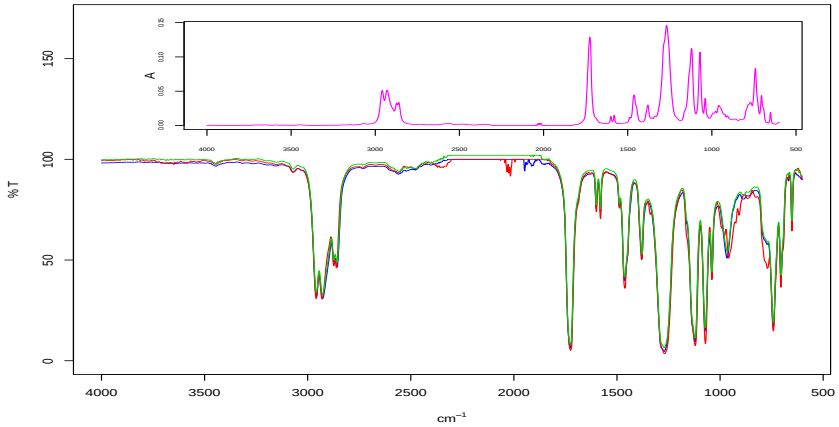

Figure 5.2: MIR spectra of pure Palatinol-N (blue), pure Palatinol-AH (red) and sample of Palatinol-N with 10 % Palatinol-AH (green).The negative bands due to total absorption by the diamond crystal are removed. The upper inserted graph is the optimal difference spectrum in absorbance.

5.1.1.2 Recording of spectra

The spectra were acquired using a PerkinElmer 2000 FT-IR spectrometer. The sampling unit used is an external ATR unit from SensIR-Technologies. After initialization, the instrument was set to the specifications mentioned in the Table 5.2 on page 49. A background spectrum was recorded and then the sample was pipetted onto the trough of the diamond crystal (Fig. 5.3 on page 49). Three spectra in sequence were acquired and subsequently the sampling area (trough) was cleaned thoroughly with Tetrahydrofuran (THF). Care was taken, so that no sample or THF is remaining on the crystal which can be checked by the monitoring function of the instrument (Fig. 5.4 on page 50). Then the same sample was again placed in the trough and the next three spectra were obtained. This procedure of cleaning and placing the sample and obtaining three spectra is once again repeated, so that a total of nine spectra for each individual sample were acquired. The instrumental settings were held constant during all the measurements of the samples. Nine spectra from the pure Palatinol-N were also obtained in an analogous way, the average of which forms the reference spectrum of the Palatinol-N.

Table 5.2: Instrumental specifications for recording spectra.

Specifications	Value
No. of scans	32
Digital resolution	1 cm^{-1}
Optical resolution	4 cm^{-1}
J-stop wavenumber	4000 cm^{-1}
J-stop image size	4mm
Units	%T

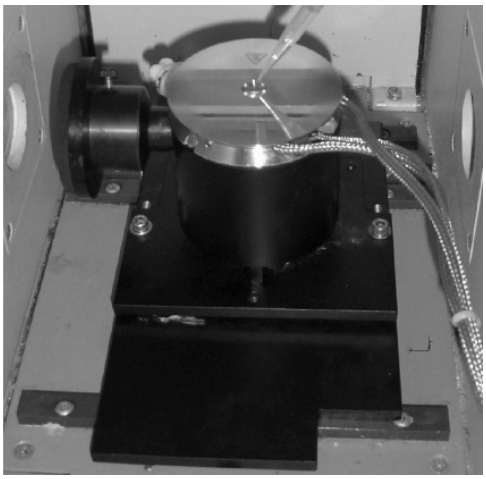

Figure 5.3: Multiple reflection Diamond ATR unit and sampling pipette. Only about 100 μL of liquid sample is required to obtain a spectrum.

5.1.1.3 Analysis of spectra by calculating spectral purity parameters

First it will be discussed how the purity can be checked with difference spectroscopy. Difference spectroscopy means in our case that from the spectrum X of contaminated sample the spectrum Y of the reference spectrum of the pure substance is subtracted after multiplication with a factor f:

$$D = X - f \times Y$$

All operations have to be performed in absorbance. The size of the factor f determines how strong the reference is compensated in the difference spectrum. Although the principle of difference spectroscopy is simple, the determination of

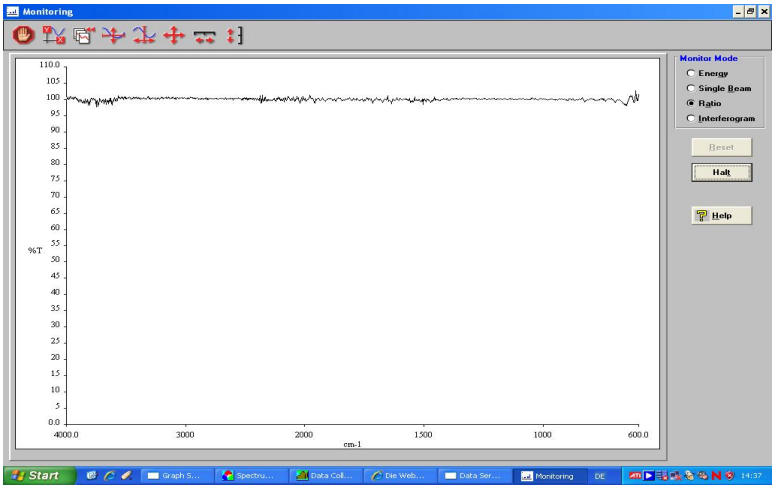

Figure 5.4: Monitor function of the software to control cleanliness of the crystal. Since the transmission is very close to 100 % over the whole spectral range the crystal is assumed to be free from residual chemicals.

the optimal factor f is tedious and has to be accomplished manually in standard application software like, e.g. Spectrum for Windows^{TM}. "Optimal" in this respect means that the reference spectrum Y is compensated completely in the difference spectrum leaving no traces of its presence.

In order to calculate f_{opt} automatically a specific algorithm ("Dynamic Difference Spectroscopy") was developed. This works by calculating a whole series of difference spectra with f increasing from -1 to $+2$ in steps of 0.001. For each value of f a difference spectrum is calculated which means that a total of 3001 difference spectra are calculated for each individual sample. The first difference spectra show strong undercompensation, i.e. only positive absorbances appear. But with increasing f gradually the true difference spectrum evolves and with a further increase of f overcompensation starts leading to negative absorbances in the difference spectrum. The aim of the algorithm is to find the state where there is neither under- nor overcompensation, i.e. the f value which is closest to a perfect compensation (f_{opt}). The finding of f_{opt} is performed with the following procedure. The negative part of the difference spectrum is integrated by summing up all negative absorbance values:

$$\chi = \int D^{-}$$

For low values of f we have only positive values in the difference spectrum, i.e. $\chi = 0$. But as f increases gradually negative values due to overcompensation will appear in the difference spectra. The optimal factor f_{opt} is at the transition between under- and overcompensation.

For finding this one could look at the plot of χ against f. However to see the limit in a more sharp and distinct way, the second order derivative of χ is calculated numerically by applying the R-function `diff(Chi,differences=2)`. Thereby differences of χ caused by a small increment of f are strongly amplified. The result is shown in Fig. 5.5. This plot of Diff2 vs f is called "Difference Operating Characteristic (DOC)".

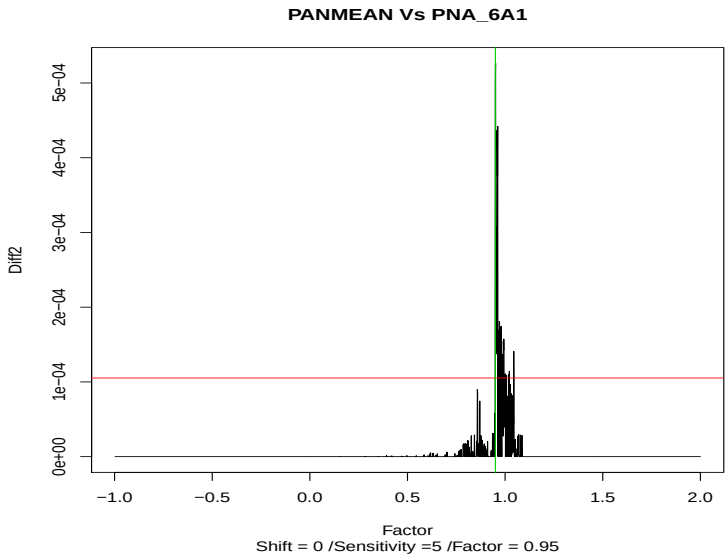

Figure 5.5: Difference Operating Characteristic-Plot. The red line characterizes the threshold for Diff2, the green line shows the optimal factor f_{opt}.

The transition between under- and overcompensation, i.e. the position where Diff2 becomes positive is now very sharp and distinct and a threshold can be set. This threshold is set at a fraction of the maximum of Diff2.

This fraction is set to 1/Sensitivity, where the default value for sensitivity is 100. The factor at the position where Diff2 is equal to the threshold gives us the factor value 'f_{opt}' we are looking for. However at this position of Diff2, a small degree of overcompensation may have already occurred. To correct for this we can

decrease the factor by a few steps. The number of backward increments employed in this way is called Shift. The default value for Shift is 0. The Shift/Sensitivity combination can be optimized for a certain reference substance. In our studies we confined the Shift to 0 and kept the sensitivity to 0 or 5.

The optimal factor 'f_{opt}' determined for a certain sample is multiplied by 100 to obtain the spectral purity parameter SPR_3 of this sample:

$$SPR_3 = 100 \times f_{opt}$$

After having determined 'f_{opt}' the optimal difference spectrum (see Fig. 5.6) is calculated as:

$$D_{opt} = X - f_{opt} \times Y$$

This should correspond to the pure spectrum of the impurity, which could be

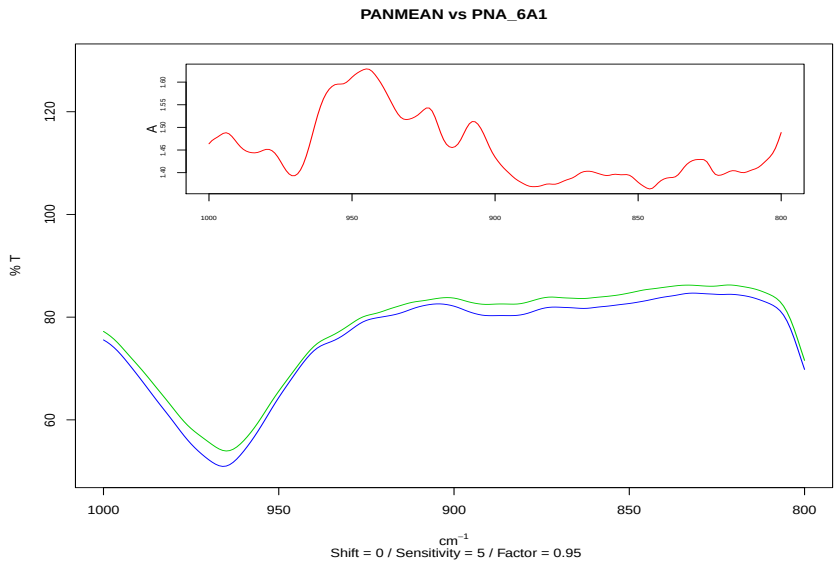

Figure 5.6: MIR spectra of reference substance Palatinol-N (blue) and a sample with 6 % Palatinol-AH in Palatinol-N (green) in the selected spectral range for analysis. The upper inserted graph is the optimal difference spectrum in aborbance (red).

used to identify the impurity, e.g. by comparing the difference spectrum with the spectra of a library. From the difference spectrum, another spectral purity parameter SPR_4 is gained. For this purpose the integral over the positive part

of D_{opt} (calculated as sum of all positive absorbance values) is set into relation to the area of the reference spectrum in the same spectral range. Then the following parameter for spectral purity is computed:

$$SPR_4 = 100 \times (1 - \frac{\int_{\bar{\nu}_1}^{\bar{\nu}_2} D_{opt}^{+}}{\int_{\bar{\nu}_1}^{\bar{\nu}_2} Y})$$

$\bar{\nu}_1$, $\bar{\nu}_2$ are lower and upper wavenumber of the spectral range used for computing the spectral purity parameters. In an ideal situation both SPR_3 and SPR_4 should be quite similar. But in reality this is not the case because we have spectral disturbances like noise, baseline distortions and small deviations in the band contours occurring often for very intense absorption bands and this causes artifacts which do not allow a perfect compensation of the reference spectrum. This is the reason why especially SPR_3 does not perform optimally for very low impurities in some cases.

Unlike the parameters SPR_1 and SPR_2 based on linear regression the spectral purity parameters SPR_3 and SPR_4 based on calculating the optimal difference spectrum D_{opt} are sensitive to intensity changes and baseline shifts caused by irreproducibility of the sample preparation. For liquids, if the ATR crystal is covered completely by the sample, reproducibilities are near to perfect and the method works quite well. But as will be shown later for solids this is not the case. This means that for solids the regression based parameters SPR_1 and SPR_2 perform considerably better than the difference based SPR_3 and SPR_4.

Fig 5.7 on page 55 and Table 9.2 on page 127 in the Appendix shows the results for all the spectral purity parameters for our experimental example. For SPR_1 and SPR_2 a typical behavior identical to that in the simulated example of the section 4.3 on page 40 can be observed, i.e. convex behavior for SPR_1 and concave behavior for SPR_2. SPR_3 and SPR_4 are are approximately linear functions of the concentration of the impurity. This allows for the calculation of the limit of detection (LOD) and capture (LOC) due to the calibration line method described in section 2.4 on page 24.

The reproducibilities for SPR_1 and SPR_2 are better than SPR_3 and SPR_4. This may be due to the fact that the spectral differences between the pure substance Palatinol-N and the impurity Palatinol-AH are very small (Fig. 5.2 on

page 48). In this case obviously the difference based SPR_3 and SPR_4 are more sensitive to small irreproducibilities than the regression based methods. This is also the reason that the limit of detection (LOD) and limit of capture (LOC) are lower in case of SPR_2 than with SPR_3 and SPR_4 (see Table 5.3).

The limit of detection is 0.402 g/100 g and the limit of capture is 0.846 g/100 g when using SPR_2 as spectral purity parameter.

This means that despite the small differences between the spectra of the pure substance and the impurity a contamination below 1 g/100 g still can be detected. To validate this experiment a new set of samples of similar concentrations were prepared. Recording of the spectra was also carried in the same way as before. Comparison with the reference spectrum (from the first experiment) shows results, which confirm the data obtained by the first experiment (a slight improvement is noticed see Fig. 5.8 on page 56 and Table 5.3).

Table 5.3: Limits of detection and capture.

Parameter	Calibration		Validation	
	LOD g/100g	LOC g/100g	LOD g/100g	LOC g/100g
SPR_1	-	-	-	-
SPR_2	0.402	0.846	0.130	0.394
SPR_3	1.316	2.632	1.187	2.374
SPR_4	1.115	2.231	1.090	2.180

5.1.1.4 Quantitative analysis

In the model studied here, univariate quantitative calibration methods are of little or no help, because of problems of selectivity due to strong overlapping of the spectra. Nevertheless, quantitative predictions can be performed with the help of multivariate calibration methods as, e.g. Partial Least Squares (PLS) Regression which we applied here.

The first sample set (see section 5.1.1.1 on page 47) was used for building the calibration model and the second sample set mentioned in section 5.1.1.3 for validation purpose. There was no spectral pretreatment performed on the spectra used for calibration and validation. It is seen from Table 5.4 on page 56 and Fig.

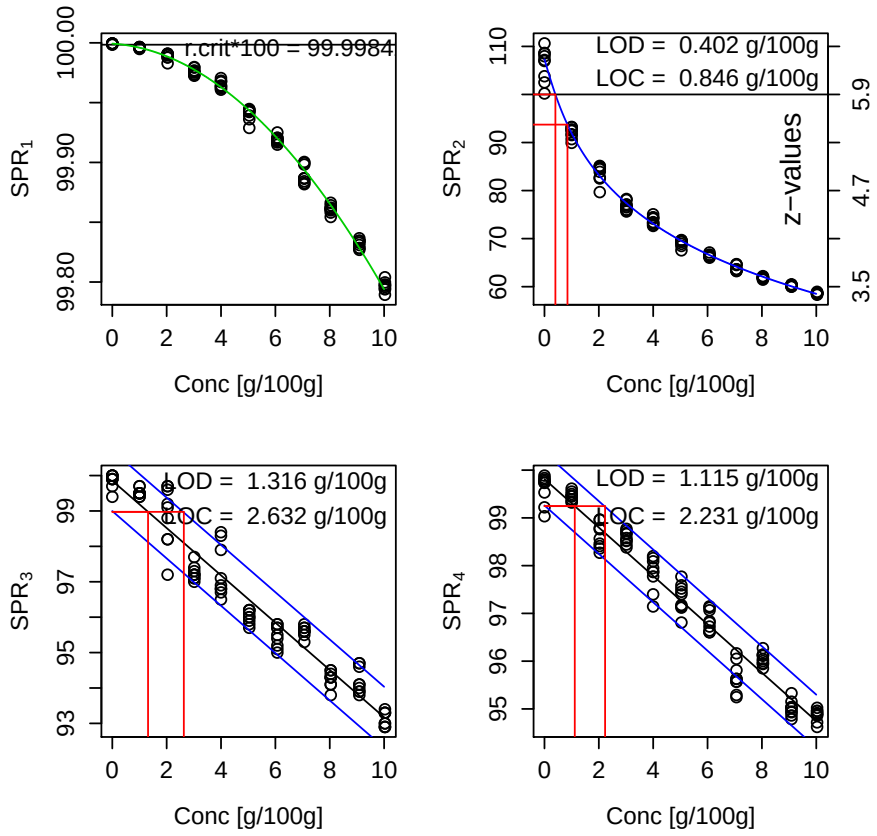

Figure 5.7: Dependency of spectral purity parameters of Palatinol-N on the concentration of the impurity Palatinol-AH in the spectral range 1000-800 cm^{-1}.

5.9 on page 57 that the calibration set is well suited for predicting the samples from the validation batch, for which a root mean square of prediction (RMSEP) of 0.3 g/100 g was obtained which is approximately equal to the limit of capture determined for SPR_2.

Of course such a prediction is only possible if the impurity is known. As already described the impurity can be determined by evaluating the difference spectrum. So, if this shows that a commonly occurring contaminant is present in the sample, it can be quantitatively predicted with a corresponding calibration set.

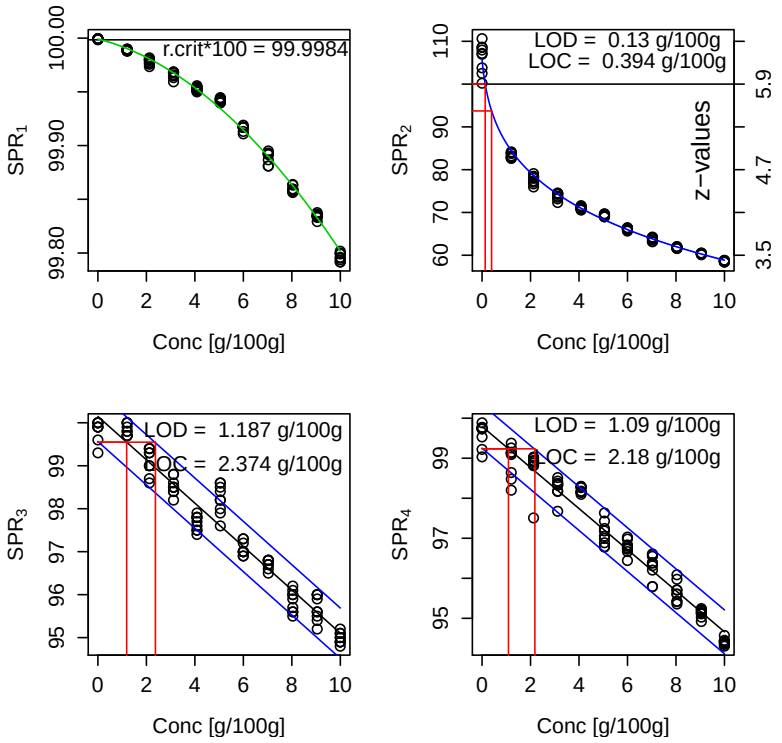

Figure 5.8: Validation experiment for dependency of spectral purity parameters of Palatinol-N on the concentration of the impurity Palatinol-AH in the spectral range 1000-800 cm^{-1}.

Table 5.4: Diagnostic parameters for PLS calibration (1000-800 cm^{-1}, 3 factors).

Diagnostic Value	Calibration	Validation
r^2	0.997	0.998
RMSEC g/100g	0.179	-
$RMSEP_{cv}$ g/100g	0.191	-
RMSEP g/100g	-	0.303

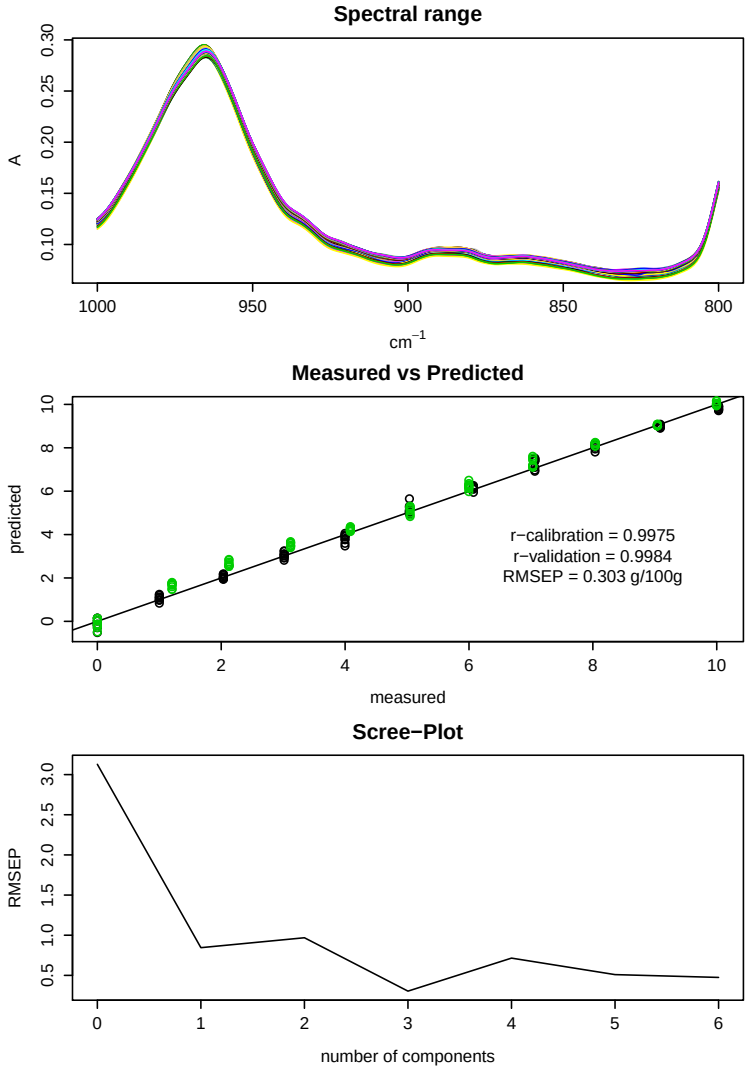

Figure 5.9: Quantitative analysis of Palatinol-AH ("Impurity") in Palatinol-N by PLS. Upper: Calibration and validation spectra. Middle: Prediction plot (black: calibration, green: validation). Lower: RMSEP Scree plot.

5.1.2 Spectral purity control employing Near-IR Palatinol-AH as impurity in Palatinol-N

An analogous study similar to that of Middle-IR was intended to be performed with NIR spectroscopy also. But, if one has a close look at the pure spectra of Palatinol-N and Palatinol-AH one notices only very small deviations even in

the Middle Infrared region (see Fig. 5.2 on page 48). This implies that one sees almost no or negligible differences in the Near Infrared region which is confirmed in Fig. 5.10.

To test the similarity between these spectra a linear regression was performed between the NIR absorbance values of pure Palatinol-N and pure Palatinol-AH and a very high correlation coefficient of $r = 0.99993$ was obtained. When a regression was performed between the spectra of these substances in the Middle Infrared region (excluding the Diamond artifacts between 2300-1850 cm^{-1}) this shows an r of 0.9884. So while in the Middle Infrared we still have discrimination between Palatinol-AH and Palatinol-N this obviously vanishes almost completely in the NIR. So further studies for these sample sets were not performed in the Near Infrared region. Nevertheless NIR studies were performed for other sample sets with other kinds of impurities which will be explained in the sections following this.

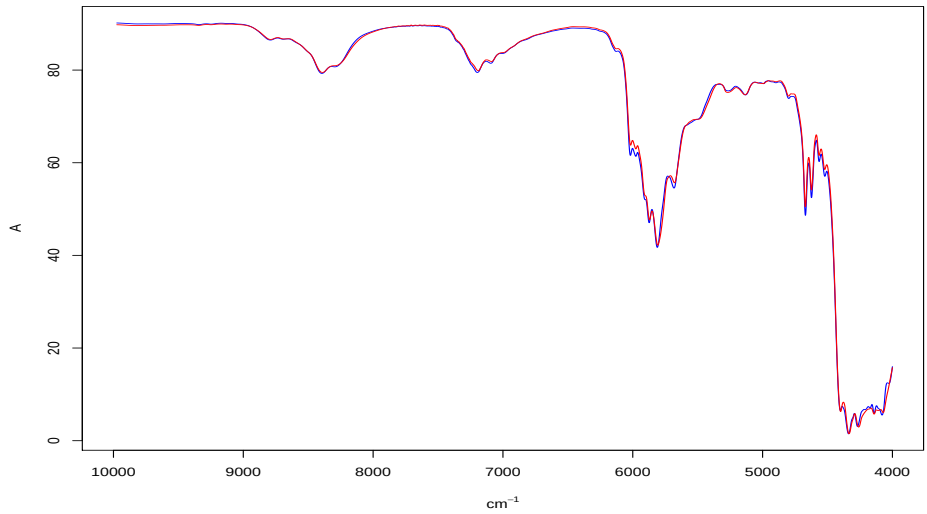

Figure 5.10: NIR spectra of pure Palatinol-N (blue), pure Palatinol-AH (red). Correlation of 0.99993 is obtained between these spectra.

5.1.3 Spectral purity control employing Middle-IR Palatinol-911P as impurity in Palatinol-N

In this model experiment the reference substance is again Palatinol-N, the impurity used for introducing a contamination is Palatinol-911P (Dialkyl Phthalate, see Fig. 5.11 on page 62). This is a linear (C9-C11) phthalate from BASF AG, Germany. As both phthalates have similar physical and chemical properties (see Table 5.5 on page 61) they form homogeneous binary mixtures. The main structural difference between these two compounds in the presence of extra $-CH_2$ functional groups in Palatinol-911P. Therefore as expected the major spectral differences are noticed in the C-H stretch region (3200-2800 cm^{-1}) and there were no or negligible differences in the fingerprint region (as it was the case between Palatinol-AH and Palatinol-N). Due to these unique spectral properties the pair of Palatinol-911P/Palatinol-N it forms an ideal model system for testing the spectral purity parameters in the C-H stretch region.

5.1.3.1 Preparation of samples and recording of spectra

The concentration range and sample preparation are similar to that described in section 5.1.1.1 on page 47. So 10 samples with contamination range 1 g/100 g-10 g/100 g were prepared. The spectra of pure Palatinol-N were once again recorded since the spectrometer had to undergo service maintenance. For the recording of the spectra of pure Palatinol-N and the samples containing the impurity Palatinol-911P the instrument was set to the same specifications (see Table 5.2 on Page 49) that in the first experiment. The cleaning of the crystal was also similarly followed along with the monitoring function for cleaning to avoid unwanted disturbances in the spectra.

5.1.3.2 Analysis of spectra by calculating spectral purity parameters

To calculate the spectral purity of the sample spectra, the same algorithms were applied as before. To find the optimal wavenumber range, a moving window approach was followed. Windows of 500 wavenumbers, followed by 400 wavenumbers down to 50 wavenumbers were used. Care has to be taken to avoid the region between 2300-1850 cm^{-1} as it has negative intensities due to total absorption of the

Diamond crystal. The spectral range between 3000-2800 cm^{-1} was found to be the optimal one in accordance with the above discussed differences in the chemical structures of the two phthalates. The z_{crit} for Palatinol-N was also calculated newly for this spectral range.

When all the spectral purity parameters were calculated and graphically represented (see Fig. 5.13 on page 63), a typical behavior in compliance with the simulated example is observed (see Fig. 4.6 on page 43). A convex curve for the first parameter SPR_1 and concave curve for the second parameter SPR_2 is obtained. And like before a linear relationship is obtained for purity parameters SPR_3 and SPR_4. The detection limit and capture limit of the impurity for SPR_2 were found to be 0.098 g/100 g and 0.324 g/100 g (see Table 5.6 on page 61). r_{crit} was calculated to be 0.99999685 (obtained from transformation of z_{crit}) and this value can be used as threshold value, and if the calculated SPR_1 value of spectrum lies below $100 \times r_{crit}$, this means that an impurity is detected. For SPR_4 a slight improvement in LOD and LOC is noticed compared to the case where Palatinol-AH is the impurity this may be due to the fact that differences are more pronounced in this example with Palatinol-911P.

5.1.3.3 Quantitative analysis

Since the impurity is self induced and therefore known in the samples for this experiment a quantitative PLS calibration could be established. No spectral pretreatment was performed. Leave one out type of validation method was used here and for the rest of the PLS models calculated in this thesis. An RMSEP value of 0.182 g/100 g was obtained which is between the LOD and LOC for SPR_2.

Table 5.5: Chemical and physical properties of Palatinol-911P.

Specifications	Palatinol-911P
Formula	$C_{28}H_{46}O_4$
Mol. Wt	450
Refractive index n_D^{20}	1.479-1.485
Density at 20°C (g/ml)	0.952-0.964

Table 5.6: Limit of detection and capture.

Parameter	LOD g/100g	LOC g/100g
SPR_1	-	-
SPR_2	0.098	0.324
SPR_3	2.521	5.043
SPR_4	0.892	1.783

5.1.4 Spectral purity control employing Near-IR Palatinol-911P as impurity in Palatinol-N

Before starting the experiment a regression between the NIR spectrum of Palatinol-N and Palatinol-911P was performed and a correlation coefficient of 0.994 was obtained. Though the spectra are similar to each other still there is lot of scope to detect the impurity caused by Palatinol-911P as the r is relatively low compared to the case before of Palatinol-N/Palatinol-AH (see Fig. 9.9 on page 131 in the Appendix).

5.1.4.1 Preparation of samples and recording of spectra

The spectra were acquired using a PerkinElmer One NTS Spectrometer. For this experiment the same sample set as in the section 5.1.3.1 on page 59 was used. Followed by initialization the instrument was set to the specifications specified in Table 5.7 on page 65 and a back ground spectrum was collected. The sample was pipetted into a 1 mm quartz cuvette (Hellma GmbH & Co. KG, Germany) and three spectra were recorded. The cuvette was cleaned with THF thoroughly followed by drying. The same sample was once again filled in the cuvette and another three subsequent spectra were acquired. This procedure was followed one more time and thus a total of nine spectra for each sample were recorded.

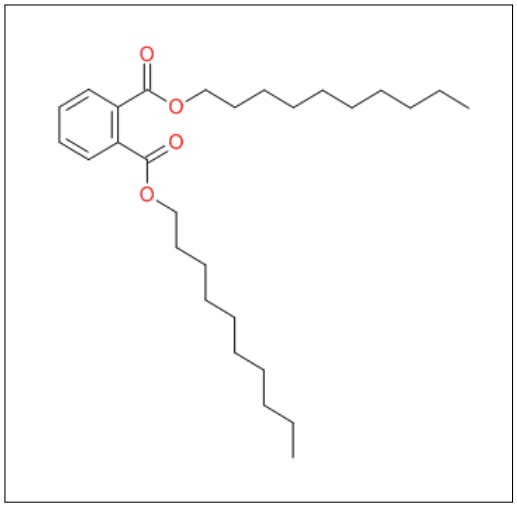

Figure 5.11: Chemical structure of Palatinol-911P.

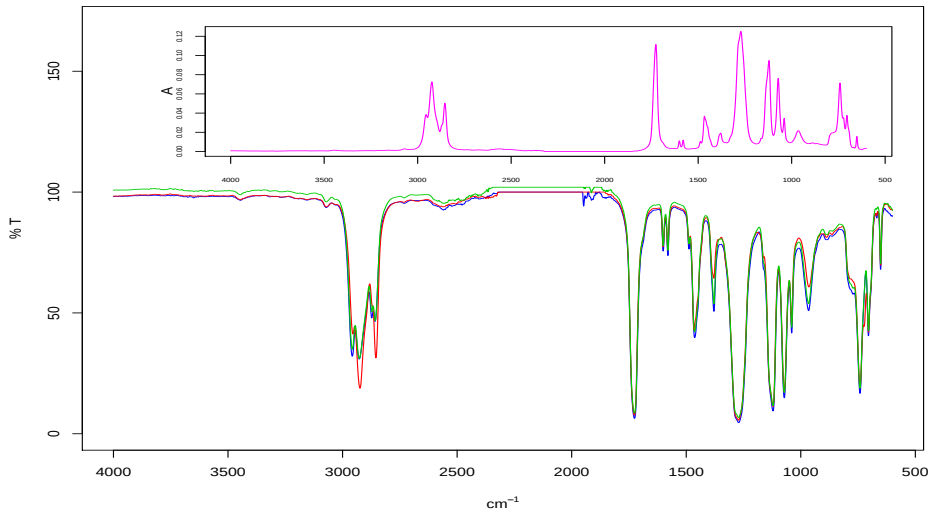

Figure 5.12: MIR spectra of pure Palatinol-N (blue), pure Palatinol-911P (red) and sample of Palatinol-N with 10 % Palatinol-911P (green). The negative bands due to total absorption by the diamond crystal are removed. The upper inserted graph is the optimal difference spectrum in absorbance.

The same procedure of cleaning and obtaining nine spectra was followed for pure Palatinol-N.

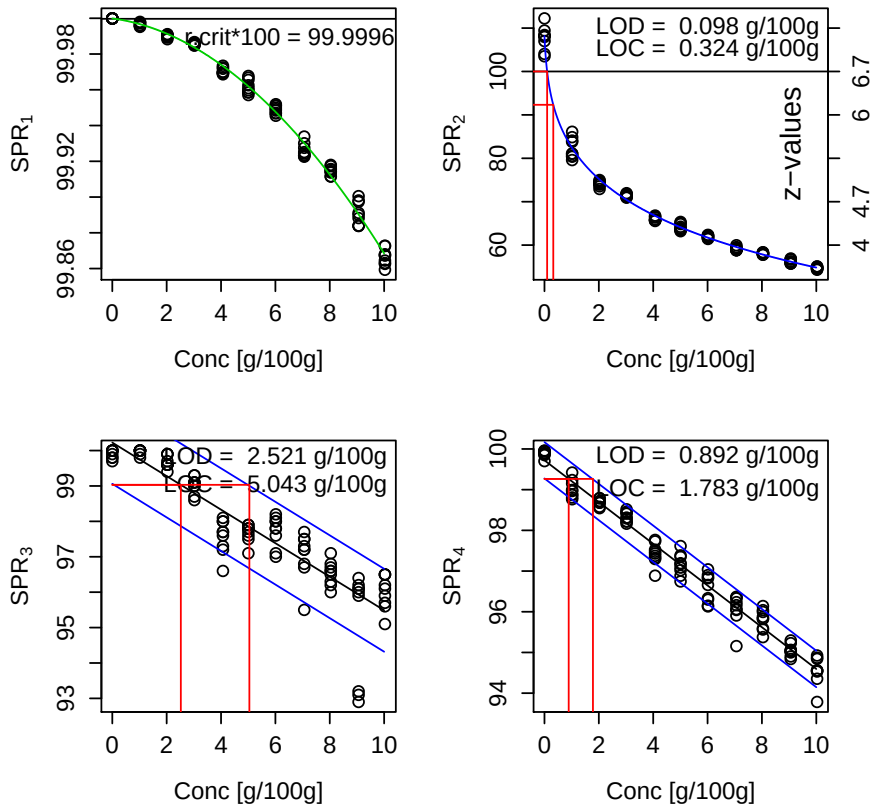

Figure 5.13: Dependency of spectral purity parameters of Palatinol-N on the concentration of the impurity Palatinol-911P in the spectral range 3000-2800 cm^{-1}.

5.1.4.2 Analysis of spectra by calculating spectral purity parameters

A moving window approach was followed to find the optimal spectral range for detecting impurities. As expected the CH overtone region between 6000-5500 cm^{-1} was the favored region for analysis of spectral purity parameters, since the major differences between these two compounds are found in C-H stretch region in Middle Infrared. Both z_{crit} and r_{crit} for this spectral range was again calculated. In Fig. 5.15 on page 65 the typical behavior for SPR_1 and SPR_2 can again observed. For SPR_2 the limit of detection (LOD) and capture (LOC) of the impurity were found to be 0.387 g/100 g and 0.557 g/100 g respectively (see Table 5.8 on page 66).

The LOD value for SPR_2 is increasing from 0.100 g/100 g in the Middle

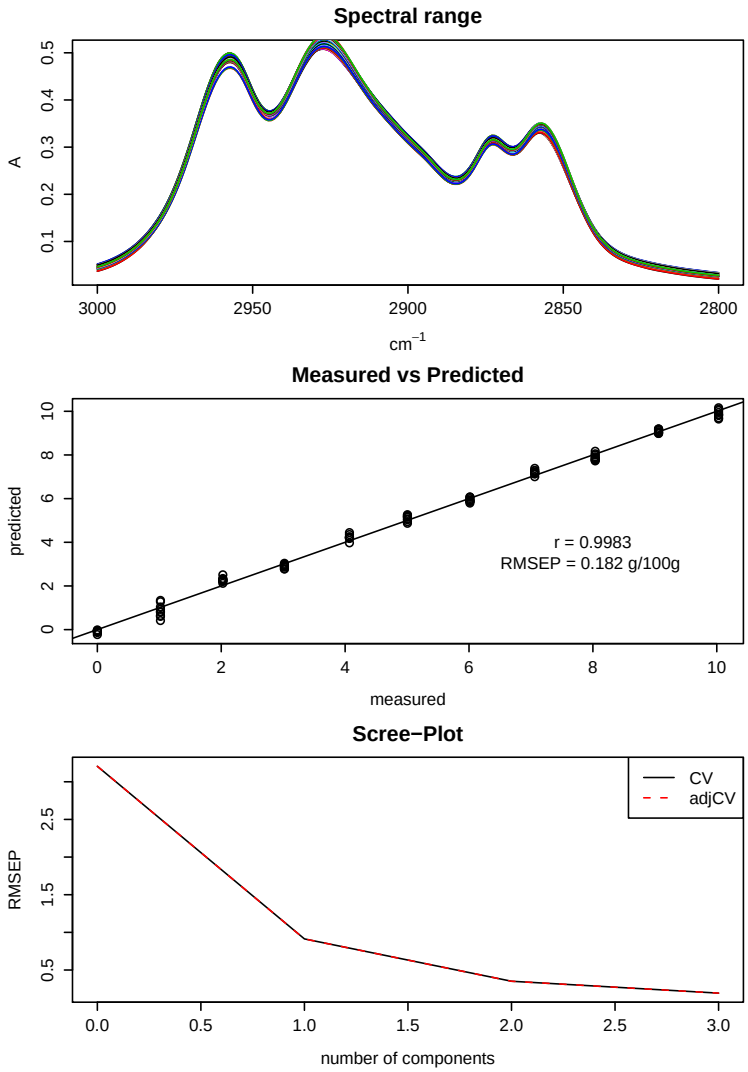

Figure 5.14: Quantitative analysis of Palatinol-911P("Impurity") in Palatinol-N by PLS in Middle Infrared. Upper: Calibration spectra. Middle: Prediction plot. Lower: RMSEP Scree plot.

Infrared to 0.387 g/100 g in the NIR. This comes by the fact that the spectral differences between the phthalates are much more pronounced in the Middle Infrared. However (astonishingly) the LOD of 0.545 g/100 g based on SPR_3 and of 0.317 g/100 g for SPR_4 is getting better in NIR compared to values of 2.521 and 0.892 g/100 g in the MIR. This is due to the fact that we have a better S/N ratio and a better reproducibility of the difference spectra in the NIR.

Table 5.7: Instrumental specifications for recording spectra (NIR).

Specifications	Value
No. of scans	32
Digital resolution	1 cm^{-1}
Optical resolution	16 cm^{-1}
Units	%T

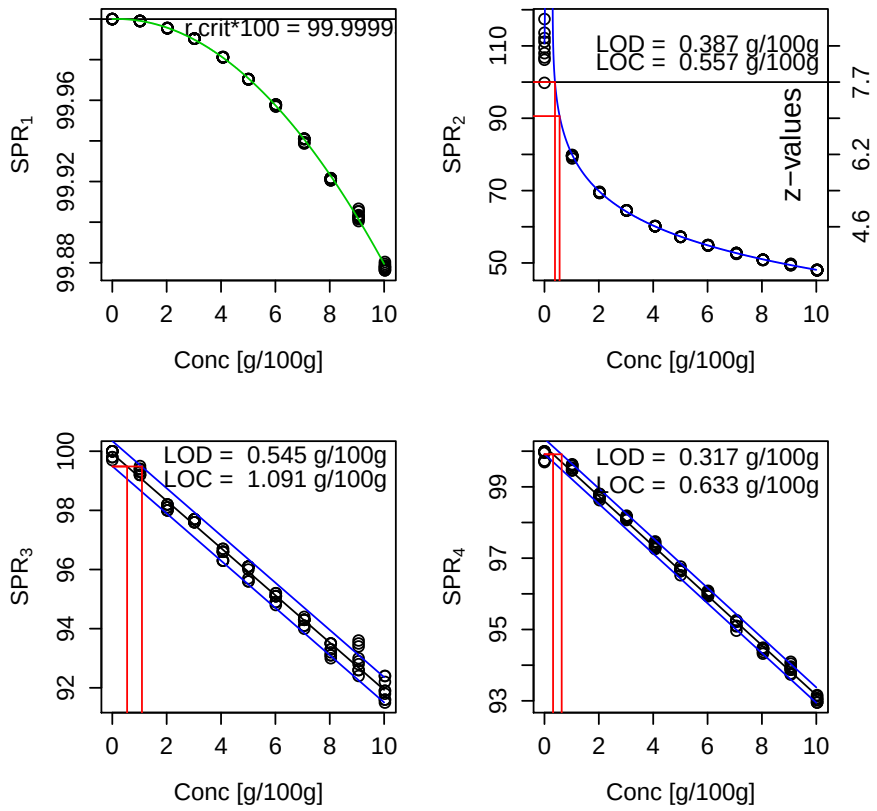

Figure 5.15: Dependency of spectral purity parameters of Palatinol-N on the concentration of the impurity Palatinol-911P in the spectral range 6000-5500 cm^{-1}.

Table 5.8: LOD and LOC values.

Parameter	LOD g/100g	LOC g/100g
SPR_1	-	-
SPR_2	0.387	0.557
SPR_3	0.545	1.091
SPR_4	0.317	0.633

5.1.4.3 Quantitative analysis

Since the impurity is self induced and therefore known in the samples for this model experiment a quantitative PLS calibration is established with three principal factors. No spectral pretreatment was performed. An RMSEP value of 0.076 g/100 g was obtained.

5.1.5 Spectral purity control employing Middle-IR Reofos-50 as impurity in Palatinol-N

In the third experimental model system for purity control of Palatinol-N, the chemical compound employed to simulate a contamination is Reofos-50. Reofos-50 (Isopropylated Triaryl Phosphate) is a registered trade name of Chemtura Corporation, USA. It is the commonly used phosphorylated flame retardant in PVC and other plastics. Although Reofos-50 is chemically and physically different from Palatinol-N (see Fig. 5.17 on page 68 and Table 5.9 on page 68 for details) both form homogeneous binary mixtures. The spectrum of Reofos-50 (Fig. 5.18 on page 69) is completely different from the spectrum of Palatinol-N due to its different chemical nature. The Reofos-50 spectrum differs both in the C-H stretch region (3200-2800 cm^{-1}) and also in the fingerprint region (1850-600 cm^{-1}). So when a contamination is imitated in the samples, both the C-H stretch and the fingerprint region can be employed for purity control.

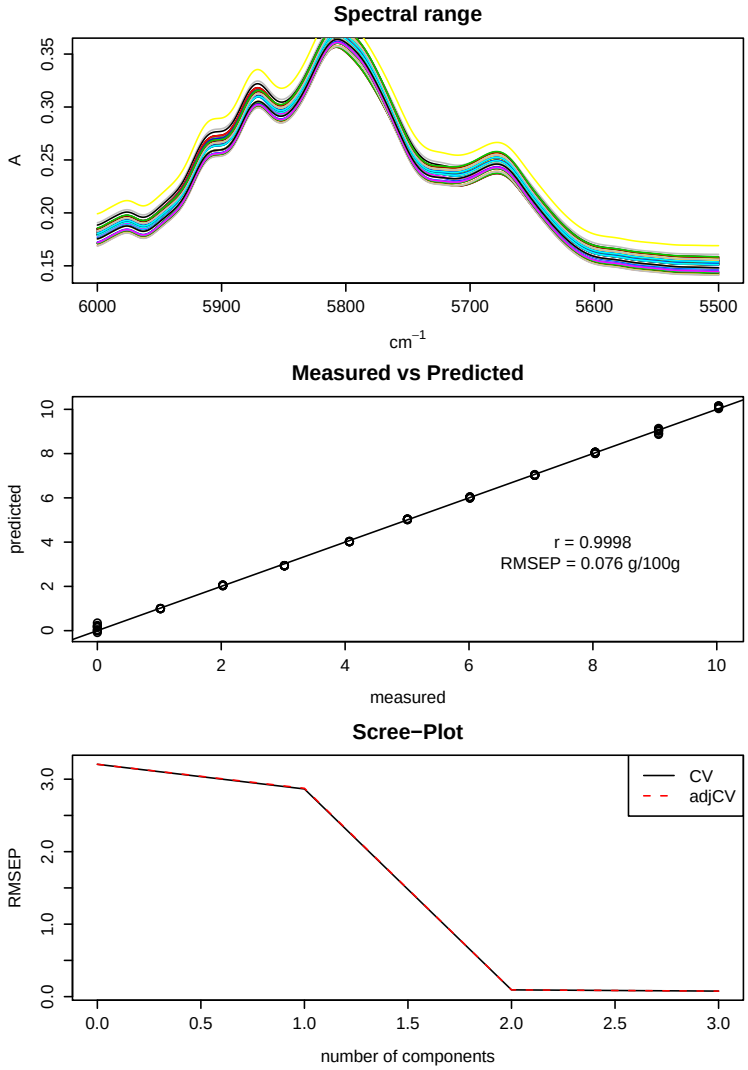

Figure 5.16: Quantitative analysis of Palatinol-911P ("Impurity") in Palatinol-N by PLS in Near Infrared (6000-5500 cm^{-1}). Upper: Calibration spectra. Middle: Prediction plot. Lower: RMSEP Scree plot.

5.1.5.1 Preparation of samples and recording of spectra

The same method as described in the previous sections was followed for the preparation of samples containing Reofos-50 as "contaminant" in Palatinol-N. As previously a concentration range of 1-10 g/100 g was used. In this experiment the nine spectra of pure Palatinol-N and their average which forms the reference

spectrum were retained from the section 5.1.3.1 on page 59. For acquiring the spectra of the samples the spectrometer was set to the same specifications like that in Table 5.2 on page 49. Cleaning and monitoring was also followed in same the fashion as in the former sections.

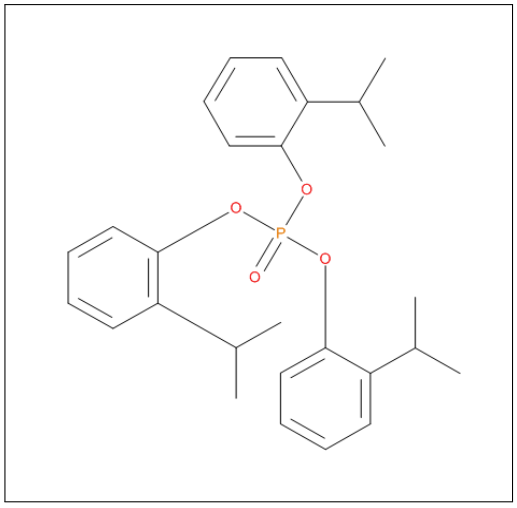

Figure 5.17: Chemical structure of Reofos-50.

Table 5.9: Chemical and physical properties of Reofos-50.

Specifications	Reofos-50
Formula	$C_{27}H_{33}O_4P$
Mol. Wt	452.522.
Refractive index n_D^{20}	1.546
Density at 20°C (g/ml)	1.17-1.18

5.1.5.2 Analysis of spectra by calculating spectral purity parameters

In principle for calculating the spectral purity parameters of the sample spectra one could apply the complete range from 4000-600 cm^{-1} (excluding the diamond

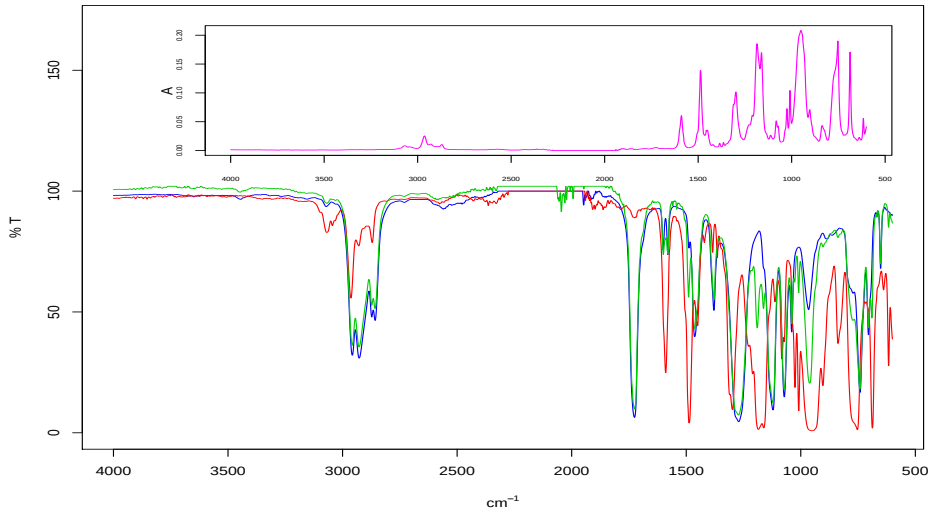

Figure 5.18: MIR spectra of pure Palatinol-N (blue), pure Reofos-50 (red) and sample of Palatinol-N with 1 % Palatinol-911P (green). The negative bands due to total absorption by the Diamond crystal are removed. The upper inserted graph is the optimal difference spectrum in absorbance.

regions containing negative values) as there are prominent differences in both the fingerprint and C-H stretch regions. With the moving window approach both the ranges 1850-900 cm^{-1} and 3100-2800 cm^{-1} were found to be suitable for determining the spectral purity parameters. But the region 1850-900 cm^{-1} (fingerprint region) gave slightly better results (see Table 5.10 on page 70). All the spectral purity parameters were calculated along with their respective threshold values and represented graphically in the Fig. 5.19 on page 70 (wavenumber range 1850-900 cm^{-1}). The figure for the range in C-H stretch region is placed in the Appendix on page 133.

SPR_1 and SPR_2 show the usual behavior. The reproducibility is very good and compared to the experiments before we get an extremely low limit of detection of 0.002 g/100 g for SPR_2. This is certainly due to the fact that the spectral differences between Palatinol-N and Reofos-50 are very pronounced.

In contrast to this difference spectroscopy gives not so optimal results. This may be due to baseline problems and artifacts in the regions of strong absorptions.

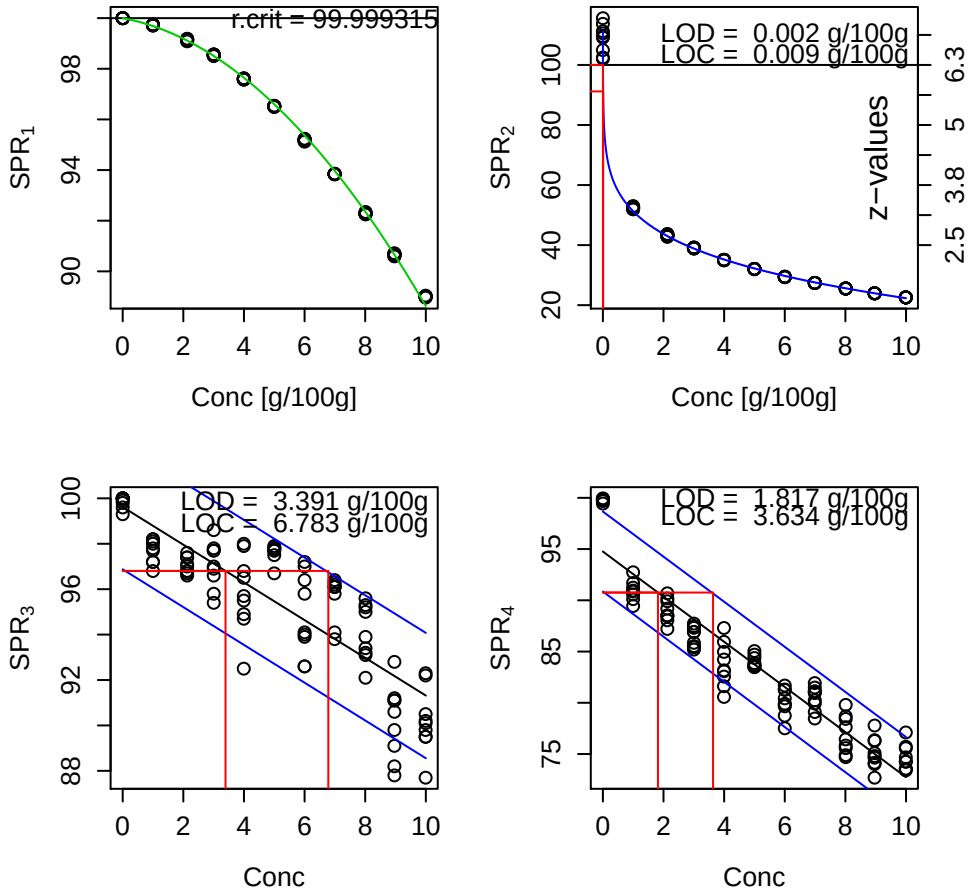

Figure 5.19: Dependency of spectral purity parameters of Palatinol-N on the concentration of the impurity Reofos-50 in wavenumber range of 1850-900 cm^{-1}.

Table 5.10: LOD and LOC values for experiment with impurity Reofos-50 in Middle Infrared regions 1850-900 cm^{-1} and 3100-2800 cm^{-1}.

	1850-900 cm^{-1}		3100-2800 cm^{-1}	
Parameter	LOD g/100g	LOC g/100g	LOD g/100g	LOC g/100g
SPR_1	-	-	-	-
SPR_2	0.002	0.009	0.017	0.071
SPR_3	3.391	6.783	2.407	4.814
SPR_4	1.817	3.634	3.129	6.258

5.1.5.3 Quantitative analysis

PLS calibration with three principal factors was performed in the spectral range of 1850-900 cm^{-1} (see Fig. 5.20). This gives a RMSEP value of 0.034 g/100 g. This is around the fourfold of the limit of capture for SPR_2.

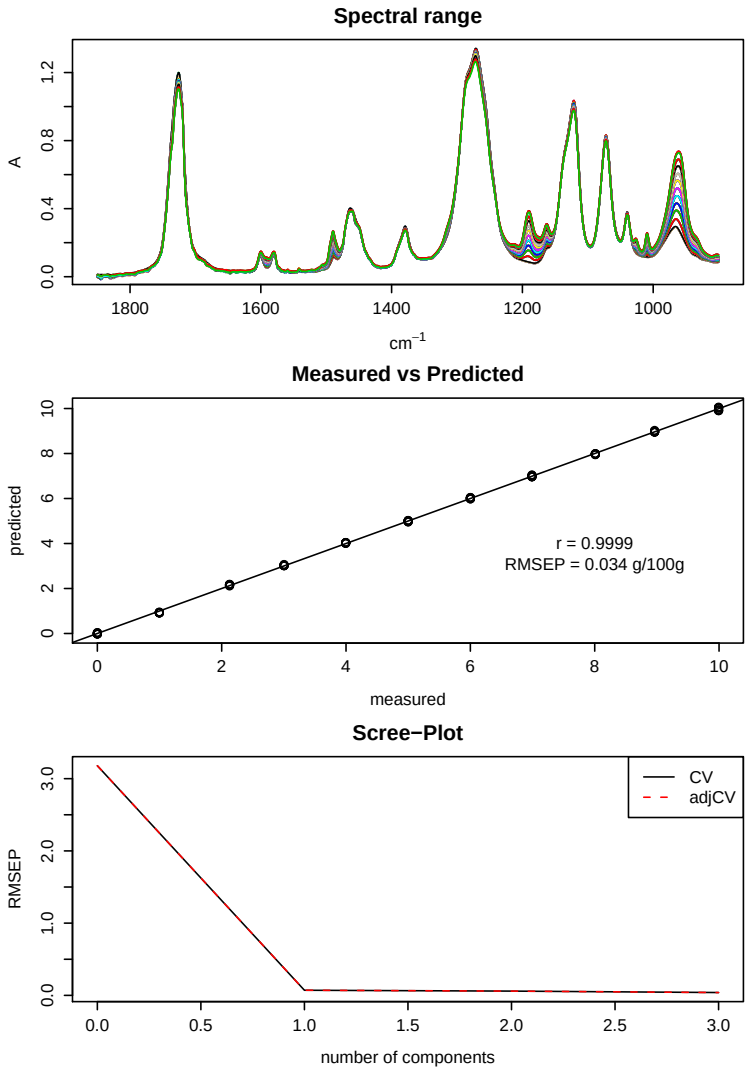

Figure 5.20: Quantitative analysis of Reofos-50 ("Impurity") in Palatinol-N by PLS in Middle Infrared. Upper: Calibration spectra. Middle: Prediction plot. Lower: RMSEP Scree plot.

5.1.6 Spectral purity control employing Near-IR Reofos-50 as impurity in Palatinol-N

The chemical and spectral nature of the impurity Reofos-50 is so diverse from Palatinol-N that in this case not only Middle Infrared but also the Near Infrared spectra show quite different features (see Fig. 9.10 on page 131 in the Appendix).

5.1.6.1 Preparation of samples and recording of spectra

The sample set used in the purity control in Middle Infrared in section 5.1.5.1 on page 67 was used for recording the spectra in NIR with a Spectrum One NTS spectrometer. Instrumental settings were held constant during the measurements as specified in the Table 5.7 on page 65. The procedure of cleaning and recording of nine spectra for each sample was also the same as mentioned in the section 5.1.4.1 on page 61.

5.1.6.2 Analysis of spectra by calculating spectral purity parameters

Nine spectra of pure Palatinol-N and its pure reference were taken from experiment in section 5.1.4.1 on page 61. With the moving window approach the optimal wavenumber range for purity control was detected to be 9000-5500 cm^{-1} for the first two parameters SPR_1 and SPR_2 based on linear regression, and 6000-5500 cm^{-1} for the two parameters SPR_3 and SPR_4 based on difference spectroscopy. One could also use the wavenumber range 6000-5500 cm^{-1} for purity control using SPR_1 and SPR_2 (see Fig. 9.13 on page 134 in the Appendix) but the broad range of 9000-5500 cm^{-1} gave a slight improvement of the LOD (see Table 5.11 on page 74).

LOD and LOC of the impurity were found to be 0.105 g/100 g and 0.305 g/100 g with SPR_2, 0.613 g/100 g and 1.227 g/100 g with SPR_3, 0.255g/100 g and 0.510 g/100 g with SPR_4 (see Fig. 5.21 on page 73 and Table 5.11 on page 74). The LOD and LOC values for SPR_2 are still low but not as low as in the Middle Infrared (see Table 5.10 on page 70). However SPR_3 and SPR_4 based on difference spectroscopy perform now better than in the Middle Infrared.

This model experiment demonstrates that one could employ almost the complete NIR range for purity control purposes if the impurity causing substance has substantial different features to that of the pure reference substance.

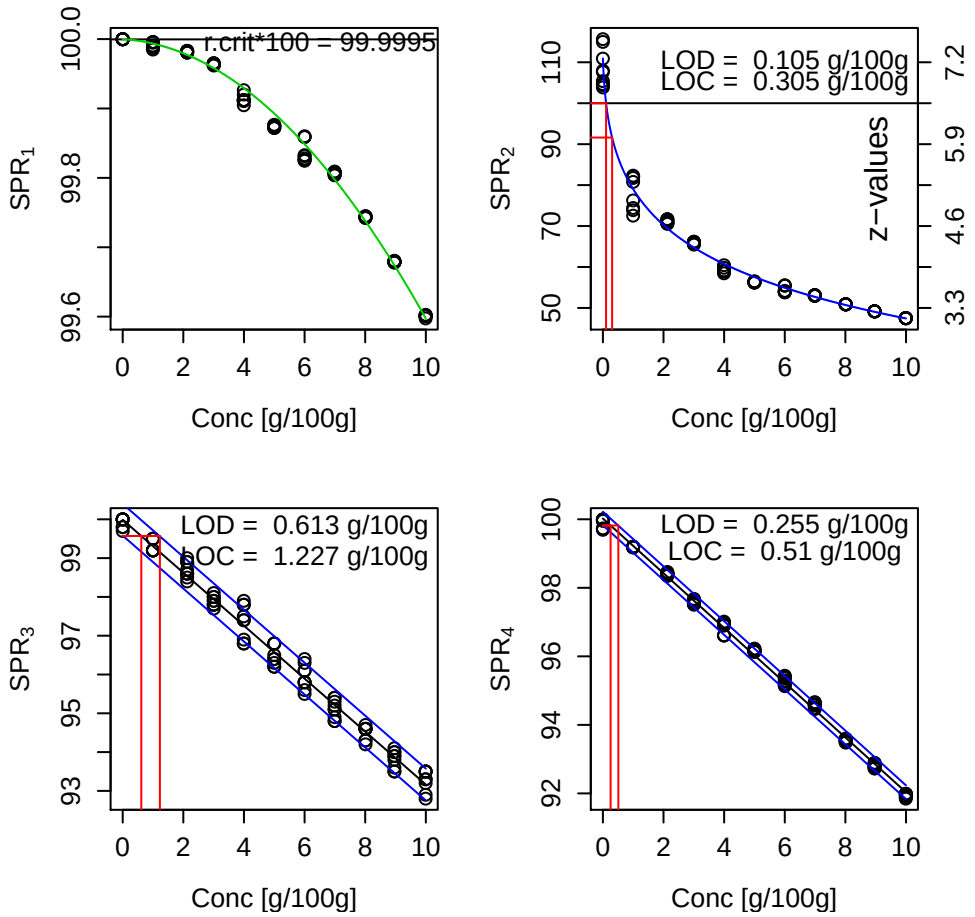

Figure 5.21: Dependency of spectral purity parameters of Palatinol-N on the concentration of the impurity Reofos-50 in the spectral range 9000-5500 cm^{-1} for SPR_1 and SPR_2 and 6000-5500 cm^{-1} for SPR_3 and SPR_4 .

Table 5.11: LOD and LOC values for experiment with impurity Reofos-50 in Near Infrared regions 9000-5500 cm^{-1} and 6000-5500 cm^{-1}.

	9000-5500 cm^{-1}		6000-5500 cm^{-1}	
Parameter	LODg/100g	LOC g/100g	LOD g/100g	LOC g/100g
SPR_1	-	-	-	-
SPR_2	0.105	0.305	0.291	0.312
SPR_3	3.147	6.293	0.613	1.227
SPR_4	3.752	7.504	0.255	0.510

5.1.6.3 Quantitative analysis

The PLS calibration with three principal factors was performed in the wavenumber range of 9000-5500 cm^{-1}. An RMSEP value of 0.065 g/100 g was obtained (see Fig. 5.22 on page 75) which is somewhat below the LOD value for SPR_2.

5.2 Purity control of Palatinol-AH

In order to further check the applicability and adaptability for different situations of the spectral purity parameters (SPR_1- SPR_4), an experiment opposite to the first experiment in which Palatinol-AH is used for inducing contamination in samples of Palatinol-N is performed. In this experiment Palatinol-N forms the contaminant and the pure reference substance is Palatinol-AH whose purity is to be determined using our spectral purity parameters. The chemical and physical properties of these compounds were discussed already in section 5.1 on page 46.

5.2.1 Spectral purity control employing Middle-IR Palatinol-N as impurity in Palatinol-AH

5.2.1.1 Preparation of samples and recording of spectra

To imitate the contamination, about ten samples were prepared by addition of Palatinol-N to Palatinol-AH. Approximately 1 g of Palatinol-N was added to a

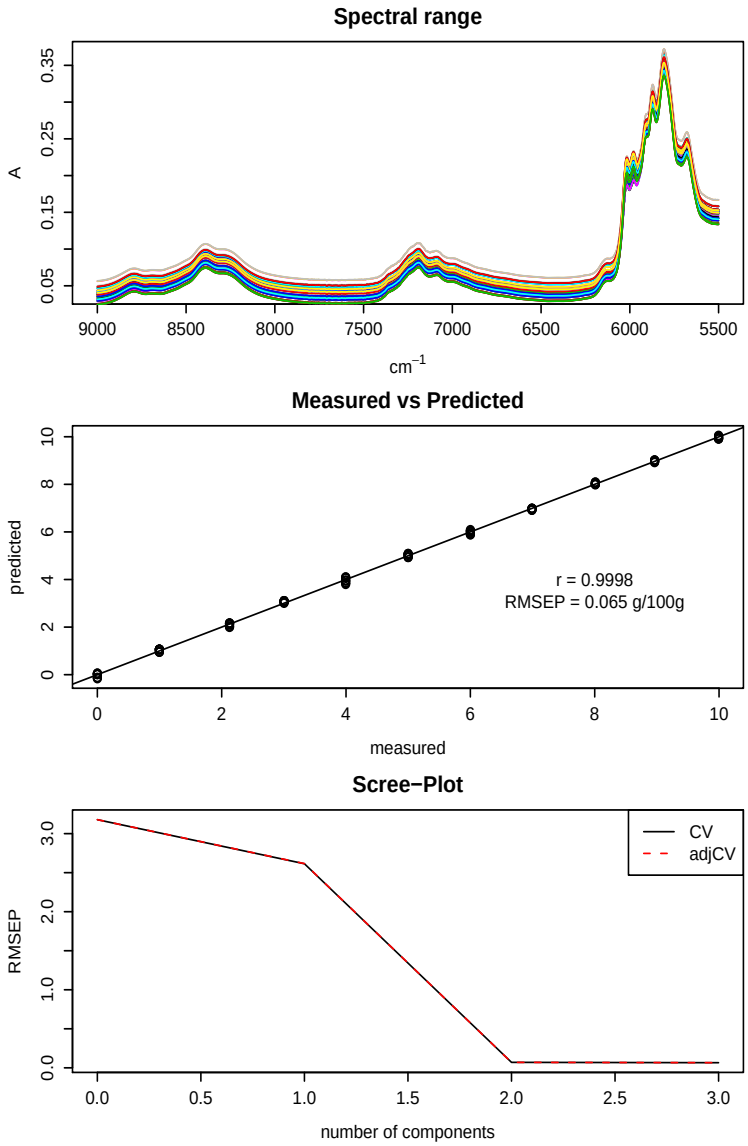

Figure 5.22: Quantitative analysis of Reofos-50 ("Impurity") in Palatinol-N by PLS in Near Infrared. Upper: Calibration spectra. Middle: Prediction plot. Lower: RMSEP Scree plot.

clean and empty glass vial, then Palatinol-AH was used to make up to the weight of 10 g approx., this makes a concentration of 1 g/100 g. This procedure was followed to prepare the rest of the samples in the concentration range of 1-10 g/100 g.

The spectra were recorded by using the PerkinElmer 2000 FT-IR spectrometer. The sampling unit was an external Diamond ATR unit. The instrumental settings were same as that mentioned in Table 5.2 on page 49. Nine spectra for each sample and pure Palatinol-AH were obtained in same way as explained in the section 5.1.1.2 in page 48.

5.2.1.2 Analysis of spectra by calculating spectral purity parameters

By applying the moving window approach the optimal wavenumber range for the purity control was found to be in the range of 1000-900 cm^{-1}. This wavenumber range is almost similar as the one used for purity control of Palatinol-N in Middle Infrared, when the samples contained impurity Palatinol-AH (1000-800 cm^{-1}). This is due to the fact that the major differences between the spectrum of Palatinol-AH and the spectrum of Palatinol-N are found in this region (see Fig. 5.2 on page 48).

The LOD/LOC of the impurity were found to be 0.184 g/ 100 g and 0.500 g/100 g with SPR_2, 1.748 g/100 g and 3.497 g/100 g using SPR_3, 1.515 g/100 g and 3.030 g/100 g using SPR_4 (see Fig. 5.23 on page 77 and Table 5.12). These values are in a similar range as in the case of experiment with Palatinol-AH as impurity in Palatinol-N (see Table 5.3 on page 54).

Table 5.12: LOD and LOC values for experiment with impurity Palatinol-N in Palatinol-AH (Middle Infrared region).

Parameter	LOD g/100g	LOC g/100g
SPR_1	-	-
SPR_2	0.184	0.478
SPR_3	1.748	3.497
SPR_4	1.515	3.030

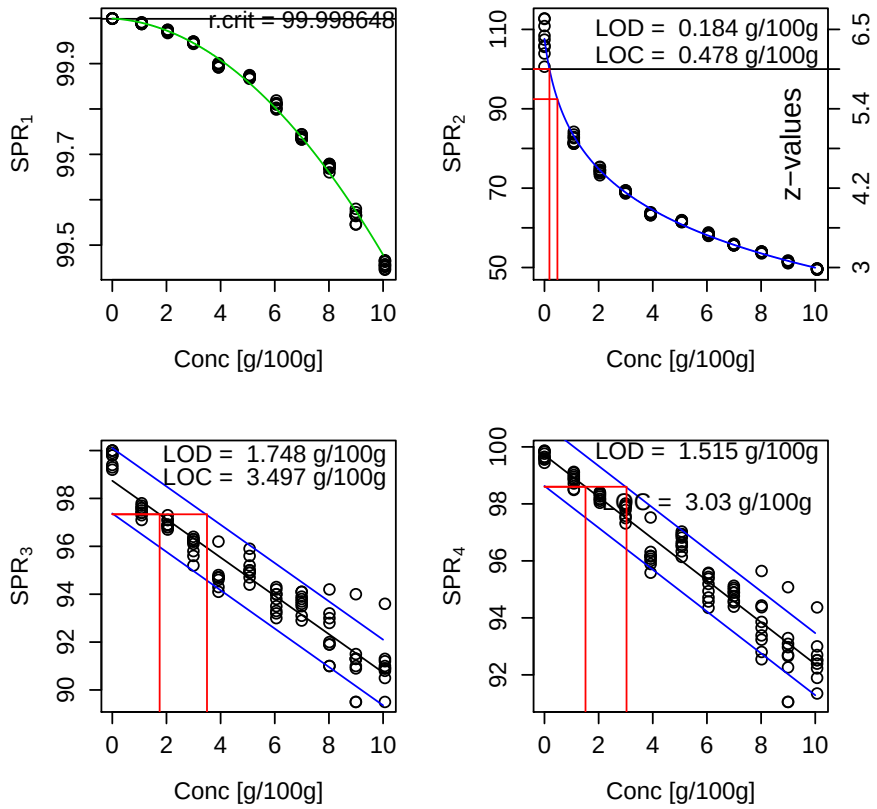

Figure 5.23: Dependency of spectral purity parameters of Palatinol-AH on the concentration of the impurity Palatinol-N in the spectral range 1000-900 cm^{-1}.

5.2.1.3 Quantitative analysis

PLS calibration with three principal factors was performed in the spectral range of 1000-900 cm^{-1} (see Fig. 5.24 on page 78). This gives a RMSEP value of 0.124 g/100 g. This is a little smaller than the limit of detection for SPR_2.

Near Infrared studies for this samples was not performed due to the reason mentioned in section 5.1.2 on page 57.

5.3 Purity control of Water

Water is an omnipresent solvent used for many purposes in pharmaceutical and food industries, etc. and its analysis in the Infrared can be easily performed

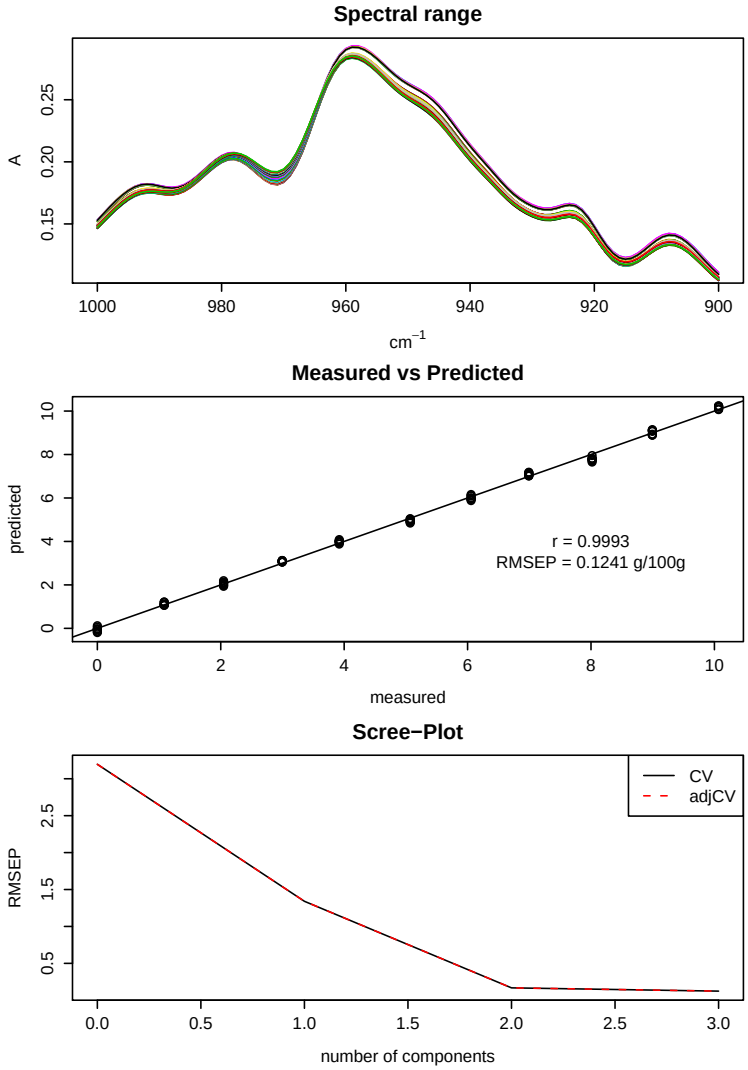

Figure 5.24: Quantitative analysis of Palatinol-N ("Impurity") in Palatinol-AH by PLS in Middle Infrared. Upper: Calibration spectra. Middle: Prediction plot. Lower: RMSEP Scree plot.

using ATR spectroscopy. Due its strong absorbances water overrides many of the spectral features of the dissolved species (see Fig. 5.25 on page 79), but the remaining spectral windows allow for a very efficient quality control of aqueous solutions as shown by the experiments in the following sections.

5.3.1 Spectral purity control employing Middle-IR Potassium Hydrogen Phthalate as impurity in water

In this experiment of purity control of water, Potassium Hydrogen Phthalate (KHP) was used to induce an organic contamination in the water samples. KHP has a relatively a high solubility (25 g/100 ml) in water.

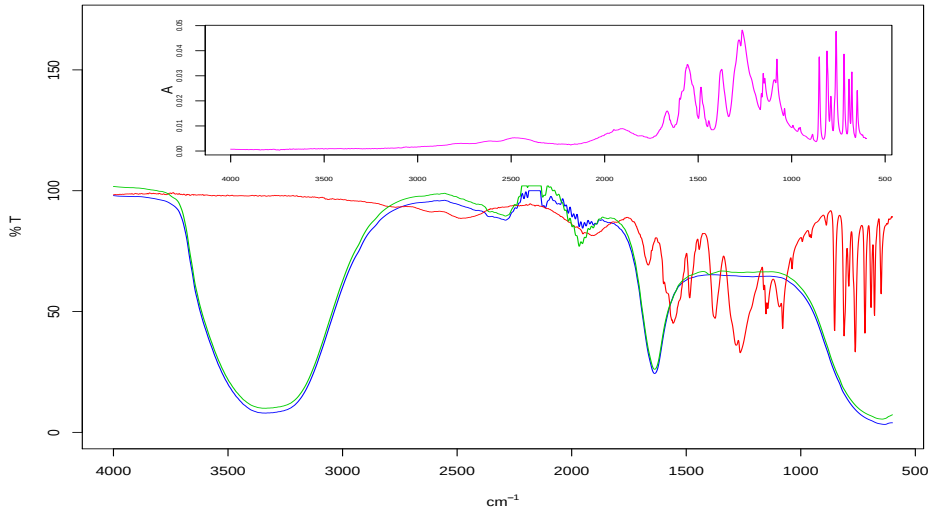

Figure 5.25: MIR spectra of pure water (blue), pure Potassium Hydrogen Phthalate (red) and sample of water with 1 % KHP (green). The negative bands due to total absorption by the diamond crystal are removed. The upper inserted graph is the optimal difference spectrum in absorbance.

5.3.1.1 Preparation of samples and recording of spectra

Approximately 0.1 g of KHP (Merck KGaA, Darmstadt, Germany) was added into a clean empty glass vial and distilled water (obtained from Milli Q Academic A10 of Millipore GmbH, Germany) was added to make weight up to 10 g and mixed well to obtain a homogeneous solution, with a concentration of 0.1 g/100 g. This procedure of preparation was followed further with increasing amounts of KHP in water to get a concentration range between 0.1-10 g/100 g. This

concentration range is 10 fold lower than in the experiments with Palatinol-N and Palatinol-AH.

The spectrometer was set to the specifications like to that in the previous experiments. The sample was pipetted to the trough of the ATR unit. Three spectra in sequence were recorded. Then the sample was removed and the crystal was cleaned with water and dried. The same sample was again placed onto the trough then the next three spectra were obtained. This procedure of cleaning and recording of the spectra was once again followed so that a total on nine spectra for the sample are obtained. This method was followed for all the samples and also with the pure distilled water.

5.3.1.2 Analysis of spectra by calculating spectral purity parameters

The wavenumber range 1700-1000 cm^{-1} was found to be the optimal range for analysis with spectral purity parameters. This region is the favored one because KHP has strong absorptions in this part of fingerprint region. They are not really disturbed by the OH-deformation absorption of water because this is very broad and unspecific. This is why in comparison to organic solvents in water very low detection limits can be achieved as the following results show.

With SPR_2 the LOD and LOC of the impurity KHP were determined to be 0.008 g/100 g and 0.056 g/100 g. And with SPR_4 the LOD and the LOC of impurity were found to be 0.219 g/100 g and 0.438g/100 g (see Fig. 5.26 on page 81 and Table 5.13).

Again as in the model experiment before the regression method delivering SPR_2 gives much better results than difference spectroscopy (SPR_3 and SPR_4).

Table 5.13: LOD and LOC values for experiment with impurity KHP in water (Middle Infrared region).

Parameter	LOD g/100g	LOC g/100g
SPR_1	-	-
SPR_2	0.008	0.056
SPR_4	0.219	0.438

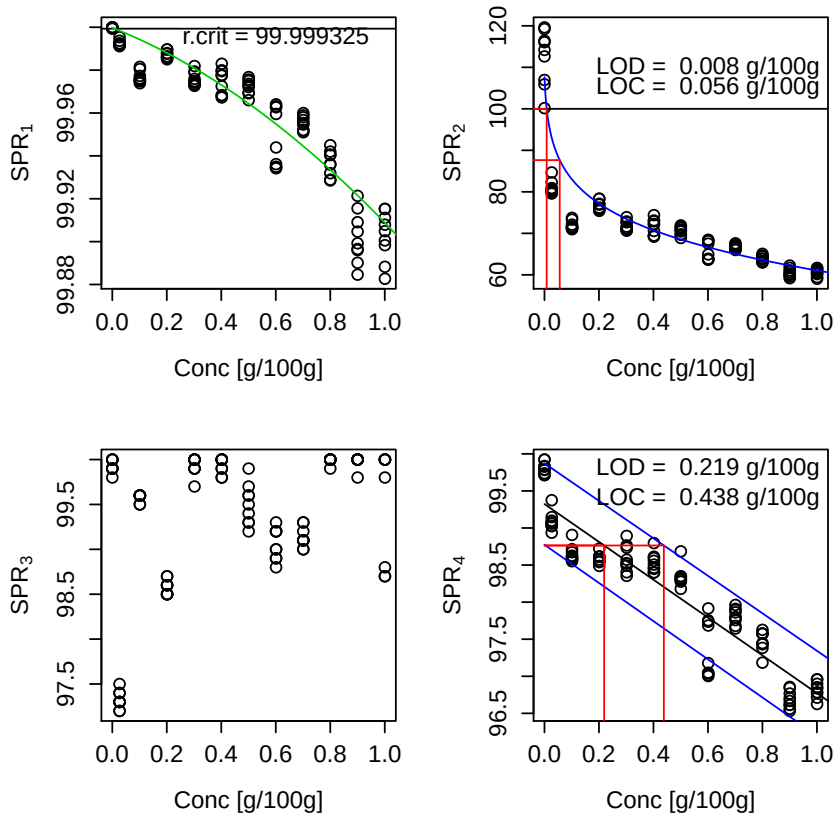

Figure 5.26: Dependency of spectral purity parameters of Water on the concentration of impurity KHP in the spectral range 1700-1000 cm^{-1}.

5.3.1.3 Quantitative analysis

For quantitative analysis of the impurity like in previous experiments a PLS calibration was performed on the spectra of the samples. Using three factors and the spectral range of 1700-1000 cm^{-1}, the RMSEP value was determined to be 0.061 g/100 g (see Fig. 5.27 on page 82). This is approximately equal to the limit of capture for SPR_2.

Another example of the quantitative analysis of organic trace contaminants in water will be discussed in Chapter 6 which is dealing with the quantitative analysis of hydrocarbons in water.

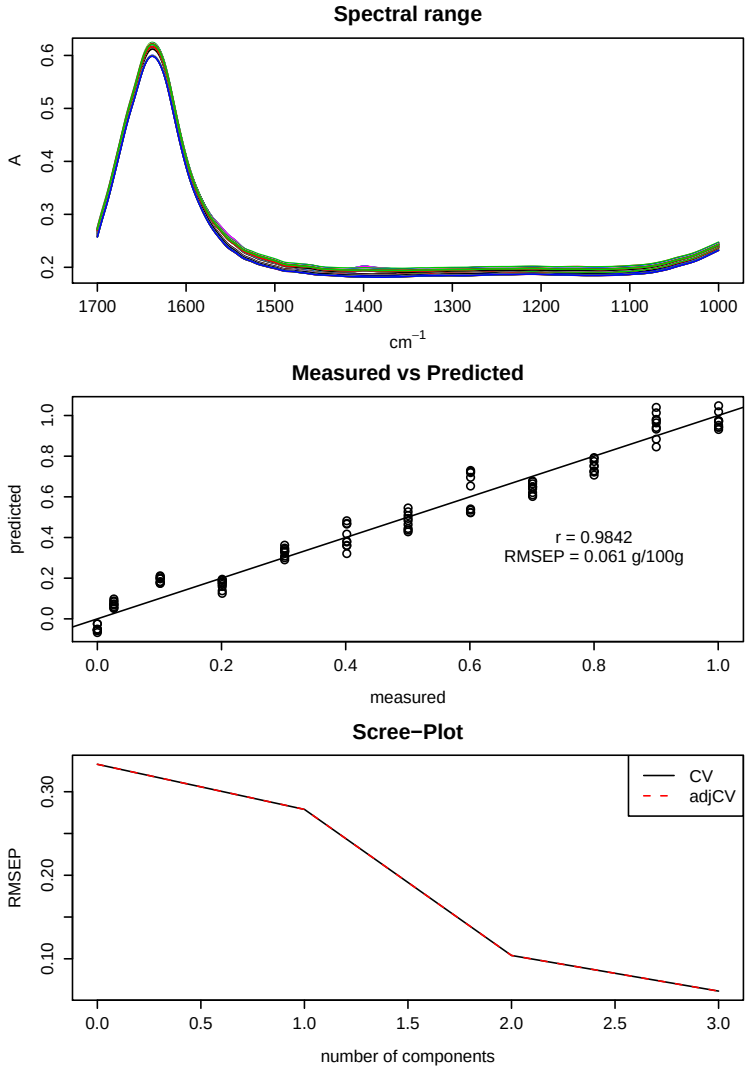

Figure 5.27: Quantitative analysis of KHP ("Impurity") in Water by PLS in Middle Infrared. Upper: Calibration spectra. Middle: Prediction plot. Lower: RMSEP Scree plot.

5.4 Purity control of Aspirin

Acetylsalicylic acid a solid also known as Aspirin is often used as an analgesic to relieve minor aches and pains, as an antipyretic to reduce fever, and as an anti-inflammatory medication. Its chemical structure is given in Fig. 5.28(a) on page 83.

Due to the availability of accessories like ATR (MIR) and Diffuse reflectance unit (NIR) nowadays it is relatively simple and easy to take spectra of solid samples.

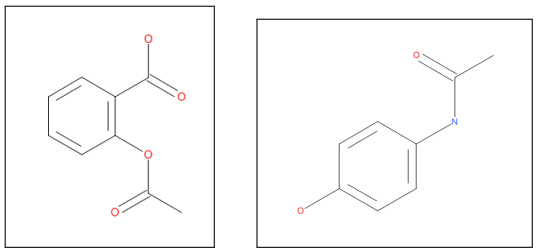

(a) Molecular structure of Aspirin.

(b) Molecular structure of Paracetamol.

Figure 5.28: Molecular structures of Pharmaceutical drugs.

5.4.1 Spectral purity control employing Middle-IR Paracetamol as impurity in Aspirin

This model experiment is performed for demonstrating the usefulness of spectral purity parameters for the purity control of solids. The solid substance chosen for this purpose is Aspirin (Merck KGaA, Darmstadt, Germany) which forms the pure reference substance. As contaminating substance also a solid substance was chosen. This was Paracetamol, i.e. N-(4-hydroxyphenyl)acetamide (Merck KGaA, Darmstadt, Germany) whose molecular structure is given in the Fig. 5.28(b).

5.4.1.1 Preparation of samples and recording of spectra

For imitating contamination of 1 g/100 g of Paracetamol in Aspirin, about 1 g of Paracetamol was taken into a glass vial followed by addition of Aspirin to make up to 10 g. In order to achieve uniform and homogeneous mixing this mixture was transfered to a vibratory micro mill, "Pulverisette 0", Fritsch GmbH, Idar-Oberstein, Germany, and this was operated for 15 minutes. The same method was followed for the preparation and mixing of samples in the concentration range

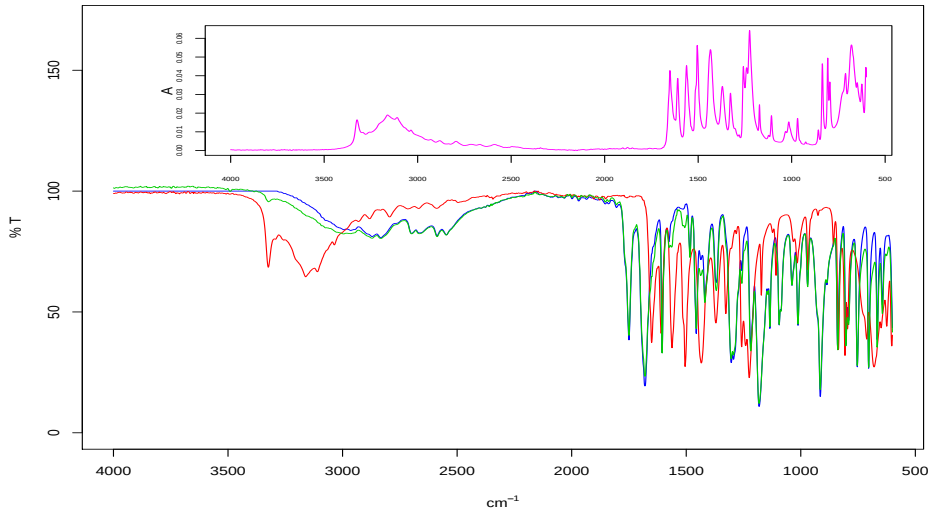

Figure 5.29: MIR spectra of pure Aspirin (blue), pure Paracetamol (red) and sample of Aspirin with 10 % Paracetamol (green). The upper inserted graph is the optimal difference spectrum in absorbance.

1-10 g/100 g. Pure Aspirin was also subjected to this mixing in order to avoid unnecessary spectral deviations especially in the Near Infrared.

In this experiment the single reflection Diamond ATR unit was used for presenting the sample for recording of the spectra as it ensures the proper contact of the sample by pressing it to the the Diamond crystal with help of a screw. In sequence three spectra were obtained when sample was placed on the crystal. This was followed by cleaning and monitoring. Once again the same sample was placed on to the crystal and three spectra were obtained. This procedure was one more time followed in order to obtain 9 spectra for each sample and also for the pure Aspirin.

5.4.1.2 Analysis of spectra using spectral purity parameters

The moving window approach gives an optimal wavenumber range between 1580-1530 cm^{-1}. The Fig. 5.30 on page 85 shows the results for this range. SPR_3, which is based on the difference factor did not prove to be useful. This is due to the fact that the baseline of the spectra is of limited reproducibility due to

the fact that the ATR spectra of solids with respect to the baseline are not as reproducible as those of liquids.

The LOD and LOC of the 'impurity' Paracetamol were found to be 0.182 g/100 g and 0.384 g/100 g with SPR_2, 0.921 g/100 g and 1.841 g/100 g using SPR_4 (see Fig. 5.30 and Table 5.14 on page 86).

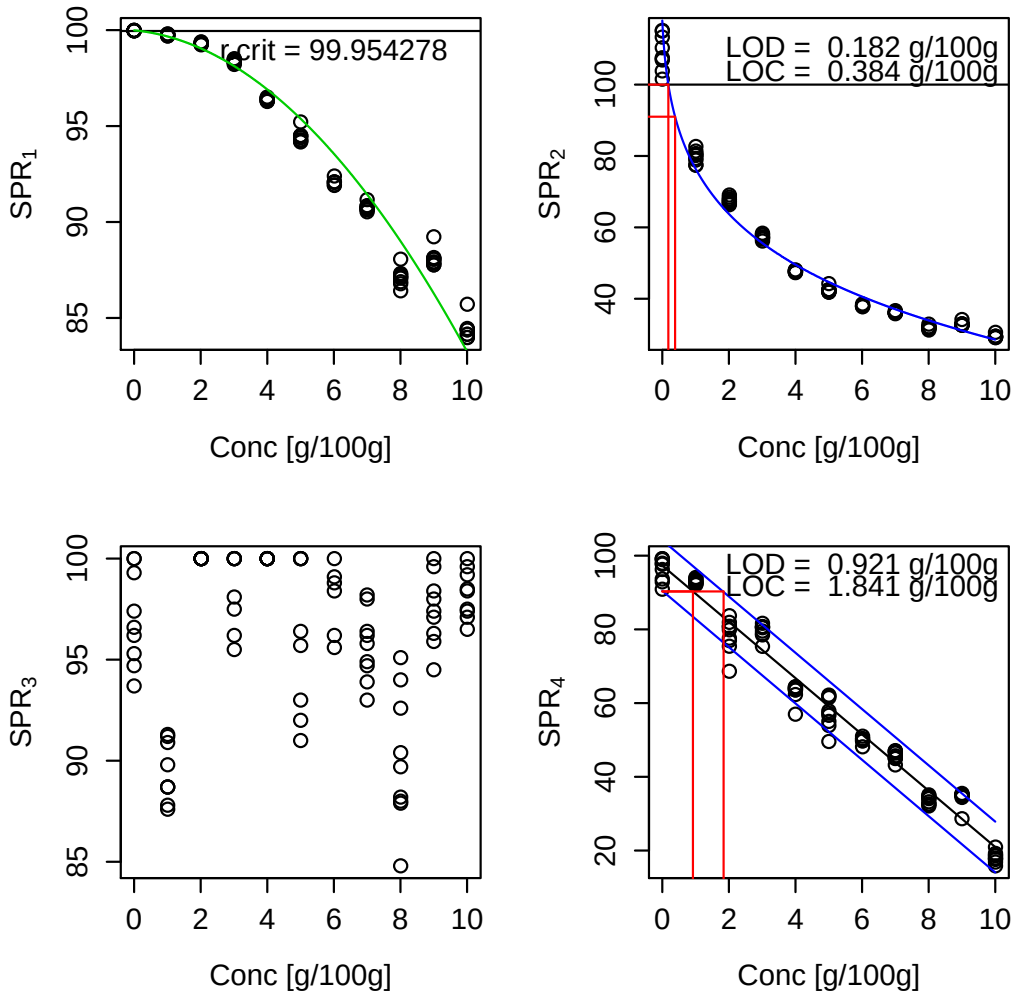

Figure 5.30: Dependency of spectral purity parameters of Aspirin on the concentration of impurity Paracetamol in the spectral range 1580-1530 cm^{-1}.

Table 5.14: LOD and LOC values for experiment with impurity Paracetamol in Aspirin (Middle Infrared region).

Parameter	LOD g/100g	LOC g/100g
SPR_1	-	-
SPR_2	0.182	0.384
SPR_3	-	-
SPR_4	0.921	1.841

5.4.1.3 Quantitative analysis

For quantitative analysis of the impurity like in previous experiments a PLS calibration was performed on the spectra of the samples. Using three factors and the spectral range of 1580-1530 cm^{-1}, the RMSEP value was determined to be 0.265 g/100 g (Fig. 5.31 on page 87). This is about the same precision as was formerly obtained with Near Infrared [63]. The RMSEP value is between the LOD and LOC for SPR_2.

5.4.2 Spectral purity control employing Near-IR Paracetamol as impurity in Aspirin

Near Infrared especially for solids with its Diffuse reflectance accessory forms an alternative to Diamond ATR in Middle infrared. The NIR spectra obtained show higher reproducibility and smaller baseline shifts. This accessory (Fig. 9.3 on page 108 in the Appendix) also presents an opportunity for presenting uniform samples in the path of the radiation because a relatively large sample mass (about 10 g) is used and no pressing which may have a dehomogenising effect is necessary. There are major differences in the Middle Infrared spectra of Aspirin and of Paracetamol this is also be the case for Near Infrared spectra (see Fig. 9.11 on page 132 in the Appendix).

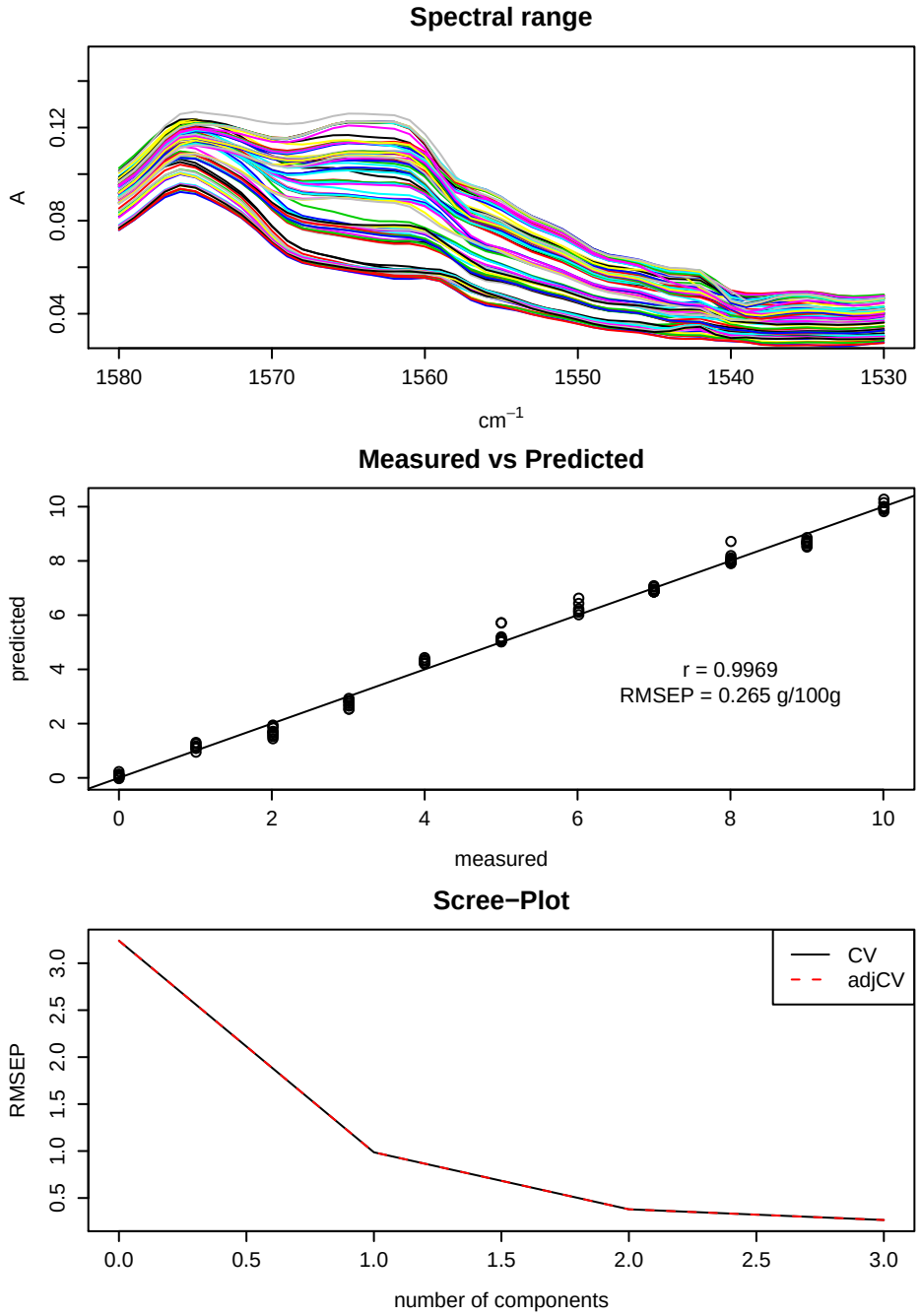

Figure 5.31: Quantitative analysis of Paracetamol ("Impurity") in Aspirin by PLS in Middle Infrared. Upper: Calibration spectra. Middle: Prediction plot. Lower: RMSEP Scree plot.

5.4.2.1 Preparation of samples and recording of spectra

The samples in this experiment are the one that were employed in section 5.4.1.1 on page 83. Care was taken to pack the powder uniformly in the glass vial by dropping the filled vial 50 times on to the cardboard for all the samples since loosely packed powder will lead to baseline shifts. The NIR spectrometer was set to the specification stated in Table 5.7 on page 65. After acquiring a background spectrum with Spectralon, three spectra of each sample were recorded in sequence, then the powder was unpacked and repacked into the glass vial. This process was performed three times resulting in nine spectra for each sample. This procedure was followed for the pure Aspirin also.

5.4.2.2 Analysis of spectra using spectral purity parameters

The moving window approach showed the spectral wavenumber range of 6800-6000 cm^{-1} to be the most suitable one for applying the spectral purity parameters. Unlike in Mid IR these parameters show a much better reproducibility from spectrum to spectrum as seen in Fig. 5.32 on page 89 (see also Fig. 5.30 on page 85 for comparison).

The LOD and LOC of the impurity paracetamol were found to be 0.034 g/100 g and 0.145 g/100 g for SPR_2 and 0.945 g/100 g and 1.891 g/100 g for SPR_4 (see Table. 5.15). As already in some former cases SPR_3 did not prove to be useful. Compared to the Middle Infrared the LOD of SPR_2 is lower by a factor of about 6.

Table 5.15: LOD and LOC values for experiment with impurity Paracetamol in Aspirin (Near Infrared region).

Parameter	LOD g/100g	LOC g/100g
SPR_1	-	-
SPR_2	0.034	0.145
SPR_3	-	-
SPR_4	0.945	1.891

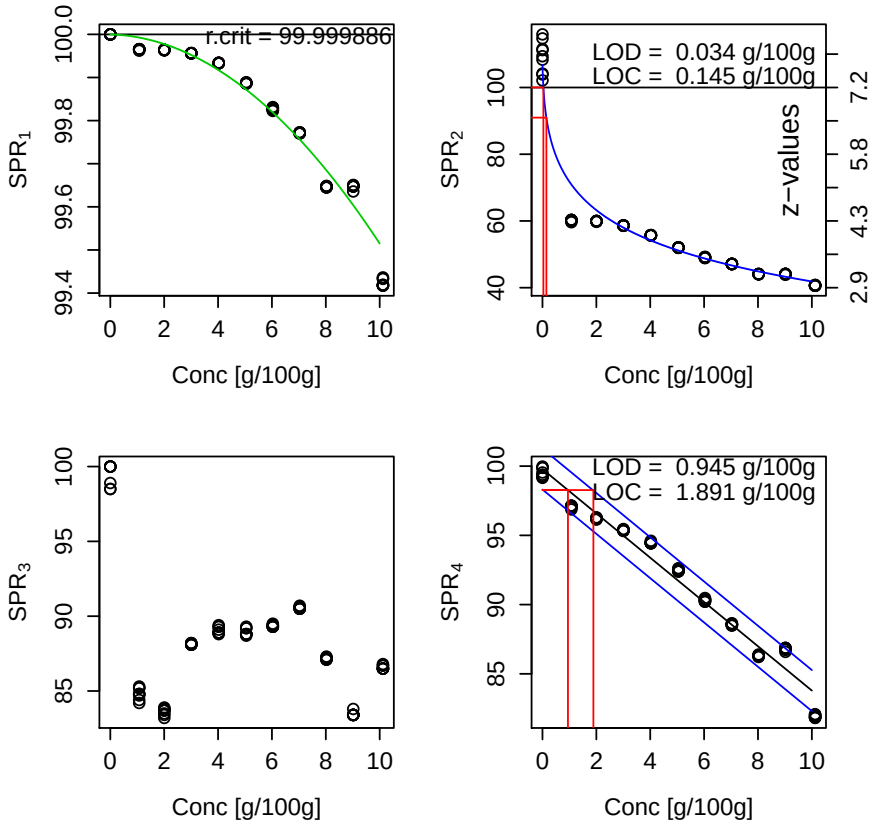

Figure 5.32: Dependency of spectral purity parameters of Aspirin on the concentration of impurity Paracetamol in the spectral range 6800-6000 cm^{-1}.

5.4.2.3 Quantitative analysis

For quantitative analysis of the impurity like in previous experiments a PLS calibration was performed on the spectra of the samples. Using three factors and the spectral range of 6800-6000 cm^{-1}, the RMSEP value was determined to be 0.249 g/100 g (Fig. 5.33 on page 90).

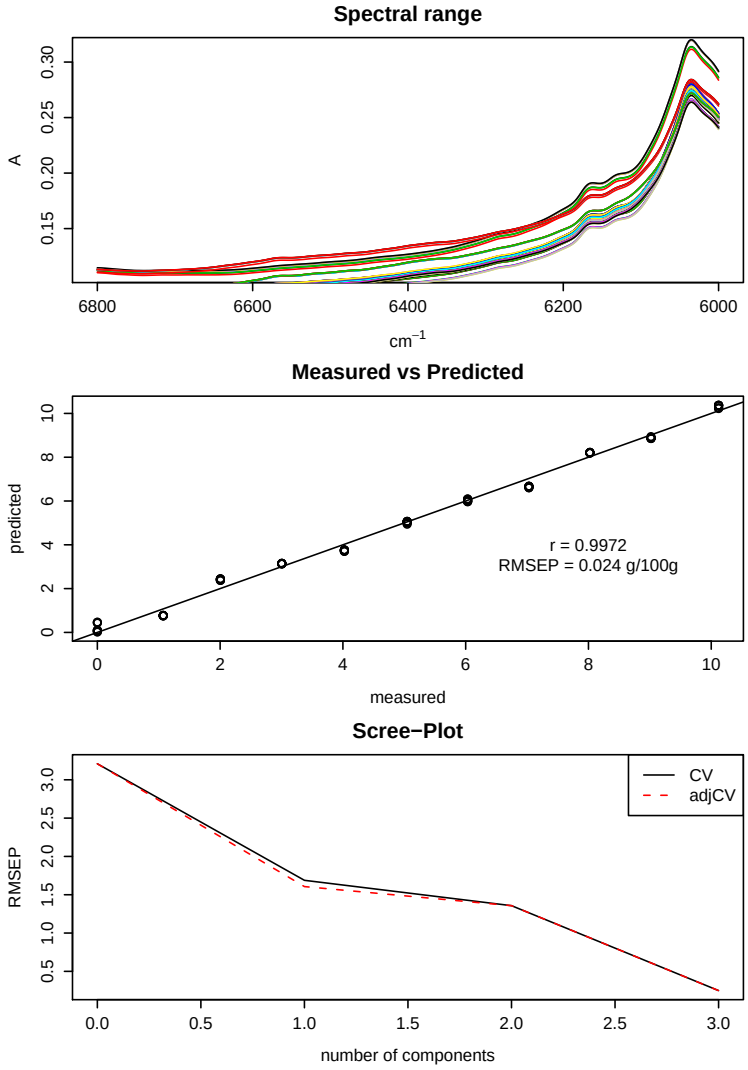

Figure 5.33: Quantitative analysis of Paracetamol ("Impurity") in Aspirin by PLS in Near Infrared. Upper: Calibration spectra. Middle: Prediction plot. Lower: RMSEP Scree plot.

6

Purity control of Water with respect to contamination by hydrocarbons

For a long time in order to determine the hydrocarbons (e.g. Mineral oil, Diesel oil, etc.) in water the DIN 38409 H18 [64] method was employed. This method demands the use Carbon tetrachloride or 1,1,2-Trichloro-1,2,2-trifluoroethane commercially known as Freon as extractant. Both are problematic solvents. Carbon tetrachloride is carcinogenic and therefore completely banned for routine analysis in labs. Freon is an "ozone killer" and by this is environmentally harmful. As an alternative solvent Tetrachloroethylene is used in USA. Meanwhile, the use of chlorofluorocarbons (CFCs) is generally prohibited by the European commission (Article 4 of Council regulation-EC.no 2037/2000) [65] in acceptance of the Montreal Protocol [66]. Tetrachloroethylene due to its probable carcinogenic nature is prohibited in some countries, e.g. Austria. Consequently, DIN 38409 H18 method has been abandoned and is replaced with DIN EN ISO 9377-2 (H53) [67], which is based on a determination using gas chromatography.

The Hydrocarbons in water can also be determined by EPA 1664 method [68]. In this method n-Hexane is used for extraction and after its evaporation the hydrocarbon content is gravimetrically obtained. Instead of gravimetric analysis, IR-ATR determination is proposed and even a device for this purpose is manufactured and sold by Wilks Enterprise Inc [69]. Both these methods have the

disadvantage of a potential loss of low volatile hydrocarbons during evaporation. As a consequence direct IR spectrometric determination in the solvent used for extraction of the water samples is favored and this has additional advantages like better accuracy than the gravimetric resp. IR-ATR methods and higher speed than the gas chromatographic methods.

n-Hexane however cannot be used as extractant in the case of an IR-spectrometric determination due to its CH_2/CH_3-absorptions. As a substitute to n-Hexane one can use Cyclohexane which in contrast to the common hydrocarbons does not posses any methyl (CH_3-) groups. The main purpose of this chapter is to compare the efficiency of a FT-IR spectrometer and a Spectrometer with a Quantum Cascade Laser (QCL) as radiation source in the determination of hydrocarbons in water because this may open also new prospects for purity control.

6.1 Calibration of Diesel oil in Cylcohexane

In this section the IR-spectrometric determination of hydrocarbons in Cyclohexane is described. As an example for hydrocarbons we use a Diesel oil standard. The determination was performed in transmittance in a CaF_2 cell.

6.1.1 Calibration with a FT-IR spectrometer

After some preliminary experiments the thickness of the CaF_2 cell was set to d = 1.7 mm. One would like to have a cell thickness as high as possible because due to Beer-Lambert's Law the sensitivity of spectrometric analytical method is directly proportional to the path length.

In the case of DIN 38409 H18 were Freon was used as solvent for extraction one could work with extraordinarily high cell thicknesses of 0.5 to 5 cm. With Cyclohexane this is not possible because at the measuring wavenumber of 1377 cm^{-1} it shows a rather high baseline absorption.

This situation is demonstrated in Fig. 6.1 on page 93 which shows the spectrum of Cyclohexane at a cell thickness of a 1.7 mm together with the ATR spectrum of Diesel oil. One can recognize easily that at the measuring wavenumber of 1377 cm^{-1}, Cyclohexane does not show any absorption bands, however its

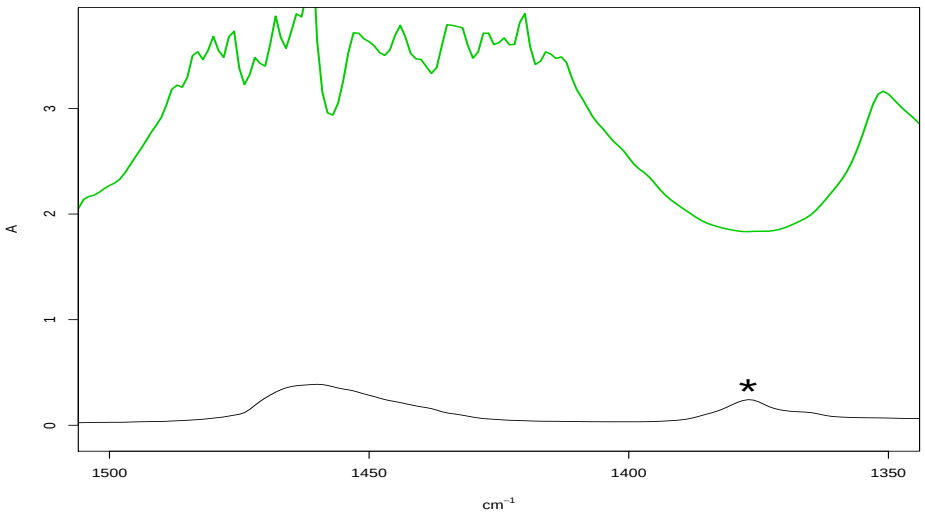

Figure 6.1: FT-IR spectrum of Cyclohexane (green) (1.7 mm thickness) and ATR spectrum of Diesel oil (black) in the CH_3/CH_2 absorption region. The measuring wavelength of 1377 cm^{-1} is marked with an asterisk.

baseline absorption at this position is about of 1.8 absorbance units. The band marked with an asterisk is the CH_3- band of Diesel oil which is utilized for the quantitative analysis.

The samples were directly prepared by adding Diesel oil to Pure Cyclohexane (SIGMA-ALDRICH GmbH, Germany), thereby avoiding the extraction process, i.e. no direct investigation of aqueous samples was performed. The presentation of analytical results however is based on Diesel oil in water under the assumption that when an extraction is performed, it gives an enrichment by a factor of 18. If one wants to refer the concentration in Cyclohexane, these concentrations must be multiplied by a factor of 18. A certain amount of Diesel oil (BAM H53 standard, Dr. Ehrenstofer GmbH, Germany) was placed in a volumetric flask and weighed followed by filling in Cyclohexane in small increments with stirring. The higher concentrations were weighed directly and the lower concentrations were produced by appropriate dilutions. Table 9.3 on page 135 in the Appendix shows the standards used for calibration.

The samples were pipetted into the CaF_2 cuvette and three consecutive spec-

tra were recorded, followed by cleaning the cuvette with pure Cyclohexane and vacuum drying. Following this method three spectra for all the samples were obtained. The same procedure was followed for the three spectra of pure Cyclohexane also. Fig. 6.2 shows spectra taken in the concentration range of 0.006 mg/L up to 54.8 mg/L Diesel oil in water. The actual concentration in Cyclohexane are higher by a factor of 18 because for the extraction of oil from water, where usually 900 ml of water is extracted with 50 ml of Cyclohexane.

For the purpose of compensating the spectrum of Cyclohexane, in the next step the spectrum of pure Cyclohexane is subtracted from the spectra of Fig. 6.2.

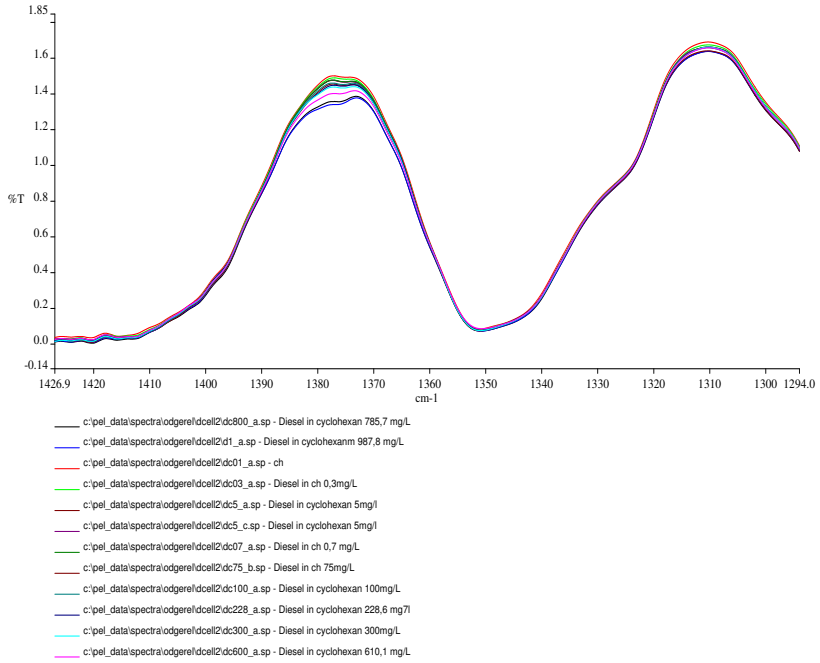

Figure 6.2: Spectra of Diesel oil (in Cyclohexane extract) in the concentration range of 0.006 - 54.8 mg/L referring to the concentration in water.

Fig. 6.3 on page 95 shows that at low concentrations the baseline shifts to higher values. Baseline shifts can be eliminated by calculating derivatives as depicted in Fig. 6.4 on page 96.

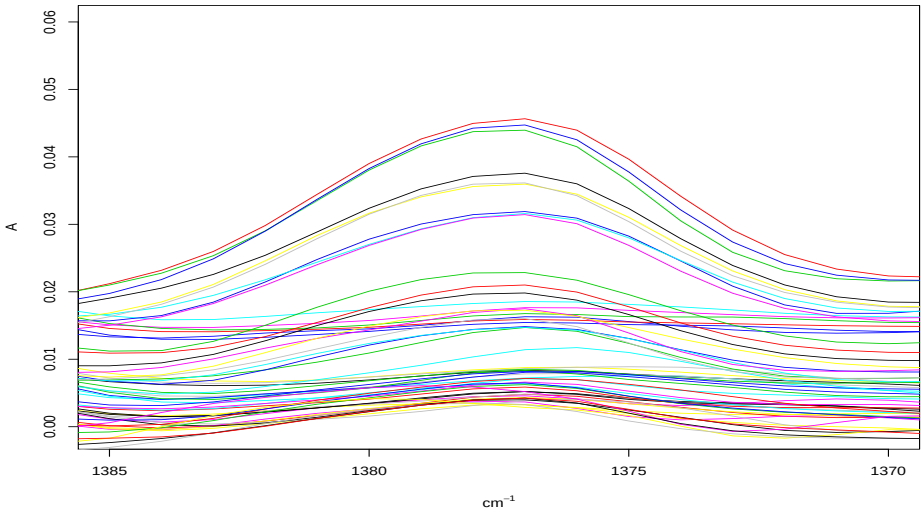

Figure 6.3: Difference spectra after subtraction of the spectrum of pure Cyclohexane from the spectra of Fig. 6.2.

As signal for this quantitative analysis of Diesel oil, the absolute values of the ordinate of the second derivative spectra at 1377 cm^{-1} were used. Fig. 6.5 on page 96 shows the resulting calibration.

The residual standard error of the method is 2.37 mg/L. The limit of detection, limit of capture and limit of quantification were determined as per section 2.4 on page 24 to be 4.02 mg/L, 8.04 mg/L and 14.39 mg/L. The residuals plot shows relative uniform distribution (Fig. 6.6 on page 97). The QQ plot confirms a near normal distribution of the residuals (Fig. 6.7 on page 97). These results above refer to concentrations in water. If we refer to the concentration of Diesel oil in Cyclohexane we get the following values, 72 mg/L LOD, 144 mg/L LOC and 259 mg/L LOQ.

6.1.2 Calibration with a Quantum Cascade Laser spectrometer

The Eracheck Laser Instrument described in the section 3.1.4 on page 29 and shown in Fig. 9.4 on page 109 in the Appendix was used for this experiment.

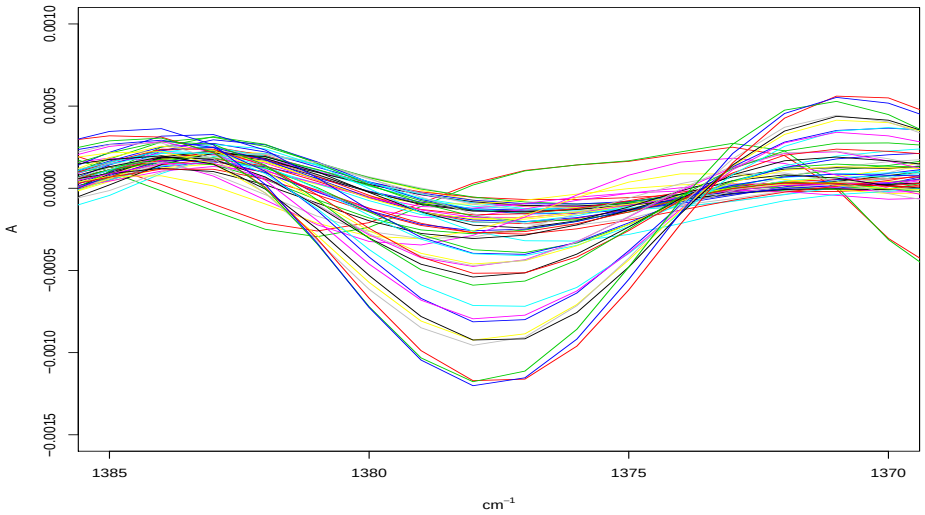

Figure 6.4: Second derivative of the difference spectra of Fig. 6.3.

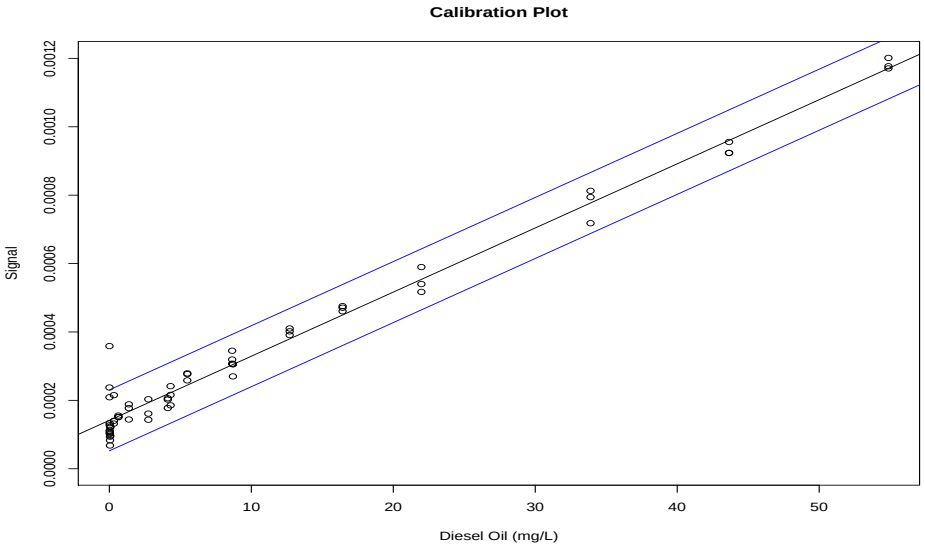

Figure 6.5: Calibration line with prediction bands for Diesel oil in the concentration range 0.006 - 54.8 mg/L (evaluation via second derivative of FT-IR spectra).

The cell thickness was between 2-3 mm. By increasing the cell thickness the sensitivity of the calibration is enhanced. However at the same time the background absorbance of Cyclohexane increases also to about 2.3 absorbance units. In the

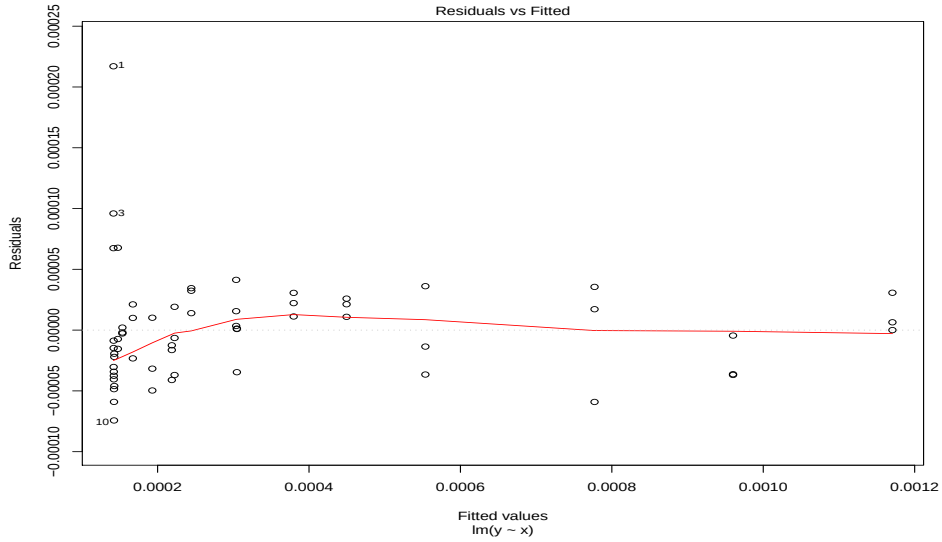

Figure 6.6: Residuals plot for the calibration in Fig. 6.5.

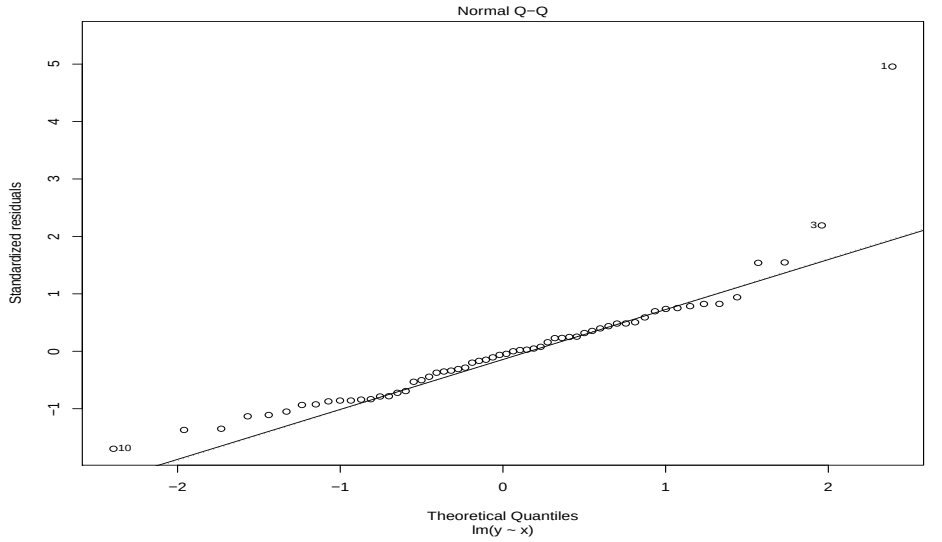

Figure 6.7: QQ plot for the calibration in Fig. 6.5.

case of a FT-IR spectrometric analysis this would lead to unacceptable high noise which is not the case here due to the high throughput of the laser.

The sample solution was transfered with an integrated membrane pump into

the cell. For this purpose 10 ml of sample solution is needed. After filling the cell the absorbance at the laser wavenumber between 1370-1380 cm^{-1} is measured. After each measurement the cell is rinsed with pure Cyclohexane (again 10 ml). While rinsing the absorbance of the pure Cyclohexane is measured at the laser wavenumber. Then the difference between the absorbance of the sample and pure Cyclohexane is stored internally and used for calibration. By repeating this procedure two times three absorbance values for each sample were obtained. Fig. 6.8 on page 99 shows the corresponding calibration which is considerably superior to the one with FT-IR spectrometer. The residual standard error is now 0.13 mg/L. The limit of detection is 0.22 mg/L, limit of capture is 0.44 mg/L and limit of quantification is 0.80g/L. This is an improvement of more than one order of magnitude compared to the measurements with a FT-IR spectrometer. The residuals show a uniform distribution around zero (Fig. 6.9 on page 99). Also with the QQ plot one can assume again a normal distribution of the residuals (Fig. 6.10 on page 100). The results above refer to water. If we refer to the concentration of Diesel oil in Cyclohexane we get the following values 3.6 mg/L LOD, 7.2 mg/L LOC and 14.4 mg/L LOQ.

This large improvement compared to the results obtained with the FT-IR spectrometer is attributed to the radiation source in the spectrometer. A QC laser provides higher power density at the sample and higher throughput, which is at least 400x times higher per wavelength compared to traditional IR sources. Therefore these QC lasers give much higher signal-to-noise ratio even at higher sample thicknesses [42].

There are spectrometers available in the market with tunable QC lasers, especially for trace analysis of gases. These spectrometers have scan ranges from 1600-1000 cm^{-1} [70]. It is expected that the overall spectral range covered by the lasers will increase to around 2000 cm^{-1} in the near future and spectral recording time will be drastically reduced to milliseconds [42]. When a full fledged laser spectrometer for the complete MIR range is available one should be able to reach very low levels of detection down to ppm levels by employing the spectral purity parameters ($SPR_1 - SPR_4$) developed in this thesis.

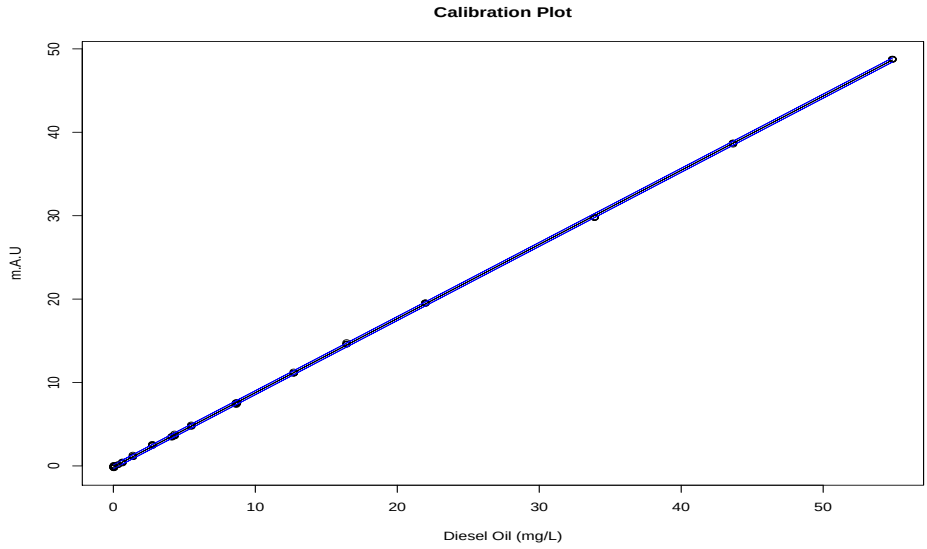

Figure 6.8: Calibration line with prediction bands for Diesel oil (in Cyclohexane extract) in concentration range 0.006 - 54.8 mg/L referring to the concentration in water. The evaluation was performed at the laser wavenumber between 1370-1380 cm^{-1}.

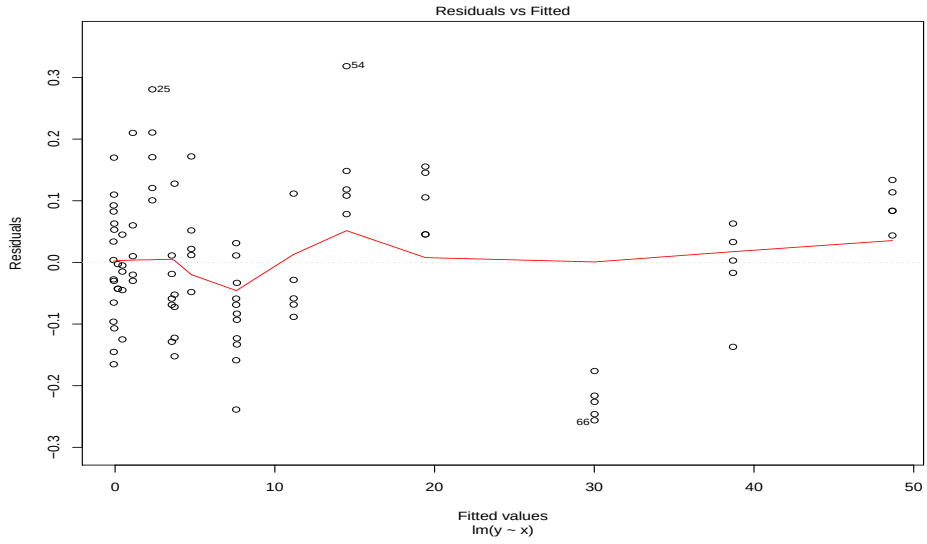

Figure 6.9: Residuals plot for the calibration in Fig. 6.8.

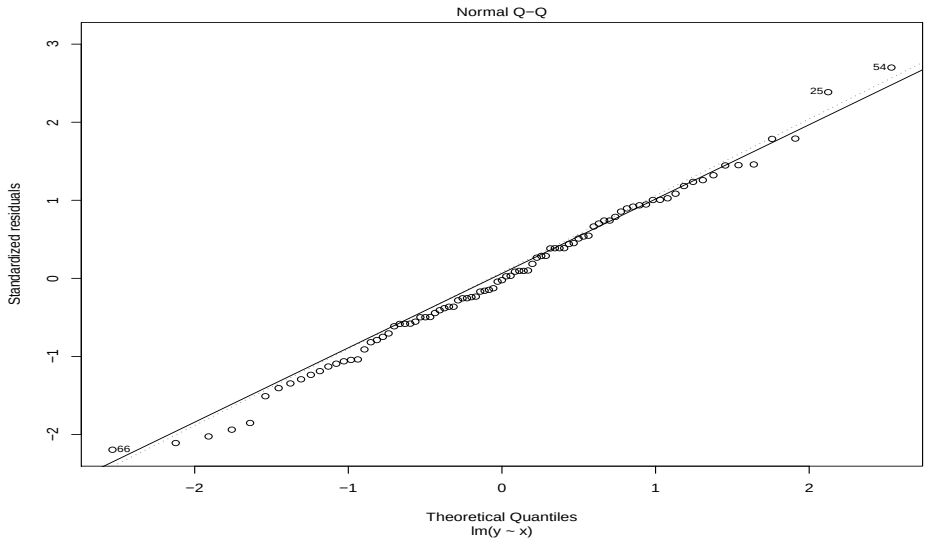

Figure 6.10: QQ plot for the calibration in Fig. 6.8.

7

Discussion and outlook

The main aim of this thesis was to develop universal methods for the detection of various types of possible impurities present in raw materials or other chemical products using Infrared spectroscopy. For this purpose four spectral purity parameters were formulated basing on the fact that each organic compound and many inorganic compounds are Infrared active and have characteristic spectra which are unique to the respective substance. When a contamination occurs the spectra may differ slightly or prominently from the spectrum of the pure reference substance depending on the nature of the impurity present.

The first two of these spectral purity parameters (SPR_1 and SPR_2) were derived from regressing the sample spectrum on the reference spectrum and the second two were derived from the principles of difference spectroscopy (SPR_3 and SPR_4).

SPR_1 corresponds to the correlation coefficient r multiplied by 100. The correlation coefficient has been used successfully in the past for the purpose of identity control [21]. However in this thesis it is shown that especially for determining detection limits it is advantageous to transform r into Fisher's z-coefficient. Therefore we defined a new purity parameter SPR_2 based on the normalized z-value [71]. As could be shown by simulation studies SPR_2 shows a concave behavior with increasing impurities and thereby is especially sensitive to small impurities.

As mentioned SPR_3 and SPR_4 are based on difference spectroscopy. Normally to find the optimal compensation, i.e. the optimal difference factor, dif-

ference spectroscopy is performed manually. But for process environments automatic routines have to be used. Therefore a method of "dynamic difference spectroscopy" was developed which determines the optimal difference factor f_{opt} automatically. SPR_3 corresponds to f_{opt} multiplied by 100. In some cases however SPR_3 did show no favorable behavior at very low impurities. In this case SPR_4 which corresponds to the integral of the difference spectrum gave somewhat better results.

Therefore in the following final discussion only SPR_2 (from regression) and SPR_4 (from difference spectroscopy) will be mentioned.

As sampling methods in the Middle Infrared we used a Diamond ATR accessory for both liquids and solids. This is much more convenient than using traditional IR cuvettes or KBr disks. In the Near Infrared we used quartz cuvettes (1 mm thickness) for liquids and a Diffuse reflection accessory for solids.

At first spectral purity parameters were applied on the spectra obtained from liquid samples (Palatinol plasticizers and water) followed by the solid samples (Aspirin).

In the first experiment the purity of Palatinol-N was tested. To imitate contaminations three different compounds were selected which uniquely differ from the spectrum of pure Palatinol-N. One differs in the finger print region, another in the C-H stretch region and still another in both the regions.

At first Palatinol-AH was used to induce the contamination. This compound has a very similar spectrum as that of Palatinol-N and differs only slightly in the fingerprint region. In spite of this, the presence of this impurity can be detected down to 0.1 g/100 g with SPR_2 and about 1 g/100 g with SPR_4 when the Middle Infrared spectra were analyzed. Due to the extreme similarity between the NIR spectrum of Palatinol-AH and Palatinol-N further analysis with spectral purity parameters was not performed in the NIR.

The second contaminant used for imitation of a contamination of Palatinol-N was Palatinol-911P, the spectrum of which differs in the C-H stretch region (3200-2800 cm^{-1}). In the Middle Infrared detection limit down to again a level of 0.1 g/100 g for SPR_2 and of 0.8 g/100 g for SPR_4 is obtained. In this case even the NIR spectra are different enough for using them for purity control and the obtained limits of detection were 0.3 g/100 g for SPR_2 and 0.8 g/100 g for

SPR_4. It is remarkable that here difference spectroscopy gives a better result than that of Middle Infrared. This is probably due to the fact that noise and reproducibility of baseline is better in the Near Infrared.

The third compound used for impurifying Palatinol-N was Reofos-50. This compound is chemically and spectrally very different from Palatinol-N. In this experiment one can use almost the complete spectral range both in MIR and NIR unlike restricted spectral ranges in the other experiments. The reason for this are the prominent differences in both the C-H stretch and the fingerprint regions. In the Middle Infrared using SPR_2 a limit of detection down to a level of 0.002 g/100 g could be achieved which corresponds to 20 ppm. With Near Infrared and SPR_2 the limit of detection is 0.1 g/100 g. So in this case the Middle Infrared is more sensitive for detecting impurities than the Near Infrared. The reason for this is the fact that the spectra in the Middle Infrared differ much more than in the Near Infrared. For SPR_4 one gets a limit of detection of 0.2 g/100 g for the Near Infrared and 1.87 g/100 g in the Middle Infrared. So the general impression that the regression method is more suitable in detecting impurities compared to the difference method is confirmed.

To further validate these results an experiment vice versa to the first experiment was performed, i.e. Palatinol-AH was used as pure substance and Palatinol-N as contaminant. Like before in this case only MIR studies were performed. The detection limits obtained were similar to that of the first experiment.

As a further example purity control of water was performed in the Middle Infrared. The contamination was induced by addition of Potassium hydrogen Phthalate to the water samples. This analysis again demonstrates the high efficiency of the spectral purity parameter SPR_2 for detecting low impurities down to a concentration of 0.008 g/100 g. SPR_4 gives a limit of detection of 0.2 g/100g.

For tests on solids an experiment with Aspirin as pure reference substance and Paracetamol as impurity was performed. For the MIR spectra detection of impurities down to a level of 0.18 g/100 g was obtained with SPR_2 and to a level of 0.9 g/100 g with SPR_4. Much better LOD result of 0.03 g/100g for SPR_2 was obtained with NIR spectra. With SPR_4 same like MIR about 0.9 g/100 g LOD was achieved with NIR.

Table 7.1: Summary of results for purity control of liquids and solids

Reference substance	Impurity	LOD g/100 g $-SPR_2$		LOD g/100 g $-SPR_4$	
		MIR	NIR	MIR	NIR
	LIQUIDS				
Palatinol-N	Palatinol-AH	0.1	-	1	-
Palatinol-N	Palatinol-911P	0.1	0.1	0.8	0.3
Palatinol-N	Reofos-50	0.002	0.1	1.8	0.2
Palatinol-AH	Palatinol-N	0.1		1	
Water	KHP	0.008	-	0.2	-
	SOLIDS				
Aspirin	Paracetamol	0.1	0.03	0.9	0.9

Table 7.1 shows a summary of the results. From this one can draw the following conclusions. SPR_4 resulting from difference spectroscopy gives not as good results as SPR_2. But in practice the calculated difference spectra might be useful for identifying an impurity.

SPR_2 resulting from linear regression was therefore found to be the most effectual parameter for detecting impurities. One can expect that for liquids one achieves a limit of detection between 0.001-0.1 g/100 g in the Middle Infrared depending on the degree of difference between the spectrum of the impurity and the reference substance. NIR is not as sensitive as MIR and we can expect an LOD of about 0.1 g/100 g.

In contrast to liquids in solids (powders) the homogeneity is considerably less than in liquids. So even when the spectra of the reference substance and the contaminant are quite different we will achieve detection limits not far below 0.1 g/100 g for the Middle Infrared and 0.03 g/100 g in the Near Infrared. It should be remarked that Diffuse reflectance in the NIR is much more powerful for detecting impurities than ATR in the Middle Infrared.

Due to the discussion above one can state that with conventional Middle and Near Infrared spectroscopy one can detect impurities of at least 0.1 % which is a goal in accordance, e.g. with a recommendation of the ICH for quality control of drugs [6].

But do we have a chance to proceed to lower trace levels with Infrared spectroscopy? Certainly not with conventional instrumentation. But it is shown in this thesis in the context of determining hydrocarbons in water that with an IR quantum cascade laser a detection limit of 4 mg Diesel oil in 1 liter of Cyclohexane can be achieved corresponding to about 4 ppm. This was with a fixed laser wavenumber between 1370-1380 cm^{-1}. But tunable quantum cascade lasers are available already in the market and rapid progress is made in this field. Using this kind of lasers and applying the spectral purity control methods developed in this thesis, routine Infrared spectrometric quality control for impurities in the ppm range may be feasible in the near future.

8

Summary

In this thesis computational methods for spectrometric purity control in Middle and Near Infrared were developed and tested with practical examples. Two different principles were applied, viz. linear regression of the spectra and difference spectroscopy.

The methods based on linear regression proved be more effective and limits of impurities down to 0.002 g/100 g for liquids and 0.03 g/100 g for solids could be achieved. Detection of impurities considerably below these limits is not possible with conventional MIR/NIR instrumentation. But in the context of the determination of hydrocarbons in water by extraction with Cyclohexane with an IR quantum cascade laser at a fixed wavenumber a limit of detection of about 4 ppm could be obtained. So there are good prospects that with the advent of broadly tunable quantum cascade lasers IR purity control in the ppm range will become possible in the near future.

All spectra and R-program codes used in this thesis are publicly available under http://bscw.uni-duisburg-essen.de/pub/bscw.cgi/11186089

9

Appendix

Figure 9.1: PerkinElmer-System 2000 FT-IR spectrometer with single reflection Diamond unit.

Figure 9.2: An enlarged picture of single reflection Diamond ATR unit. Only few mg of solid sample are required to obtain a spectrum.

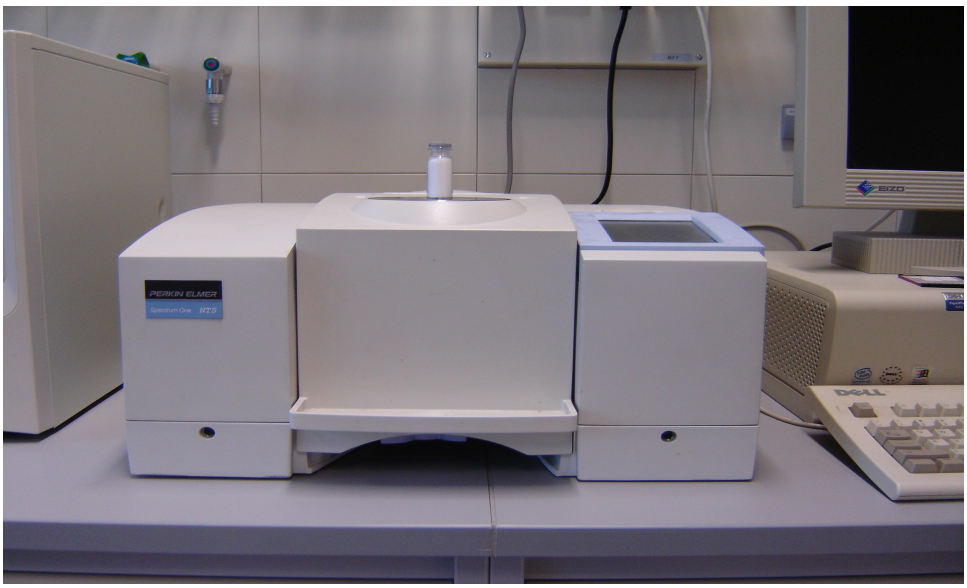

Figure 9.3: PerkinElmer-Spectrum One NTS spectrometer with Diffuse reflection accessory and a sample on it.

Figure 9.4: Eracheck spectrometer.

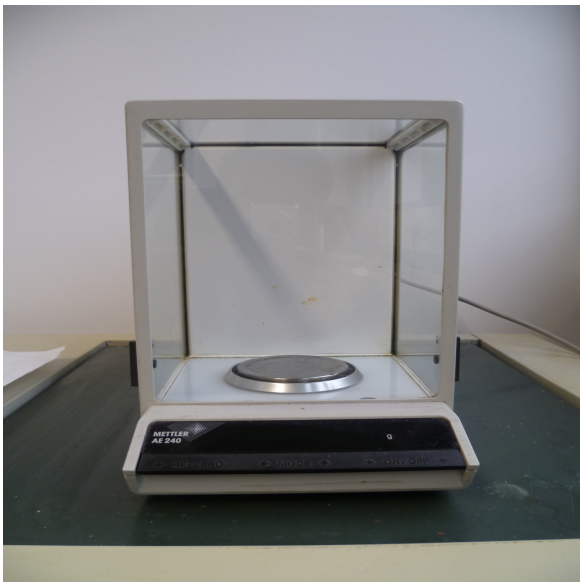

Figure 9.5: Mettler Toledo AE 240 electronic balance.

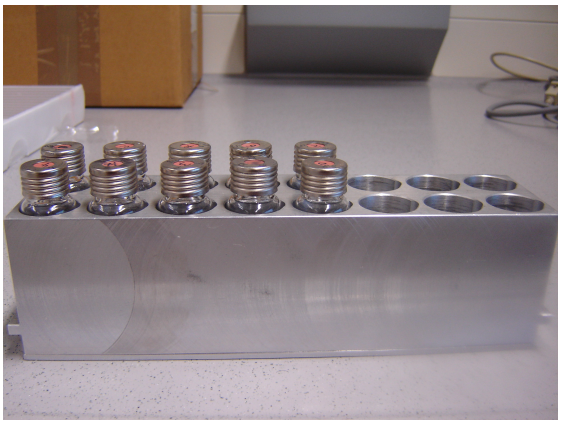

(a) Glass vials with liquid samples.

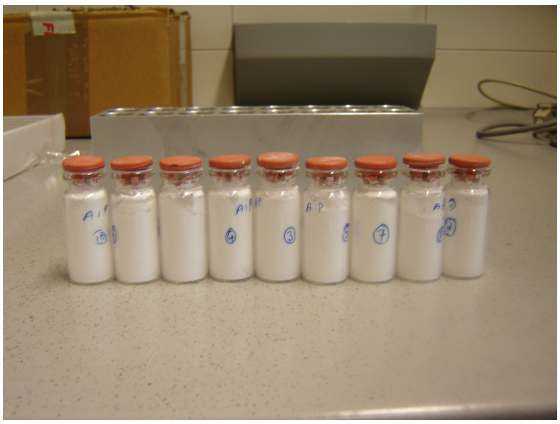

(b) Glass vials with solid samples.

Figure 9.6: Glass vials with samples.

(a) CaF_2 cell of thickness 1.7 mm.

(b) Quartz cell of thickness 1 mm.

Figure 9.7: Transmission cells.

Figure 9.8: Vibratory Micro-Mill "Pulverisette 0".

1. R-code for calculating and plotting the spectral purity parameters

```
THIS IS THE CODE FOR CALCULATIONG AND PLOTTING SPECTRAL PURITY PARAMETERS
read.spectrum <- function(SpectrumName){
con <- file(SpectrumName, "rt", blocking = FALSE)
i.line=0
zeile = "Zeile"
while(zeile != "#DATA"){
i.line=i.line +1
zeile <- readLines(con,n=1)
}
close(con)
spectrum <- read.table(SpectrumName,skip=i.line)
spectrum
}
cround <- function(x,n){
vorz <- sign(x)
z <- abs(x)*10^n
z <- z + 0.5
z <- trunc(z)
z <- z/10^n
z*vorz
}
boolA <- FALSE
boolB <- FALSE
boolC <- FALSE
boolNorm <- TRUE
Empfindlichkeit <- 5
Shift <- 0
upper.B <- 1000
lower.B <- 800
list <- read.csv2("C:/purity/mixVsPAN.csv")
n<-length(list[,1])
Reinheitsgrad1.A <- 1:n
Verunreinigung.A <- 1:n
Reinheitsgrad2.A <- 1:n
Korr1.A <- 1:n
```

```
Sigma1.A <- 1:n
Korr2.A <- 1:n
Sigma2.A <- 1:n
Z1.A<-1:n
Z2.A<-1:n
for (i in 1:n){
spec<-read.spectrum(as.character(list$MeanPalN[i]))
colnames(spec) <- c("x","y")
spec.ref <- spec[spec$x >=lower.B & spec$x <=upper.B,]
x <- spec.ref$x
y <- spec.ref$y/100
#y[spec$x <= 2400 & spec$x >= 1850] <- 1
y[y<=1e-4] <- 1e-4
y <- -log10(y)
y <- y - min(y)
N_1 <- 1
y <- N_1*y
spec.ref <- data.frame(x=x,y=y)
t.spec.ref <- 10^(2-y)
t.spec.ref <- data.frame(x=x,y=t.spec.ref)

spec<-read.spectrum(as.character(list$Mixtures[i]))
colnames(spec) <- c("x","y")
spec.gem <- spec[spec$x >=lower.B & spec$x <=upper.B,]
x <- spec.gem$x
y <- spec.gem$y/100
#y[spec$x <= 2400 & spec$x >= 1850] <- 1
y[y<=1e-4] <- 1e-4
y <- -log10(y)
y <- y - min(y)
N_2 <- 1
y <- N_2*y
spec.gem <- data.frame(x=x,y=y)
t.spec.gem <- 10^(2-y)
t.spec.gem <- data.frame(x=x,y=t.spec.gem)
sum.minus.dif <- NULL
```

```
factors <- NULL
summe <- NULL
factor <- seq(-1,2,0.001)
for (j in 1:length(factor)){
dif <- spec.gem$y-factor[j]*spec.ref$y
sum.minus.dif[j] <- -sum(dif[dif<0],na.rm=TRUE)
}
Diff2 <- diff(diff(sum.minus.dif))
(Threshold <- max(Diff2)/Empfindlichkeit)
(Faktor.Index <- which(Diff2 >= Threshold)[1])
(Faktor <- factor[Faktor.Index+2-Shift])
Faktor.direct <- Faktor
if (Faktor > 1) Faktor <- 1
Reinheitsgrad1.A[i] <- Faktor
Reinheitsgrad1.A[i]
dif<-spec.gem$y-Faktor*spec.ref$y
Verunreinigung.A [i]<- sum(dif[dif>0])/sum(spec.ref$y)
Reinheitsgrad2.A[i] <- 1-Verunreinigung.A[i]
Reinheitsgrad2.A[i]
#####Plot of Difference Spectrum
if (boolA){
dif <- dif/N_1
dif <- 10^(2-dif)
t.spec.dif <- data.frame(x,dif)
lower <- min(c(min(t.spec.gem),min(t.spec.ref),min(t.spec.dif)))
windows(7,7)
plot(t.spec.dif,ylim=c(lower,110),xlim=c(max(x),min(x)),col=2,type="l",
sub=paste("Shift = ",as.character(Shift), " /Sensitivity =" ,
 as.character(Empfindlichkeit),
 "/Factor =",as.character(Faktor),sep=""),main=paste(as.character(list$ref2[i])
 " vs ",
 as.character(list$name[i]),sep=""))
text(1600,60,paste("R1.A = ",as.character(Reinheitsgrad1.A[i]),sep=""))
text(1600,50,paste("R2.A  = ",as.character(Reinheitsgrad2.A[i]),sep=""))
text(1600,40,paste("V.A = ",as.character(Verunreinigung.A[i]),sep=""))
lines(t.spec.ref,col=4)
```

```
lines(t.spec.gem,col=1)
}
######Plot of Diff Characteristics
if (boolB){
windows(9,9)
factor.i <- (1 + 2 ):3001
Factor <- factor[factor.i]
plot(Factor,Diff2,type="l",col=1,main=paste(as.character(list$ref2[i])," Vs ",
 as.character(list$name[i]),sep=""),sub=paste("Shift = ", as.character(Shift),
  " /Sensitivity =" ,
   as.character(Empfindlichkeit)," /Factor = ", as.character(Faktor),sep=""))
abline(h=Threshold,col=2)
abline(v=Faktor,col=3)
if (Faktor.direct != Faktor) abline(v=Faktor.direct,col=4)
text(-0.6,0.4,paste("R1.A= ",as.character(Reinheitsgrad1.A[i]),sep=""))
text(0.0,0.6,paste("R2.A = ",as.character(Reinheitsgrad2.A[i]),sep=""))
text(0.0,0.8,paste("V.A  = ",as.character(Verunreinigung.A[i]),sep=""))
}
model1 <- summary(lm(spec.gem$y ~ spec.ref$y,weights=10^-spec.ref$y))
model2 <- summary(lm(spec.gem$y ~ spec.ref$y))
Korr1.A[i] <- sqrt(model1$r.squared)
Sigma1.A[i] <- model1$sigma
Z1.A[i]<- 0.5*log((1+Korr1.A[i])/(1-Korr1.A[i]))
Korr2.A[i]<- sqrt(model2$r.squared)
Sigma2.A[i] <- model2$sigma
Z2.A[i] <- 0.5*log((1+Korr2.A[i])/(1-Korr2.A[i]))
}
#######################################  2nd Part!!!! ##########################
upper.B <- 3200
lower.B <- 2750
list <- read.csv2("C:/purity/mixVsPAN.csv")
n<-length(list[,1])
Reinheitsgrad2.B <- 1:n
Verunreinigung.B <- 1:n
for (i in 1:n){
spec<-read.spectrum(as.character(list$MeanPalN[i]))
```

```
colnames(spec) <- c("x","y")
spec.ref <- spec[spec$x >=lower.B & spec$x <=upper.B,]
x <- spec.ref$x
y <- spec.ref$y/100
y[y<=1e-4] <- 1e-4
y <- -log10(y)
y <- y - min(y)
N_1 <- 1
if (boolNorm) N_1 <- 1/sqrt(sum(y^2))
y <- N_1*y
spec.ref <- data.frame(x=x,y=y)
t.spec.ref <- 10^(2-y)
t.spec.ref <- data.frame(x=x,y=t.spec.ref)

spec<-read.spectrum(as.character(list$Mixtures[i]))
colnames(spec) <- c("x","y")
spec.gem <- spec[spec$x >=lower.B & spec$x <=upper.B,]
x <- spec.gem$x
y <- spec.gem$y/100
y[y<=1e-4] <- 1e-4
y <- -log10(y)
y <- y - min(y)
N_2 <- 1
if (boolNorm) N_2 <- 1/sqrt(sum(y^2))
y <- N_2*y
spec.gem <- data.frame(x=x,y=y)
t.spec.gem <- 10^(2-y)
t.spec.gem <- data.frame(x=x,y=t.spec.gem)

#########################################################
Faktor <- Reinheitsgrad1.A[i]
dif<-spec.gem$y-Faktor*spec.ref$y
Verunreinigung.B [i]<- sum(dif[dif>0])/sum(spec.ref$y)
Reinheitsgrad2.B[i] <- 1-Verunreinigung.B[i]
Reinheitsgrad2.B[i]
#################################################################
```

```
#####Plot of Difference Spectrum
if (boolC){
dif <- dif/N_1
dif <- 10^(2-dif)
t.spec.dif <- data.frame(x,dif)
lower <- min(c(min(t.spec.gem),min(t.spec.ref),min(t.spec.dif)))
windows(7,7)
plot(t.spec.dif,ylim=c(lower,110),xlim=c(max(x),min(x)),col=2,type="l",
sub=paste("Shift = ", as.character(Shift), " /Sensitivity =" ,
 as.character(Empfindlichkeit)," /Factor = ", as.character(Faktor)
 ,sep=""),main=paste(as.character(list$name2[i])," vs ",as.character
 (list$name[i]),sep=""))
text(3400,70,paste("R2.B  = ",as.character(Reinheitsgrad2.B[i]),sep=""))
text(3400,80,paste("VB = ",as.character(Verunreinigung.B[i]),sep=""))
lines(t.spec.ref,col=4)
lines(t.spec.gem,col=1)
}
}
###################################
Reinheitsgrad1.A<- cround(Reinheitsgrad1.A,8)
Verunreinigung.A <-cround(Verunreinigung.A,8)
Reinheitsgrad2.A<-cround(Reinheitsgrad2.A,8)
Korr1.A <-cround (Korr1.A,8)
Sigma1.A<-cround (Sigma1.A,8)
Korr2.A <-cround(Korr2.A,8)
Sigma2.A<-cround(Sigma2.A,8)
Z1.A<-cround(Z1.A,8)
Z1.A.mean <- mean(Z1.A[1:9])
Z1.A.sd <- sd(Z1.A[1:9])
Z1.A.crit <- Z1.A.mean - qt(0.95,df=8)*Z1.A.sd
Z1.A.det <- Z1.A.mean - 2*qt(0.95,df=8)*Z1.A.sd
Korr1.A.mean<-mean(Korr1.A[1.9])
Korr1.A.sd<- sd(Korr1.A[1:9])
Korr1.A.crit <- Korr1.A.mean - qt(0.95,df=8)*Korr1.A.sd
Korr1.A.det <- Korr1.A.mean - 2*qt(0.95,df=8)*Korr1.A.sd
```

```
Z2.A<-cround(Z2.A,8)
Verunreinigung.B <-cround(Verunreinigung.B,8)
Reinheitsgrad2.B<-cround(Reinheitsgrad2.B,8)

z1.lower <- mean(Z1.A) - 2*sd(Z1.A)
Rz.1 <- Z1.A/z1.lower*100
Rz.1[Rz.1>100] <- 100

z2.lower <- mean(Z2.A) - 2*sd(Z2.A)
Rz.2 <- Z2.A/z2.lower*100
Rz.2[Rz.2>100] <- 100


d1 <- data.frame (list$name,Reinheitsgrad1.A, Verunreinigung.A,Reinheitsgrad2.A
Korr1.A, Sigma1.A, Korr2.A, Sigma2.A, Z1.A,Rz.1, Z2.A,Rz.2, Verunreinigung.B,
Reinheitsgrad2.B)


write.csv2 (d1, file="C:/purity/WPmixvsPAN.csv",row.names=FALSE)
print <- read.csv2("C:/purity/WPmixvsPAN.csv")
print
SPR_1<-Korr1.A*100
SPR_2<-(Z1.A/Z1.A.crit)*100
SPR_3<- Reinheitsgrad1.A*100
SPR_4<-Reinheitsgrad2.A*100

Conc<-list$conc
spectraNames<-list$name
r1<-data.frame(spectraNames,Conc,SPR_1,SPR_2,SPR_3,SPR_4)
write.csv2(r1,file="C:/purity/puritygrades.csv",row.names=FALSE)

print<-read.cs2v("C:/purity/puritygrades.csv")
print
windows(9,9)
opar<-par(mfrow=c(2,2),mex=0.8,mar=c(3,3,2,1)+1)
Conc<-list$conc
```

```
plot(Conc,SPR_1,xlab="Conc [g/100g]",ylab = expression(paste(SPR[1],sep="")))
z<-Z1.A.crit
p<-exp(2*z)
r<-(p-1)/(p+1)
k<-r*100
k<-round(k,6)
abline(h=k,col=4)

text(7,99.990,paste("r.crit =",as.character(k)) )

sm.model <- lm(SPR_1 ~ I(Conc) + I(Conc^2),weights=1/(1-Korr1.A))
Concentration <- seq(0,10,0.1)
Conc.for.pred <- data.frame(Conc=Concentration)
SPR_1.pred <- predict(sm.model,newdata=Conc.for.pred)
lines(Concentration,SPR_1.pred,col=3)

#######################################################
idummy <- which.min(abs(SPR_1.pred-100))
conc.crit <- Concentration[idummy]
conc.crit

idummy <- which.min(abs(SPR_1.pred- Korr1.A.det/Korr1.A.crit*100))
conc.delt <- Concentration[idummy]
conc.delt
#############################################################

SPR_2.pred<-0.5*log((1+SPR_1.pred/100)/(1-SPR_1.pred/100))/Z1.A.crit*100

plot(Conc,SPR_2,xlab="Conc [g/100g]",ylab = expression(paste(SPR[2],sep="")))

lines(Concentration,SPR_2.pred,col=4)
abline(h=100,col=1,lwd=1)
idummy <- which.min(abs(SPR_2.pred-100))
conc.crit <- Concentration[idummy]
conc.crit
lines(c(-1,conc.crit),rep(100,2),col=2)
```

```
lines(rep(conc.crit,2),c(100,0),col=2)
text(6,110,paste("LOD = ",as.character(conc.crit), "g/100g" ))

idummy <- which.min(abs(SPR_2.pred- Z1.A.det/Z1.A.crit*100))
conc.delt <- Concentration[idummy]
conc.delt
lines(c(-1,conc.delt),rep(Z1.A.det/Z1.A.crit*100,2),col=2)
lines(rep(conc.delt,2),c(Z1.A.det/Z1.A.crit*100,0),col=2)
text(6,105,paste("LOD = ",as.character(conc.delt), "g/100g" )

lm.yx<-lm(SPR_3~Conc)
s <- summary(lm.yx)
s.y <- s$sigma
a <- s$coef[1]
b <- s$coef[2]
x<-Conc
Q.xx <- sum(x^2) -sum(x)^2/n
m<-1
t.Wert <- qt(1-0.05,df=n-2)
x.NG <- s.y/b*t.Wert*sqrt(1/n + 1/m + mean(x)^2/Q.xx)
pred.frame<-data.frame(Conc)
pp<- predict(lm.yx,int="p",newdata=pred.frame)
pc<- predict(lm.yx,int="c",newdata=pred.frame)
plot(Conc,SPR_3,ylab = expression(paste(SPR[3],sep="")))
pred.conc<-pred.frame$Conc
matlines(pred.conc,pp,lty=c(1,1,1),col=c(1,4,4))


x.NG #limit of detection
x.EG <- 2*x.NG  #limit of capture
d<-SPR_3[-x.NG]
x.EG<- (-x.NG)*2
e<-SPR_3[x.EG]
x.NG<- round(x.NG,3)
x.EG<-round(x.EG,3)
text(6,99.8,paste("LOD = ",as.character(-x.NG), "g/100g" ))
```

```
text(6,99,paste("LOC = ",as.character(x.EG), "g/100g" ))
lm.yx<-lm(SPR_4~Conc)
s <- summary(lm.yx)
s.y <- s$sigma
a <- s$coef[1]
b <- s$coef[2]
x<-Conc
Q.xx <- sum(x^2) -sum(x)^2/n
m<-1
t.Wert <- qt(1-0.05,df=n-2)
x.NG <- s.y/b*t.Wert*sqrt(1/n + 1/m + mean(x)^2/Q.xx)
pred.frame<-data.frame(Conc)
pp<- predict(lm.yx,int="p",newdata=pred.frame)
pc<- predict(lm.yx,int="c",newdata=pred.frame)
plot(Conc,SPR_4,ylab = expression(paste(SPR[4],sep="")))
pred.conc<-pred.frame$Conc
matlines(pred.conc,pp,lty=c(1,1,1),col=c(1,4,4))

x.NG #limit of detection
x.EG <- 2*x.NG  #limit of capture
b<-SPR_4[-x.NG]
x.EG<- -x.NG*2
c<-SPR_4[x.EG]
x.NG<- round(x.NG,3)
x.EG<-round(x.EG,3)
text(6,99.8,paste("LOD = ",as.character(-x.NG), "g/100g" ))
text(6,99,paste("LOC = ",as.character(x.EG), "g/100g" ))

par(opar)
```

2. R-code for quantitative analysis using PLS

```
library(pls)
upper<-3000
lower<-2800
List <- read.csv2("C:/purity/quant911.csv")
Spectra.names <- as.character(List$Mixtures)
n <- length(Spectra.names)
for (i in 1:n){
FileName <- Spectra.names[i]
spec <- read.table(FileName,skip=86)
colnames(spec) <- c("x","y")
x <- spec$x[spec$x <= upper & spec$x >= lower]
y <- spec$y[spec$x <= upper & spec$x >= lower]
y<- log10(100/y)
spec <- data.frame(x=x,y=y)

if (i==1){
y.values <- spec$y
}
if (i>1){
y.values <- data.frame(y.values,spec$y)
}
}
Dicke<-List$conc
X<-spec$x
MSpektren<-y.values
MSpektren <- t(MSpektren)
Liste <- data.frame(d=Dicke,Specs=I(MSpektren))
calibration<- Liste[1:99,]
validation<-Liste[100:198,]
windows(9,12)
opar<-par(mfrow=c(3,1),mex=0.8,mar=c(3,3,2,1)+1)

plot(X,Liste$Specs[1,],type="l",xlab=expression(cm^-1),ylab="A",xlim=
c(upper,lower),main="Spectral range")
for (i in 2:198){
```

```
lines(X,Liste$Specs[i,],col=i)
}
quant.pcr <- plsr(d~Specs,ncomp=3,data=calibration, validation="LOO")

predplot(quant.pcr,main="Measured Vs Predicted")
abline(0,1)
s<-predict(quant.pcr,ncomp=3,newdata=validation)
p<- data.frame(s)
v<- p[,1]
points(Liste$d[100:198],v,col=3)
corr<- summary(lm(v~Liste$d[100:198]))
r<- corr$r.squared
r<-sqrt(r)
r<-round(r,4)

b<-predict(quant.pcr,ncomp=3,newdata=calibration)
f<-data.frame(b)
g<-f[,1]
corr1<- summary(lm(g~Liste$d[1:99]))
r1<-corr1$r.squared
r1<-sqrt(r1)
r1<-round(r1,4)
text(8,4,paste("r-calibration = ",as.character(r1),sep=""))
text(8,2,paste("r-validation = ",as.character(r2),sep=""))
summary(quant.pcr)
plot(RMSEP(quant.pcr,newdata=validation),main="Scree-Plot")

par(opar)
RMSEP(quant.pcr)# leave one out valdiation
par(opar)
predict(quant.pcr,ncomp=3,newdata=validation)
RMSEP(quant.pcr,newdata=validation)
```

3. A .csv table containing the directory path of the spectra

Table 9.1: Table containing paths of the directory with spectra in ASCII format.

name	conc	Mixtures	MeanPalN	ref2
PAN1	0	C:/purity/pan/ascii/PAN1.asc	C:/purity/pan/MITTEL/PANMEAN.asc	PANMEAN
PAN2	0	C:/purity/pan/ascii/PAN2.asc	C:/purity/pan/MITTEL/PANMEAN.asc	PANMEAN
PAN3	0	C:/purity/pan/ascii/PAN3.asc	C:/purity/pan/MITTEL/PANMEAN.asc	PANMEAN
PAN4	0	C:/purity/pan/ascii/PAN4.asc	C:/purity/pan/MITTEL/PANMEAN.asc	PANMEAN
PAN5	0	C:/purity/pan/ascii/PAN5.asc	C:/purity/pan/MITTEL/PANMEAN.asc	PANMEAN
PAN6	0	C:/purity/pan/ascii/PAN6.asc	C:/purity/pan/MITTEL/PANMEAN.asc	PANMEAN
PAN7	0	C:/purity/pan/ascii/PAN7.asc	C:/purity/pan/MITTEL/PANMEAN.asc	PANMEAN
PAN8	0	C:/purity/pan/ascii/PAN8.asc	C:/purity/pan/MITTEL/PANMEAN.asc	PANMEAN
PAN9	0	C:/purity/pan/ascii/PAN9.asc	C:/purity/pan/MITTEL/PANMEAN.asc	PANMEAN
PNA_1A1	1.00053	C:/purity/PNA_1A1.asc	C:/purity/pan/MITTEL/PANMEAN.asc	PANMEAN
PNA_1A2	1.00053	C:/purity/PNA_1A2.asc	C:/purity/pan/MITTEL/PANMEAN.asc	PANMEAN
PNA_1A3	1.00053	C:/purity/PNA_1A3.asc	C:/purity/pan/MITTEL/PANMEAN.asc	PANMEAN
PNA_1B1	1.00053	C:/purity/PNA_1B1.asc	C:/purity/pan/MITTEL/PANMEAN.asc	PANMEAN
PNA_1B2	1.00053	C:/purity/PNA_1B2.asc	C:/purity/pan/MITTEL/PANMEAN.asc	PANMEAN
PNA_1B3	1.00053	C:/purity/PNA_1B3.asc	C:/purity/pan/MITTEL/PANMEAN.asc	PANMEAN
PNA_1C1	1.00053	C:/purity/PNA_1C1.asc	C:/purity/pan/MITTEL/PANMEAN.asc	PANMEAN
PNA_1C2	1.00053	C:/purity/PNA_1C2.asc	C:/purity/pan/MITTEL/PANMEAN.asc	PANMEAN
PNA_1C3	1.00053	C:/purity/PNA_1C3.asc	C:/purity/pan/MITTEL/PANMEAN.asc	PANMEAN
PNA_2A1	2.03454	C:/purity/PNA_2A1.asc	C:/purity/pan/MITTEL/PANMEAN.asc	PANMEAN
PNA_2A2	2.03454	C:/purity/PNA_2A2.asc	C:/purity/pan/MITTEL/PANMEAN.asc	PANMEAN
PNA_2A3	2.03454	C:/purity/PNA_2A3.asc	C:/purity/pan/MITTEL/PANMEAN.asc	PANMEAN
PNA_2B1	2.03454	C:/purity/PNA_2B1.asc	C:/purity/pan/MITTEL/PANMEAN.asc	PANMEAN
PNA_2B2	2.03454	C:/purity/PNA_2B2.asc	C:/purity/pan/MITTEL/PANMEAN.asc	PANMEAN
PNA_2B3	2.03454	C:/purity/PNA_2B3.asc	C:/purity/pan/MITTEL/PANMEAN.asc	PANMEAN
PNA_2C1	2.03454	C:/purity/PNA_2C1.asc	C:/purity/pan/MITTEL/PANMEAN.asc	PANMEAN
PNA_2C2	2.03454	C:/purity/PNA_2C2.asc	C:/purity/pan/MITTEL/PANMEAN.asc	PANMEAN
PNA_2C3	2.03454	C:/purity/PNA_2C3.asc	C:/purity/pan/MITTEL/PANMEAN.asc	PANMEAN
PNA_3A1	3.01558	C:/purity/PNA_3A1.asc	C:/purity/pan/MITTEL/PANMEAN.asc	PANMEAN
PNA_3A2	3.01558	C:/purity/PNA_3A2.asc	C:/purity/pan/MITTEL/PANMEAN.asc	PANMEAN

PNA_3A3	3.01558	C:/purity/PNA_3A3.asc	C:/purity/pan/MITTEL/PANMEAN.asc	PANMEAN
PNA_3B1	3.01558	C:/purity/PNA_3B1.asc	C:/purity/pan/MITTEL/PANMEAN.asc	PANMEAN
PNA_3B2	3.01558	C:/purity/PNA_3B2.asc	C:/purity/pan/MITTEL/PANMEAN.asc	PANMEAN
PNA_3B3	3.01558	C:/purity/PNA_3B3.asc	C:/purity/pan/MITTEL/PANMEAN.asc	PANMEAN
PNA_3C1	3.01558	C:/purity/PNA_3C1.asc	C:/purity/pan/MITTEL/PANMEAN.asc	PANMEAN
PNA_3C2	3.01558	C:/purity/PNA_3C2.asc	C:/purity/pan/MITTEL/PANMEAN.asc	PANMEAN
PNA_3C3	3.01558	C:/purity/PNA_3C3.asc	C:/purity/pan/MITTEL/PANMEAN.asc	PANMEAN
PNA_4A1	3.99824	C:/purity/PNA_4A1.asc	C:/purity/pan/MITTEL/PANMEAN.asc	PANMEAN
PNA_4A2	3.99824	C:/purity/PNA_4A2.asc	C:/purity/pan/MITTEL/PANMEAN.asc	PANMEAN
PNA_4A3	3.99824	C:/purity/PNA_4A3.asc	C:/purity/pan/MITTEL/PANMEAN.asc	PANMEAN
PNA_4B1	3.99824	C:/purity/PNA_4B1.asc	C:/purity/pan/MITTEL/PANMEAN.asc	PANMEAN
PNA_4B2	3.99824	C:/purity/PNA_4B2.asc	C:/purity/pan/MITTEL/PANMEAN.asc	PANMEAN
PNA_4B3	3.99824	C:/purity/PNA_4B3.asc	C:/purity/pan/MITTEL/PANMEAN.asc	PANMEAN
PNA_4C1	3.99824	C:/purity/PNA_4C1.asc	C:/purity/pan/MITTEL/PANMEAN.asc	PANMEAN
PNA_4C2	3.99824	C:/purity/PNA_4C2.asc	C:/purity/pan/MITTEL/PANMEAN.asc	PANMEAN
PNA_4C3	3.99824	C:/purity/PNA_4C3.asc	C:/purity/pan/MITTEL/PANMEAN.asc	PANMEAN
PNA_5A1	5.03848	C:/purity/PNA_5A1.asc	C:/purity/pan/MITTEL/PANMEAN.asc	PANMEAN
PNA_5A2	5.03848	C:/purity/PNA_5A2.asc	C:/purity/pan/MITTEL/PANMEAN.asc	PANMEAN
PNA_5A3	5.03848	C:/purity/PNA_5A3.asc	C:/purity/pan/MITTEL/PANMEAN.asc	PANMEAN
PNA_5B1	5.03848	C:/purity/PNA_5B1.asc	C:/purity/pan/MITTEL/PANMEAN.asc	PANMEAN
PNA_5B2	5.03848	C:/purity/PNA_5B2.asc	C:/purity/pan/MITTEL/PANMEAN.asc	PANMEAN
PNA_5B3	5.03848	C:/purity/PNA_5B3.asc	C:/purity/pan/MITTEL/PANMEAN.asc	PANMEAN
PNA_5C1	5.03848	C:/purity/PNA_5C1.asc	C:/purity/pan/MITTEL/PANMEAN.asc	PANMEAN
PNA_5C2	5.03848	C:/purity/PNA_5C2.asc	C:/purity/pan/MITTEL/PANMEAN.asc	PANMEAN
PNA_5C3	5.03848	C:/purity/PNA_5C3.asc	C:/purity/pan/MITTEL/PANMEAN.asc	PANMEAN
PNA_6A1	6.07166	C:/purity/PNA_6A1.asc	C:/purity/pan/MITTEL/PANMEAN.asc	PANMEAN
PNA_6A2	6.07166	C:/purity/PNA_6A2.asc	C:/purity/pan/MITTEL/PANMEAN.asc	PANMEAN
PNA_6A3	6.07166	C:/purity/PNA_6A3.asc	C:/purity/pan/MITTEL/PANMEAN.asc	PANMEAN
PNA_6B1	6.07166	C:/purity/PNA_6B1.asc	C:/purity/pan/MITTEL/PANMEAN.asc	PANMEAN
PNA_6B2	6.07166	C:/purity/PNA_6B2.asc	C:/purity/pan/MITTEL/PANMEAN.asc	PANMEAN
PNA_6B3	6.07166	C:/purity/PNA_6B3.asc	C:/purity/pan/MITTEL/PANMEAN.asc	PANMEAN
PNA_6C1	6.07166	C:/purity/PNA_6C1.asc	C:/purity/pan/MITTEL/PANMEAN.asc	PANMEAN
PNA_6C2	6.07166	C:/purity/PNA_6C2.asc	C:/purity/pan/MITTEL/PANMEAN.asc	PANMEAN

PNA_6C3	6.07166	C:/purity/PNA_6C3.asc	C:/purity/pan/MITTEL/PANMEAN.asc	PANMEAN
PNA_7A1	7.0628	C:/purity/PNA_7A1.asc	C:/purity/pan/MITTEL/PANMEAN.asc	PANMEAN
PNA_7A2	7.0628	C:/purity/PNA_7A2.asc	C:/purity/pan/MITTEL/PANMEAN.asc	PANMEAN
PNA_7A3	7.0628	C:/purity/PNA_7A3.asc	C:/purity/pan/MITTEL/PANMEAN.asc	PANMEAN
PNA_7B1	7.0628	C:/purity/PNA_7B1.asc	C:/purity/pan/MITTEL/PANMEAN.asc	PANMEAN
PNA_7B2	7.0628	C:/purity/PNA_7B2.asc	C:/purity/pan/MITTEL/PANMEAN.asc	PANMEAN
PNA_7B3	7.0628	C:/purity/PNA_7B3.asc	C:/purity/pan/MITTEL/PANMEAN.asc	PANMEAN
PNA_7C1	7.0628	C:/purity/PNA_7C1.asc	C:/purity/pan/MITTEL/PANMEAN.asc	PANMEAN
PNA_7C2	7.0628	C:/purity/PNA_7C2.asc	C:/purity/pan/MITTEL/PANMEAN.asc	PANMEAN
PNA_7C3	7.0628	C:/purity/PNA_7C3.asc	C:/purity/pan/MITTEL/PANMEAN.asc	PANMEAN
PNA_8A1	8.0362	C:/purity/PNA_8A1.asc	C:/purity/pan/MITTEL/PANMEAN.asc	PANMEAN
PNA_8A2	8.0362	C:/purity/PNA_8A2.asc	C:/purity/pan/MITTEL/PANMEAN.asc	PANMEAN
PNA_8A3	8.0362	C:/purity/PNA_8A3.asc	C:/purity/pan/MITTEL/PANMEAN.asc	PANMEAN
PNA_8B1	8.0362	C:/purity/PNA_8B1.asc	C:/purity/pan/MITTEL/PANMEAN.asc	PANMEAN
PNA_8B2	8.0362	C:/purity/PNA_8B2.asc	C:/purity/pan/MITTEL/PANMEAN.asc	PANMEAN
PNA_8B3	8.0362	C:/purity/PNA_8B3.asc	C:/purity/pan/MITTEL/PANMEAN.asc	PANMEAN
PNA_8C1	8.0362	C:/purity/PNA_8C1.asc	C:/purity/pan/MITTEL/PANMEAN.asc	PANMEAN
PNA_8C2	8.0362	C:/purity/PNA_8C2.asc	C:/purity/pan/MITTEL/PANMEAN.asc	PANMEAN
PNA_8C3	8.0362	C:/purity/PNA_8C3.asc	C:/purity/pan/MITTEL/PANMEAN.asc	PANMEAN
PNA_9A1	9.08744	C:/purity/PNA_9A1.asc	C:/purity/pan/MITTEL/PANMEAN.asc	PANMEAN
PNA_9A2	9.08744	C:/purity/PNA_9A2.asc	C:/purity/pan/MITTEL/PANMEAN.asc	PANMEAN
PNA_9A3	9.08744	C:/purity/PNA_9A3.asc	C:/purity/pan/MITTEL/PANMEAN.asc	PANMEAN
PNA_9B1	9.08744	C:/purity/PNA_9B1.asc	C:/purity/pan/MITTEL/PANMEAN.asc	PANMEAN
PNA_9B2	9.08744	C:/purity/PNA_9B2.asc	C:/purity/pan/MITTEL/PANMEAN.asc	PANMEAN
PNA_9B3	9.08744	C:/purity/PNA_9B3.asc	C:/purity/pan/MITTEL/PANMEAN.asc	PANMEAN
PNA_9C1	9.08744	C:/purity/PNA_9C1.asc	C:/purity/pan/MITTEL/PANMEAN.asc	PANMEAN
PNA_9C2	9.08744	C:/purity/PNA_9C2.asc	C:/purity/pan/MITTEL/PANMEAN.asc	PANMEAN
PNA_9C3	9.08744	C:/purity/PNA_9C3.asc	C:/purity/pan/MITTEL/PANMEAN.asc	PANMEAN
PNA_10A1	10.02971	C:/purity/PNA_10A1.asc	C:/purity/pan/MITTEL/PANMEAN.asc	PANMEAN
PNA_10A2	10.02971	C:/purity/PNA_10A2.asc	C:/purity/pan/MITTEL/PANMEAN.asc	PANMEAN
PNA_10A3	10.02971	C:/purity/PNA_10A3.asc	C:/purity/pan/MITTEL/PANMEAN.asc	PANMEAN
PNA_10B1	10.02971	C:/purity/PNA_10B1.asc	C:/purity/pan/MITTEL/PANMEAN.asc	PANMEAN
PNA_10B2	10.02971	C:/purity/PNA_10B2.asc	C:/purity/pan/MITTEL/PANMEAN.asc	PANMEAN

PNA_10B3	10.02971	C:/purity/PNA_10B3.asc	C:/purity/pan/MITTEL/PANMEAN.asc	PANMEAN
PNA_10C1	10.02971	C:/purity/PNA_10C1.asc	C:/purity/pan/MITTEL/PANMEAN.asc	PANMEAN
PNA_10C2	10.02971	C:/purity/PNA_10C2.asc	C:/purity/pan/MITTEL/PANMEAN.asc	PANMEAN
PNA_10C3	10.02971	C:/purity/PNA_10C3.asc	C:/purity/pan/MITTEL/PANMEAN.asc	PANMEAN

Table 9.2: Spectral purities of Palatinol-N as function of the concentration of impurity Palatinol-AH, spectral range 1000-800 cm^{-1}.

spectranames	Conc	SPR_1	SPR_2	SPR_3	SPR_4
PAN1	0	99.998466	100.207955	99.7	99.802007
PAN2	0	99.999549	110.633279	99.9	99.77263
PAN3	0	99.999424	108.542923	99.9	99.88625
PAN4	0	99.999384	107.964801	99.9	99.733295
PAN5	0	99.999431	108.643923	100	99.034382
PAN6	0	99.999307	106.970393	100	99.532121
PAN7	0	99.99883	102.51093	100	99.221299
PAN8	0	99.999324	107.182372	100	99.742614
PAN9	0	99.998994	103.797279	99.4	99.835289
PNA_1A1	1.00053	99.996493	93.1741272	99.5	99.551292
PNA_1A2	1.00053	99.996302	92.7215149	99.5	99.464484
PNA_1A3	1.00053	99.996523	93.2461592	99.4	99.613
PNA_1B1	1.00053	99.996253	92.6095375	99.4	99.45135
PNA_1B2	1.00053	99.995841	91.7226895	99.5	99.344344
PNA_1B3	1.00053	99.996172	92.4286152	99.5	99.45372
PNA_1C1	1.00053	99.995756	91.5502675	99.7	99.388368
PNA_1C2	1.00053	99.994866	89.9300061	99.7	99.320689
PNA_1C3	1.00053	99.995312	90.7044229	99.5	99.500965
PNA_2A1	2.03454	99.989576	83.9051498	99.7	98.269618
PNA_2A2	2.03454	99.990367	84.576538	99.7	98.410579
PNA_2A3	2.03454	99.990592	84.7774647	99.6	98.565864

PNA_2B1	2.03454	99.990861	85.0244454	98.8	98.787957
PNA_2B2	2.03454	99.990977	85.1331024	99.1	98.461374
PNA_2B3	2.03454	99.990238	84.463214	99.2	98.359656
PNA_2C1	2.03454	99.982879	79.6831458	97.2	98.956998
PNA_2C2	2.03454	99.987726	82.5148833	98.2	98.965887
PNA_2C3	2.03454	99.988026	82.7252808	98.2	98.763195
PNA_3A1	3.01558	99.976917	77.1408749	97.2	98.442156
PNA_3A2	3.01558	99.979745	78.252597	97.4	98.771336
PNA_3A3	3.01558	99.979283	78.0607208	97.7	98.578346
PNA_3B1	3.01558	99.972485	75.6462582	97.2	98.515667
PNA_3B2	3.01558	99.975313	76.568964	97.1	98.662919
PNA_3B3	3.01558	99.976242	76.8955418	97.1	98.731501
PNA_3C1	3.01558	99.973654	76.0156612	97.3	98.381228
PNA_3C2	3.01558	99.973446	75.948888	97	98.684135
PNA_3C3	3.01558	99.975249	76.5470074	97.2	98.526475
PNA_4A1	3.99824	99.968345	74.4535554	98.4	97.14505
PNA_4A2	3.99824	99.970552	75.0684136	97.9	98.157347
PNA_4A3	3.99824	99.967239	74.1612947	98.3	97.399573
PNA_4B1	3.99824	99.96372	73.293031	97.1	98.090887
PNA_4B2	3.99824	99.964322	73.4355595	96.9	97.949318
PNA_4B3	3.99824	99.967923	74.3409658	96.8	98.199442
PNA_4C1	3.99824	99.960823	72.6394594	96.5	97.86908
PNA_4C2	3.99824	99.961886	72.8734112	96.7	97.868351
PNA_4C3	3.99824	99.963038	73.1345225	96.8	97.77472
PNA_5A1	5.03848	99.942143	69.3214599	96.1	97.148229
PNA_5A2	5.03848	99.944675	69.7022108	95.8	97.769779
PNA_5A3	5.03848	99.942603	69.3893689	96.2	97.39985
PNA_5B1	5.03848	99.928859	67.5624104	96	96.809356

PNA_5B2	5.03848	99.944082	69.6116243	96.2	97.588551
PNA_5B3	5.03848	99.943679	69.550494	96	97.453544
PNA_5C1	5.03848	99.936097	68.4755583	95.9	97.120983
PNA_5C2	5.03848	99.94261	69.3904088	95.7	97.520495
PNA_5C3	5.03848	99.939265	68.9083117	96.2	97.175735
PNA_6A1	6.07166	99.914852	66.032646	95	97.147616
PNA_6A2	6.07166	99.916681	66.2174448	95.2	97.120195
PNA_6A3	6.07166	99.918075	66.3611377	95.1	97.066767
PNA_6B1	6.07166	99.919379	66.4976662	95.8	96.606562
PNA_6B2	6.07166	99.920707	66.6390458	95.8	96.642274
PNA_6B3	6.07166	99.925089	67.1228956	95.7	96.724852
PNA_6C1	6.07166	99.918271	66.3814629	95.4	96.836372
PNA_6C2	6.07166	99.920487	66.6153988	95.5	96.80675
PNA_6C3	6.07166	99.91844	66.3990559	95.7	96.604577
PNA_7A1	7.0628	99.900414	64.6993984	95.3	96.049632
PNA_7A2	7.0628	99.899501	64.621753	95.5	96.163682
PNA_7A3	7.0628	99.898211	64.5132136	95.6	95.810617
PNA_7B1	7.0628	99.882821	63.3146044	95.6	95.246747
PNA_7B2	7.0628	99.886435	63.5812867	95.6	95.630055
PNA_7B3	7.0628	99.886823	63.6104293	95.7	95.629454
PNA_7C1	7.0628	99.881789	63.2399815	95.6	95.291842
PNA_7C2	7.0628	99.88681	63.6094401	95.7	95.568518
PNA_7C3	7.0628	99.884253	63.4192575	95.8	95.571386
PNA_8A1	8.0362	99.861029	61.8625303	94.3	95.958031
PNA_8A2	8.0362	99.862184	61.9335929	94.3	96.113194
PNA_8A3	8.0362	99.861649	61.900568	94.5	96.131106
PNA_8B1	8.0362	99.861003	61.8609584	94.5	96.041435
PNA_8B2	8.0362	99.866293	62.1913109	94.4	96.138091

PNA_8B3	8.0362	99.864182	62.0578825	93.8	96.272275
PNA_8C1	8.0362	99.854392	61.4653294	94.1	95.940256
PNA_8C2	8.0362	99.858046	61.681698	94.1	95.849351
PNA_8C3	8.0362	99.859919	61.7947981	94.3	96.00159
PNA_9A1	9.08744	99.834361	60.367835	94.6	94.788582
PNA_9A2	9.08744	99.836624	60.4850029	94.7	94.944129
PNA_9A3	9.08744	99.834361	60.3678536	94.7	94.863801
PNA_9B1	9.08744	99.828372	60.0653836	93.8	94.929519
PNA_9B2	9.08744	99.832768	60.2863581	94	95.152264
PNA_9B3	9.08744	99.834535	60.3768184	94.1	95.036759
PNA_9C1	9.08744	99.828376	60.065584	93.9	95.00998
PNA_9C2	9.08744	99.826915	59.9933967	93.9	95.329263
PNA_9C3	9.08744	99.830967	60.1951552	94.1	95.03616
PNA_10A1	10.02971	99.79389	58.5062871	92.9	94.85933
PNA_10A2	10.02971	99.797782	58.6686543	92.9	94.899879
PNA_10A3	10.02971	99.79586	58.5880728	93.3	94.912744
PNA_10B1	10.02971	99.794375	58.5263362	93.3	94.88309
PNA_10B2	10.02971	99.797772	58.6682244	93.4	94.718265
PNA_10B3	10.02971	99.803989	58.9341539	93.3	94.958897
PNA_10C1	10.02971	99.789363	58.3212516	93	94.622944
PNA_10C2	10.02971	99.797001	58.6358275	93	94.958486
PNA_10C3	10.02971	99.799698	58.7497184	92.9	95.023665

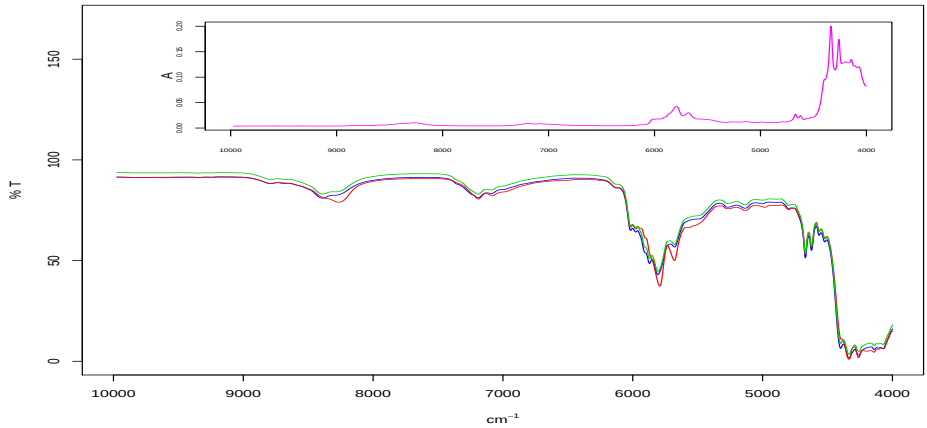

Figure 9.9: NIR spectra of pure Palatinol-N (blue), pure Palatinol-911P (red) and sample of Palatinol-N with 10 % Palatinol-911P (green). The upper inserted graph is the optimal difference spectrum in absorbance.

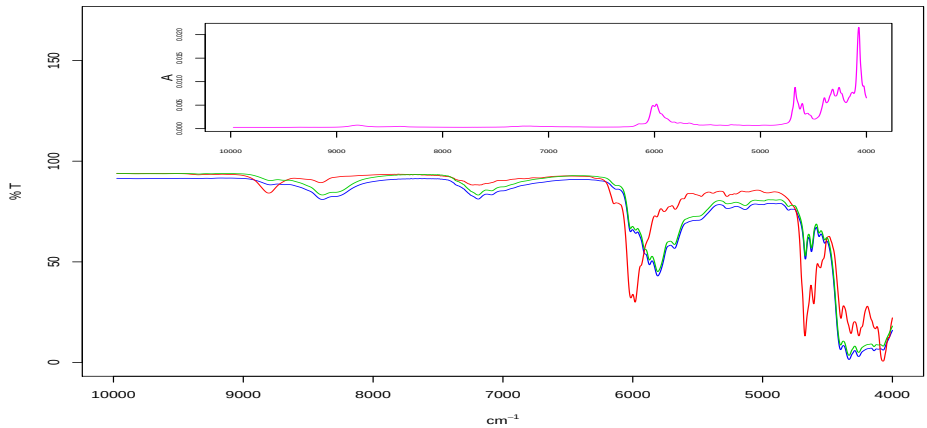

Figure 9.10: NIR spectra of pure Palatinol-N (blue), pure Reofos-50 (red) and sample of Palatinol-N with 1 % Reofos-50 (green). The upper inserted graph is the optimal difference spectrum in absorbance.

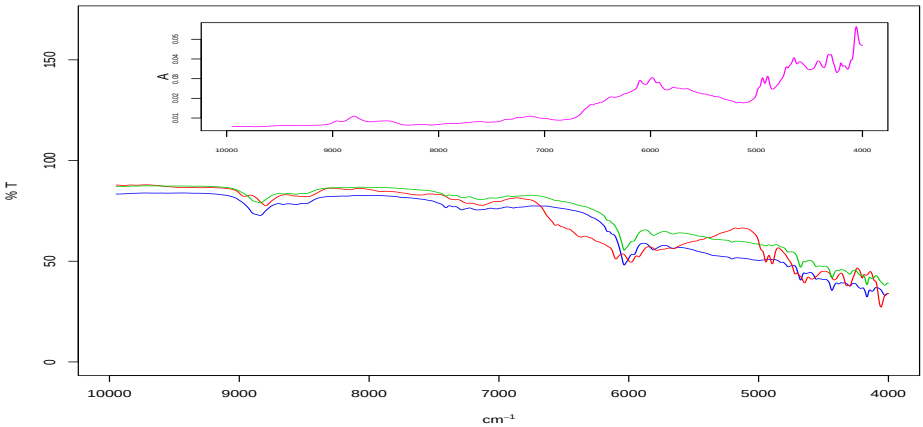

Figure 9.11: NIR spectra of pure Aspirin (blue), pure Paracetamol(red) and sample of Aspirin with 10 % Paracetamol (green). The upper inserted graph is the optimal difference spectrum in absorbance.

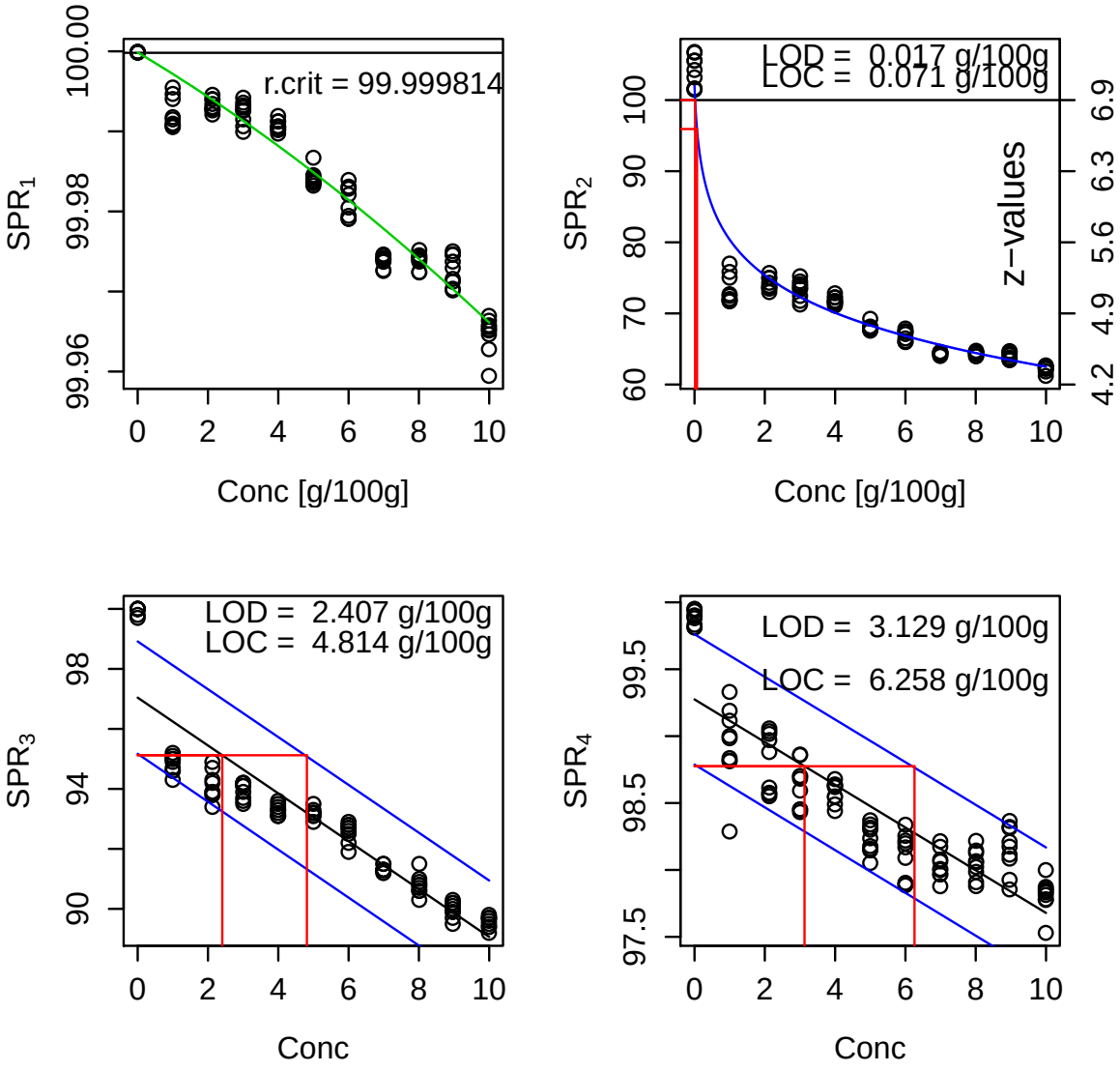

Figure 9.12: Dependency of spectral purity parameters of Palatinol-N on the concentration of the impurity Reofos-50 in spectral range of 3100-2800 cm^{-1}.

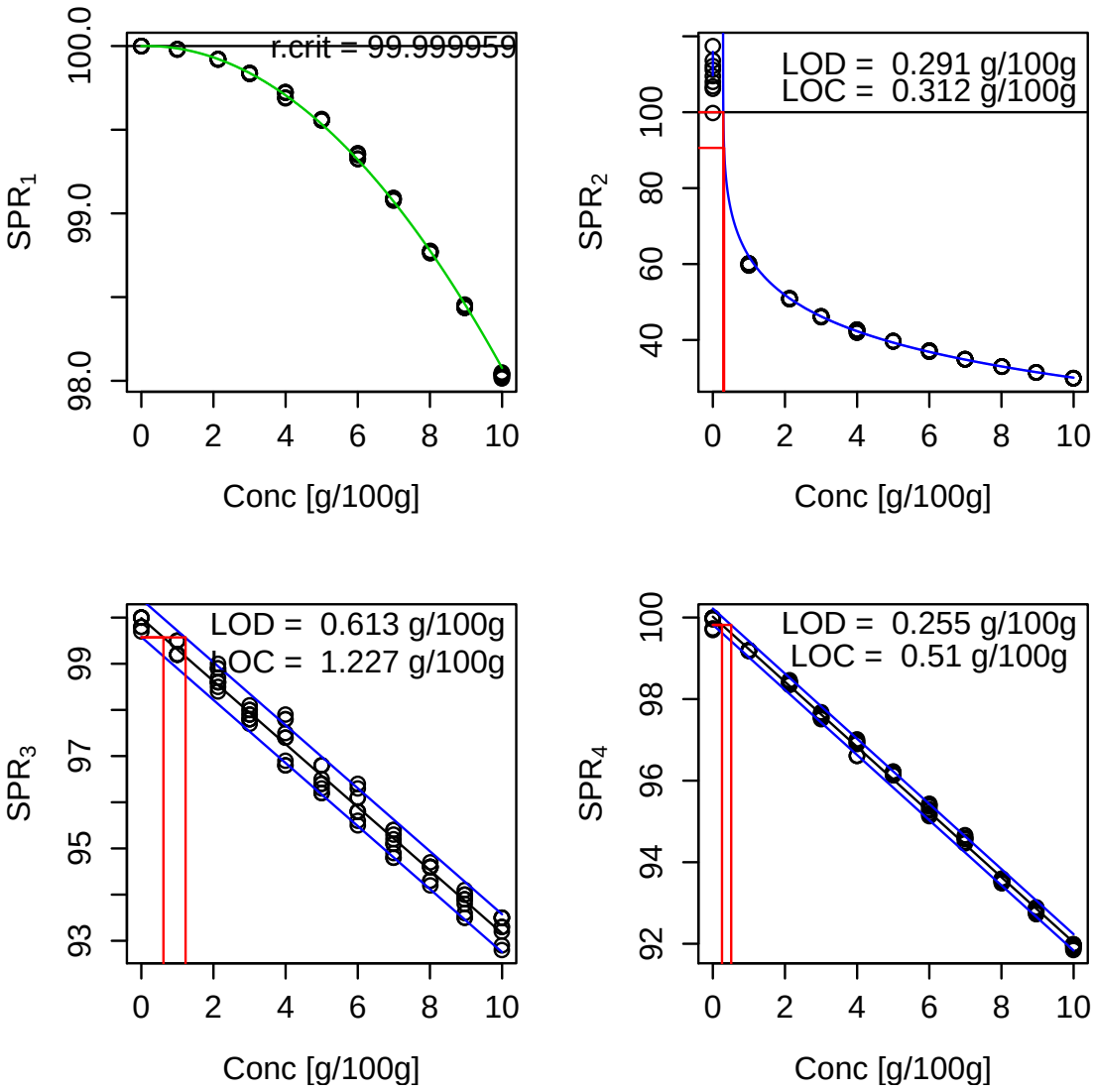

Figure 9.13: Dependency of spectral purity parameters of Palatinol-N on the concentration of the impurity Reofos-50 in the spectral range of 6000-5500 cm^{-1}.

Table 9.3: Calibration standards in concentration range of 0.006-54.4 mg/L referring to water

No	Name	mg/L
1	DC01	0.006
2	DC03	0.019
3	DC04	0.027
4	DC07	0.04
5	DC1	0.06
6	DC5	0.3
7	DC10	0.6
8	DC25	1.37
9	DC50	2.7
10	DC75	4.1
11	DC77	4.3
12	DC100	5.4
13	DC155	8.6
14	DC156	8.7
15	DC200	12.7
16	DC300	16.4
17	DC400	21.9
18	DC600	33.8
19	DC800	43.6
20	D1	54.8

Bibliography

[1] K. Molt and D. Ihlbrock. Principles and applications of Quality Control by Near Infrared Spectroscopy using the example of polymer additives. *Fresenius J. Anal. Chem*, 348:523–529, July 1994.

[2] K. Molt and A. Schlachter. Infrarotspektroskopische Untersuchungen von unterschiedlich hergestellten PVC-Sorten und bei der Herstellung und Verarbeitung von PVC-Plastisolen verwendeten Additiven. In *VDI Berichte-1959*, pages 3–26. VDI-Verlag GmbH, 2006.

[3] J. P. Coates. Industrial Applications of computerized Dispersive Infrared Spectroscopy for Analysis in Solutions. *Anal.Chim.Acta*, 103:323–338, July 1978.

[4] N. Cecconi. Using NIR Spectroscopy for Raw Materials Characterization, 2007. http://www.pharmamanufacturing.com/articles/2007/097.html.

[5] Jiben Roy. Pharmaceutical Impurities- A Mini-Review. *AAPS PharmSciTech 2002*, 3.

[6] International Conference on Harmonization of Technical Requirements for the Registration of Pharmaceuticals for Human Use-Geneva. Q3A(R2): Impurities in NewDrug Substances, 2006. http://www.ich.org.

[7] M. Blanco et al. Near-infrared spectroscopy in the Pharmaceutical Industry. *Analyst*, 123:135R– 150R, 1998.

[8] N. Colthup, L. Daly, and S. Wiberely. *Introduction to Infrared and Raman Spectroscopy*. San Diego : Academic press, San Diego, 3rd edition, 1990.

[9] D. Lin-Vien and N. Colthup. *The handbook of Infrared and Raman Characteristic Frequencies of Organic Molecules*. Academic press, Boston, 1991.

[10] A. N. Davies. *Nachr. Chem. Techn. Lab*, 263:37, 1989.

[11] 2010. http://www.sadtler.info.

[12] *EUROPÄISCHE PHARMAKOPÖE,5*. Europäische Arzneibuch Kommission, Strasbourg, Ausgabe 5.0-5.8 edition, 2006.

[13] K. Molt. Rechnerische Interpretations- und Bibliotheks suchverfahren in der Infrarotspektroskopie. ANGEWANDTE INFRAROTSPEKTROSKOPIE, Heft-20, 1985, PerkinElmer GmbH, Überlingen.

[14] R. Gnanadesikan. *Methods for Statistical Data Analysis of Multivariate Observations*. Wiley & Sons, New York, 2 edition, 1997.

[15] ASTM:Committee E13.03 on Infrared and Near Infrared Spectroscopy. *Annual Book of ASTM Standards: Molecular Spectroscopy; Surface Analysis*. ASTM International, West Conshohocken,USA, 3.06 edition, 2009. ASTM E2310 - 04(2009) Standard Guide for Use of Spectral Searching by Curve Matching Algorithms with Data Recorded Using Mid-Infrared Spectroscopy.

[16] R. Bossarta, H. Kellera, H. Kellerhalsa, and J. Oelichmann. Principal components analysis as a tool for identity control using Near Infrared spectroscopy. *Journal of Molecular Structure*, 661-662:112–323, 2003.

[17] Büchi Labortechnik AG, Flawil, Switzerland. *NIRCal Version 4.3:Chapter 6*, 2008.

[18] R. Bossarta, H. Kellera, H. Kellerhalsa, and J. Oelichmann. Use of high order principal components in NIR spectroscopy. *Journal of Near Infrared Spectroscopy*, 1:209–219, 1993.

[19] Jerome J. Workman JR, Paul R. Mobley, Bruce R. Kowalski, and Rasmus Bro. Review of chemometrics applied to spectroscopy. *Applied Spectroscopy Review*, 31:73–124, 1996.

[20] K. Tanabe and S. Saeki. Computer Retrieval of Infrared Spectra by a Correlation Coefficient Method. *Anal.Chem*, 47:118–122, 1974.

[21] Robert Hoult. Method and apparatus for comparing spectra, 1991. Patent number US5023804.

[22] W. Plugge and C. van der Vlies. The use of near infrared spectroscopy in the quality control laboratory of the pharmaceutical industry. *Journal of Pharmaceutical and Biomedical Analysis*, 10:797–803, 1992.

[23] P. R. Griffiths and L. I. Shao. Self-Weighted Correlation Coefficients and Their Application to Measure Spectral Similarity. *Applied Spectroscopy*, 63:916–919, 2009.

[24] Good Manufacturing Practice (GMP) Guidelines/Inspection Checklist, 2008. http://www.fda.gov/cosmetics/guidancecomplianceregulatory information/goodmanufacturingpracticegmpguidelinesinspectionchecklist/ default.htm.

[25] http://www.sigmaaldrich.com/analytical-chromatography/analytical-standards/ certified-reference.html.

[26] http://irmm.jrc.ec.europa.eu/reference_materials_catalogue/catalogue/ Pages/index.aspx.

[27] http://www.nist.gov/srm/.

[28] H. Weitkamp und D. Wortig. Vollautomatische Identitätsprüfung von Arzneimitteln durch rechnergekoppelte IR-Spektroskopie. *Mikrochimita Acta*, 2:31–57, 1983.

[29] H. U. Gremlich. *Infrared and Raman Spectroscopy, in Ullman's Encyclopedia of Industrial Chemistry*. Wiley-VCH Verlag GmbH, Weinheim, 6th edition, 2000.

[30] Strahlungsphysik im optischen Bereich und Lichttechnik, Benennung der Wellenlängenbereiche, 1984. BEUTH VERLAG GmbH: DIN 5031.

[31] http://orgchem.colorado.edu/hndbksupport/irtutor/tutorial.html.

[32] C. Gerthsen. *Gerthsen Physik- Ein Lehrbuch zum Gebrauch neben Vorlesungen.* Springer-Verlag, Heidelberg, 6 edition, 1960.

[33] L. D Landau and E. M. Lifshitz. *Mechanics.* Pergamon Press, 3 edition.

[34] B. G. Osborne, T. Fearn, and P. T. Hindle. *Practical NIR Spectroscopy With Applications in Food and Beverage Analysis.* Longman Scientific and Technical, New York, 2nd edition, 1993.

[35] T. Naes, T. Issakson, T. Fearn, and T. Davies. *A user-friendly guide to Multivariate Calibration and Classification.* NIR Publications, West Sussex,UK, 1 edition, 2002.

[36] J. R. Ferraro and K. K. Krishnan. *Practical Fourier Transform Infrared Spectroscopy: Industrial and Laboratory Chemical Analysis.* Academic Press, San Diego, 6 edition, 1990.

[37] P. R. Griffiths. *Chemical Infrared Fourier Transform Spectroscopy.* Wiley, New York, 1975.

[38] P. R. Griffiths and J. A. De Haseth. *Fourier Transform Spectrometry.* Wiley, New York, 1986.

[39] R. J Bell. *Introductory Fourier Transform Spectroscopy.* Academic Press, New York, 1972.

[40] http://en.wikipedia.org/wiki/Fourier_transform_infrared_spectroscopy.

[41] H. W. Siesler, Y. Ozaki, S. Kawata, and H. M. Heise (Editors). *Near-Infrared Spectroscopy.* Wiley-VCH, Weinheim, 1 edition, 2002.

[42] J. P. Coates. Shedding new light on materials analysis: Tunable mid-ir laser spectrometry. *A supplement to Spectroscopy*, pages 51–60, 2010.

[43] http://pubs.acs.org/cen/science/88/8846sci2.html.

[44] http://www.optoiq.com/index/photonics-technologies-applications/lfw-display/lfw-article-display/1840186236/articles/laser-focus-world/volume-46/issue-10/features/photonic-frontiers-quantum-cascade-lasers-prepare-to-compete-for-terahertz-applications.html.

[45] F. Capasso et al. Quantum Cascade Laser. *Science*, 264:553–556, 1994.

[46] H. Guenzler und H. U. Gremlich. *IR Spectroscopy, An Introduction*. Wiley-VCH Verlag GmbH, Weinheim, 2002.

[47] N. J Harrick. *Internal Reflection Spectroscopy*. John Wiley and Sons Inc, New York, 1967.

[48] F . M. Mirabella Jr. *Internal reflection spectroscopy: Theory and applications*. Marcel Dekker, Inc., New York, 1993.

[49] P. Kubelka and F. Munk. Ein Beitrag zur Optik der Farbenstriche. *Z. Tech. Phys*, 12:593–598, 1931.

[50] DIN 32465:2008-11, Chemische Analytik - Nachweis, Erfassungs- and Bestimmungsgrenze unter Wiederholbedingungen - Begriffe, Verfahren, Auswertung,.

[51] K. Molt and U. Telgeheder. Kalibrierung "All inclusive". *GIT Labor-Fachzeitscrift*, pages 292–294, 2010.

[52] http://www.quira.de, 2010.

[53] R Development Core Team. *R: A Language and Environment for Statistical Computing*. R Foundation for Statistical Computing, Vienna, Austria, 2008. ISBN 3-900051-07-0.

[54] http://www.mathworks.com/products/matlab/.

[55] Jose Claudio Faria. *Resources of Tinn-R GUI/Editor for R Environment*. UESC, Ilheus, Bahia, Brasil, 2009.

[56] B. H. Mevik and R. Wehrens. The pls package: Principal component and partial least squares regression in r. *Journal of Statistical Software*, 18(2):1–24, 2007.

[57] J. Cohen. A power primer. *Psychological Bulletin*, 112:155–159, 1992.

[58] R. A. Fisher. *Statistical Methods for Research Workers, 1925.* Oliver and Boyd, Edinburgh, Scotland, 1 edition, 1925.

[59] J. Cohen. *Statistical Power Analysis for the Behavioural Sciences.* Lawrence Erlbaum Associates, Inc., Hove and London, 2 edition, 1988.

[60] D. Shen and Z. Lu. Computation of Correlation Coefficient and Its Confidence Interval in SAS, 2006. http://www2.sas.com/proceedings/sugi31/170-31.pdf.

[61] http://www.analyticjournal.de/downloads_firmen/bruker_MATRIX_MF_Flyer_EN.pdf, 2009.

[62] http://www.thermoscientific.fr/com/cda/product/detail/0,1055,1000001344534,00.html, 2010.

[63] K. Molt and M. Egelkraut. Quantitative Mehrkomponentenanalyse von Pulvergemischen mittels NIRS. *GIT Labor-Fachzeitscrift für das Laboratorium*, pages 1311–1313, 1989.

[64] DIN 38409 H18, Deutsche Einheitsverfahren zur Wasser-, Abwasser- und Schlammuntersuchung (1981).

[65] REGULATION (EC) No 2037/2000 OF THE EUROPEAN PARLIAMENT AND OF THE COUNCIL of 29 June 2000 on substances that deplete the ozone layer. http://eur-lex.europa.eu/LexUriServ/LexUriServ.do?uri=OJ:L:2000:244:0001:0024:EN:PDF.

[66] Secretariat of The Vienna Convention for the Protection of the Ozone Layer & The Montreal Protocol on Substances that Deplete the Ozone Layer.

Handbook for the Montreal Protocol on Substances that Deplete the Ozone Layer. Lawrence Erlbaum Associates, Inc., United Nations Environment Programme, Vienna, 7 edition, 2006.

[67] DIN EN ISO 9377-2 Wasserbeschaffenheit Bestimmung des Kohlenwasserstoff-Index - Verfahren nach der Lösungsmittelextraktion und Gaschromatographie (2001).

[68] Method 1664, Revision A: N-Hexane Extractable Material (HEM; Oil and Grease) and Silica Gel Treated N-Hexane Extractable Material (SGTHEM; Non-polar Material) by Extraction and Gravimetry. United States Environmental Protection Agency, Washington.

[69] http://www.wilksir.com/oilgrease-analyzers.

[70] http://www.blockeng.com/products/qcl.html.

[71] Fayaz. K and K. Molt. Infrared Spectrometric Purity Control of Organic Liquids and Water. *CLEAN*, 37(12):955–962, 2009.

Curriculum Vitae

Fayaz Kondagula

Local Address
Eckenberg Str. 11/Zi-117
45307 Essen
Germany
Tel.no: 0049-17680105404

Permanent Address
Flat No 104, India House, Press Colony
Saidabad, Hyderabad, India
Tel.no: 0091-40-24151740
E-Mail: fayazpharm@yahoo.co.in

EDUCATION

1. PhD in Analytical Chemistry
   Instrumental Analytical Chemistry
   University-Duisburg Essen, Germany

2. M.Sc: Water Sciences
   University-Duisburg Essen, Germany

3. B.Pharm: Bachelor of Pharmacy
   Jawaharlal Nehru Technological University
   Hyderabad, India

EXPERIENCE

Research Scholar from 07/07-04/11
University-Duisburg Essen

PUBLICATION

Infrared Spectrometric Purity Control of Organic Liquids and Water, Fayaz Kondagula and Karl Molt, International Journal *CLEAN: Water, Soil and Air*, 37(12):955-962, 2009.

POSTERS

1. Reinheitskontrolle von chemischen und pharmazeutischen Produkten mit Hilfe der Infrarot-Spektroskopie, OPTAM-2008, in Dortmund, Germany.
2. Reinheitskontrolle von chemischen und pharmazeutischen Produkten mit Hilfe der Infrarot-Spektroskopie, ANAKON-2009, in Berlin, Germany
3. Infrared Spectrometric Purity control of Organic liquids and Water, enviro-Water-2009, Stellenbosch, South Africa.
4. Infrared Spectrometric Purity Control of Chemical and Pharmaceutical Substances in Process Environments, EuroAnalysis-2009, Innsbruck, Austria.
5. Infrared Spectrometric Purity Control of Chemical Substances in Process Environments,4. interdisziplinäres Doktorandenseminar, Attendorn-2010, Germany.
6. Infrared Spectrometric Purity Control of Chemical Substances using-R, useR! Conference-2010, NIST, Gaithersburg, USA.